



Commonwealth Edison
One First National Plaza, Chicago, Illinois
Address Reply to: Post Office Box 767
Chicago, Illinois 60690

June 27, 1983

Mr. Harold R. Denton, Director
Office of Nuclear Reactor Regulation
U.S. Nuclear Regulatory Commission
Washington, DC 20555

Subject: Dresden Station Units 2 and 3
Quad Cities Station Units 1 and 2
BWR Mark I Containment Program
Plant Unique Analysis Reports
NRC Docket Nos. 50-237, 50-249,
50-254 and 50-265

- References (a): L. O. DelGeorge letter to H. R. Denton
dated October 8, 1981.
- (b): T. J. Rausch letter to D. B. Vassallo
dated April 6, 1982.

Dear Mr. Denton:

Per the referenced letters, Commonwealth Edison committed to providing Plant Unique Analysis Report (PUARs) for the Mark I Containment Program. Enclosed for your review and use are ten (10) copies of this report for each station.

These plant unique reports (PUARs) document the efforts undertaken to address and resolve each of the applicable NUREG-0661 requirements. They demonstrate that the design of the primary containment system is adequate and that original design safety margins have been restored in accordance with NUREG-0661 acceptance criteria. Each Station's PUAR is composed of seven volumes; 14 volumes in total for both Stations, as follows:

- Volume 1 - General Criteria and Loads Methodology
- Volume 2 - Suppression Chamber Analysis
- Volume 3 - Vent System Analysis
- Volume 4 - Internal Structures Analysis
- Volume 5 - Safety Relief Valve Discharge Line Piping Analysis
- Volumes 6&7 - Torus Attached Piping and Suppression Chamber Penetration Analysis

8307070176 830627
PDR ADOCK 05000237
P PDR

A025
1/20
Limited DIST.

June 27, 1983

Volumes 1 through 4, 6, and 7 have been prepared by NUTECH Engineers, Incorporated, acting as an agent to the Commonwealth Edison Company. Volume 5 has been prepared by Sargent & Lundy (also acting as an agent to the Commonwealth Edison Company), who performed the safety relief valve discharge line piping analysis.

Please direct any questions you may have concerning this matter to this office.

One (1) signed original and sixty (60) copies of this letter is provided for your use. Due to the size of the reports, only ten (10) copies are being supplied.

Very truly yours,



B. Rybak
Nuclear Licensing Administrator

lm

cc: NRC Resident Inspector - Dresden
NRC Resident Inspector - Quad Cities
R. Gilbert - NRR
R. Bevan - NRR

6846N



Commonwealth Edison Company

Dresden Nuclear Generating Station

Units 2 & 3

NRC Docket Numbers 50-237 and 50-249

Plant Unique Analysis Report

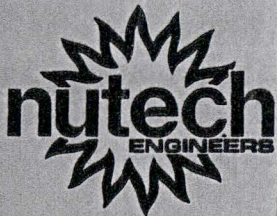
Volumes 3 & 4

— NOTICE —

THE ATTACHED FILES ARE OFFICIAL RECORDS OF THE DIVISION OF DOCUMENT CONTROL. THEY HAVE BEEN CHARGED TO YOU FOR A LIMITED TIME PERIOD AND MUST BE RETURNED TO THE RECORDS FACILITY BRANCH 016. PLEASE DO NOT SEND DOCUMENTS CHARGED OUT THROUGH THE MAIL. REMOVAL OF ANY PAGE(S) FROM DOCUMENT FOR REPRODUCTION MUST BE REFERRED TO FILE PERSONNEL.

DEADLINE RETURN DATE _____

RECORDS FACILITY BRANCH



Docket # 50-237
Control # 8307070176
Date 6-27-83 of Document
REGULATORY DOCKET FILE

REGULATORY DOCKET FILE COPY

COM-02-041-3
Revision 0
May 1983
64.305.1102

DRESDEN NUCLEAR
POWER STATION
UNITS 2 AND 3
PLANT UNIQUE ANALYSIS REPORT
VOLUME 3
VENT SYSTEM ANALYSIS

Prepared for:
Commonwealth Edison Company

Prepared by:
NUTECH Engineers, Inc.
San Jose, California

Approved by:



M. Shamszad, P.E.
Project Engineer

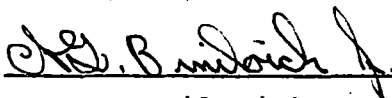


I. D. McInnes, P.E.
Engineering Manager



R. H. Adams, P.E.
Engineering Director

Issued by:



A. G. Brnilovich
Project Manager



R. H. Buchholz
Project Director

REGULATORY DOCKET FILE COPY

nutech
ENGINEERS

REVISION CONTROL SHEET

TITLE: Dresden Station, Units 2 and 3
Plant Unique Analysis Report
Volume 3

REPORT NUMBER: COM-02-041-3
Revision 0

N. G. Cofie/Consultant I

NGC
Initials

I. D. McInnes/Engineering Manager

IDM
Initials

C. F. Parker/Technician II

CFP
Initials

M. Shamszad/Project Engineer

MS
Initials

C. T. Shyy/Senior Engineer

CTS
Initials

D. C. Talbott/Consultant I

DC
Initials

R. E. Wise/Consultant I

REW
Initials

REVISION CONTROL SHEET
(Continued)

TITLE: Dresden Station, Units 2 and 3
Plant Unique Analysis Report
Volume 3

REPORT NUMBER: COM-02-041-3
Revision 0

EFFEC-TIVE PAGE (S)	REV	PRE-PARED	ACCURACY CHECK	CRITERIA CHECK	EFFEC-TIVE PAGE (S)	REV	PRE-PARED	ACCURACY CHECK	CRITERIA CHECK
3-v through 3-vi	0	REW	MS	CTS	3-2.76	0	NGC	MS	CTS
					3-2.77		MS	NGC	CTS
3-vii through 3-xvi		MS	OKP	CTS	3-2.78 through 3-2.84		NGC	MS	CTS
3-1.1 through 3-1.7		MS	CTS	IDM	3-2.85 through 3-2.92		CTS	MS	IDM
3-2.1 through 3-2.28		MS	DCT	CTS	3-2.93		NGC	MS	CTS
3-2.29 through 3-2.60		MS	REW	CTS	3-2.94 through 3-2.95		MS	NGC	CTS
3-2.61		REW	MS	CTS	3-2.96 through 3-2.113		MS	CTS	IDM
3-2.62 through 3-2.64		MS	NGC	CTS	3-2.114 through 3-2.116		MS	NGC	CTS
3-2.65 through 3-2.67		NGC	MS	CTS	3-2.117 through 3-2.137		MS	CTS	IDM
3-2.68 through 3-2.70		MS	NGC	CTS	3-2.138 through 3-2.150		MS	NGC	CTS
3-2.71 through 3-2.72		NGC	MS	CTS	3-2.151 through 3-2.161		NGC	MS	CTS
3-2.73 through 3-2.75	0	MS	NGC	CTS	3-2.162 through 3-2.178	0	MS	CTS	IDM

QEP-001.4-00

REVISION CONTROL SHEET
(Concluded)

TITLE: Dresden Station, Units 2 and 3
Plant Unique Analysis Report
Volume 3

REPORT NUMBER: COM-02-041-3
Revision 0

EFFEC-TIVE PAGE (S)	REV	PRE-PARED	ACCURACY CHECK	CRITERIA CHECK	EFFEC-TIVE PAGE (S)	REV	PRE-PARED	ACCURACY CHECK	CRITERIA CHECK
3-2.179	0	NGC	MP	CTS					
3-2.180 through 3-2.181		MS	CTS	IDMM					
3-2.182 through 3-2.185		MS	NGC	CTS					
3-2.186 through 3-2.187		NGC	MS	CTS					
3-2.188 through 3-2.189		MS	NGC	CTS					
3-2.190 through 3-2.191		MS	CTS	IDMM					
3-2.192 through 3-2.196		MS	CTS	IDMM					
3-3.1	0	MS	CTS	IDMM					

ABSTRACT

The primary containments for the Dresden Nuclear Power Station Units 2 and 3 were designed, erected, pressure-tested, and N-stamped in accordance with the ASME Boiler and Pressure Vessel Code, Section III, 1965 Edition with Addenda up to and including Winter 1965 for the Commonwealth Edison Company (CECo) by the Chicago Bridge and Iron Company. Since then, new requirements have been established. These requirements affect the design and operation of the primary containment system and are defined in the Nuclear Regulatory Commission's (NRC) Safety Evaluation Report, NUREG-0661. This report provides an assessment of containment design loads postulated to occur during a loss-of-coolant accident or a safety relief valve discharge event. In addition, it provides an assessment of the effects that the postulated events have on containment systems operation.

This plant unique analysis report (PUAR) documents the efforts undertaken to address and resolve each of the applicable NUREG-0661 requirements. It demonstrates that the design of the primary containment system is adequate and that original design safety margins have been restored, in accordance with NUREG-0661 acceptance criteria. The Dresden Units 2 and 3 PUAR is composed of the following seven volumes:

- o Volume 1 - GENERAL CRITERIA AND LOADS METHODOLOGY
- o Volume 2 - SUPPRESSION CHAMBER ANALYSIS
- o Volume 3 - VENT SYSTEM ANALYSIS
- o Volume 4 - INTERNAL STRUCTURES ANALYSIS
- o Volume 5 - SAFETY RELIEF VALVE DISCHARGE LINE PIPING ANALYSIS
- o Volume 6 - TORUS ATTACHED PIPING AND SUPPRESSION CHAMBER PENETRATION ANALYSES (DRESDEN UNIT 2)

- o Volume 7 - TORUS ATTACHED PIPING AND SUPPRESSION
CHAMBER PENETRATION ANALYSES (DRESDEN
UNIT 3)

This volume documents the evaluation of the vent system. Volumes 1 through 4 and 6 and 7 have been prepared by NUTECH Engineers, Incorporated (NUTECH), acting as an agent to the Commonwealth Edison Company. Volume 5 has been prepared by Sargent and Lundy (also acting as an agent to the Commonwealth Edison Company), who performed the safety relief valve discharge line (SRVDL) piping analysis. Volume 5 describes the methods of analysis and procedures used in the SRVDL piping analysis.

TABLE OF CONTENTS

	<u>Page</u>
ABSTRACT	3-v
LIST OF ACRONYMS	3-viii
LIST OF TABLES	3-x
LIST OF FIGURES	3-xiii
3-1.0 INTRODUCTION	3-1.1
3-1.1 Scope of Analysis	3-1.3
3-1.2 Summary and Conclusions	3-1.5
3-2.0 VENT SYSTEM ANALYSIS	3-2.1
3-2.1 Component Description	3-2.2
3-2.2 Loads and Load Combinations	3-2.29
3-2.2.1 Loads	3-2.30
3-2.2.2 Load Combinations	3-2.96
3-2.3 Acceptance Criteria	3-2.111
3-2.4 Methods of Analysis	3-2.117
3-2.4.1 Analysis for Major Loads	3-2.118
3-2.4.2 Analysis for Asymmetric Loads	3-2.162
3-2.4.3 Analysis for Local Effects	3-2.169
3-2.4.4 Methods for Evaluating Analysis Results	3-2.175
3-2.5 Analysis Results	3-2.180
3-2.5.1 Discussion of Analysis Results	3-2.192
3-2.5.2 Closure	3-2.195
3-3.0 LIST OF REFERENCES	3-3.1

LIST OF ACRONYMS

ADS	Automatic Depressurization System
ASME	American Society of Mechanical Engineers
CO	Condensation Oscillation
DC	Downcomer
DC/VH	Downcomer/Vent Header
DBA	Design Basis Accident
DBE	Design Basis Earthquake
DLF	Dynamic Load Factor
ECCS	Emergency Core Cooling System
FSI	Fluid-Structure Interaction
FSTF	Full-Scale Test Facility
IBA	Intermediate Break Accident
ID	Inside Diameter
IR	Inside Radius
LDR	Load Definition Report
LOCA	Loss-of-Coolant Accident
MB	Midbay
MJ	Miter Joint
NEP	Non-Exceedance Probability
NOC	Normal Operating Conditions
NPS	Nominal Pipe Size
NRC	Nuclear Regulatory Commission
NVB	Non-Vent Line Bay
OBE	Operating Basis Earthquake

LIST OF ACRONYMS
(Concluded)

OD	Outside Diameter
PUAAG	Plant Unique Analysis Applications Guide
PUAR	Plant Unique Analysis Report
PULD	Plant Unique Load Definition
QSTF	Quarter-Scale Test Facility
RPV	Reactor Pressure Vessel
SAR	Safety Analysis Report
SBA	Small Break Accident
SRSS	Square Root of the Sum of the Squares
SRV	Safety Relief Valve
SRVDL	Safety Relief Valve Discharge Line
SSE	Safe Shutdown Earthquake
VB	Vent Line Bay
VH	Vent Header
VL	Vent Line
VL/DW	Vent Line/Drywell
VL/VH	Vent Line/Vent Header

LIST OF TABLES

<u>Number</u>	<u>Title</u>	<u>Page</u>
3-2.2-1	Vent System Component Loading Information	3-2.60
3-2.2-2	Suppression Pool Temperature Response Analysis Results - Maximum Temperatures	3-2.61
3-2.2-3	Vent System Pressurization and Thrust Loads For DBA Event	3-2.62
3-2.2-4	Pool Swell Impact Loads for Vent Line and Spherical Junction	3-2.63
3-2.2-5	Downcomer Longitudinal Bracing and Lateral Bracing Pool Swell Drag and Fallback Submerged Structure Load Distribution	3-2.64
3-2.2-6	Support Column LOCA Water Jet and Bubble-Induced Drag Load Distribution	3-2.65
3-2.2-7	Downcomer LOCA Bubble-Induced Drag Load Distribution	3-2.66
3-2.2-8	Downcomer Longitudinal Bracing and Lateral Bracing LOCA Bubble-Induced Drag Load Distribution	3-2.67
3-2.2-9	IBA Condensation Oscillation Downcomer Loads	3-2.68
3-2.2-10	DBA Condensation Oscillation Downcomer Loads	3-2.69
3-2.2-11	IBA and DBA Condensation Oscillation Vent System Internal Pressures	3-2.70
3-2.2-12	Support Column DBA Condensation Oscillation Submerged Structure Load Distribution	3-2.71
3-2.2-13	Downcomer Longitudinal Bracing and Lateral Bracing DBA Condensation Oscillation Submerged Structure Load Distribution	3-2.72

LIST OF TABLES
(Continued)

<u>Number</u>	<u>Title</u>	<u>Page</u>
3-2.2-14	Maximum Downcomer Chugging Load Determination	3-2.73
3-2.2-15	Multiple Downcomer Chugging Load Magnitude Determination	3-2.74
3-2.2-16	Chugging Lateral Loads for Multiple Downcomers - Maximum Overall Effects	3-2.75
3-2.2-17	Load Reversal Histogram for Chugging Downcomer Lateral Load Fatigue Evaluation	3-2.76
3-2.2-18	Chugging Vent System Internal Pressures	3-2.77
3-2.2-19	Support Column Pre-Chug Submerged Structure Load Distribution	3-2.78
3-2.2-20	Downcomer Longitudinal Bracing and Lateral Bracing Pre-Chug Submerged Structure Load Distribution	3-2.79
3-2.2-21	Support Column Post-Chug Submerged Structure Load Distribution	3-2.80
3-2.2-22	Downcomer Longitudinal Bracing and Lateral Bracing Post-Chug Submerged Structure Load Distribution	3-2.81
3-2.2-23	Support Column SRV Discharge Submerged Structure Load Distribution	3-2.82
3-2.2-24	Downcomer T-quencher Bubble Drag Submerged Structure Load Distribution	3-2.83
3-2.2-25	Downcomer Longitudinal Bracing and Lateral Bracing T-quencher Bubble Drag Submerged Structure Load Distribution	3-2.84
3-2.2-26	Mark I Containment Event Combinations	3-2.104
3-2.2-27	Controlling Vent System Load Combinations	3-2.105
3-2.2-28	Enveloping Logic for Controlling Vent System Load Combinations	3-2.107

LIST OF TABLES
(Concluded)

<u>Number</u>	<u>Title</u>	<u>Page</u>
3-2.3-1	Allowable Stresses for Vent System Components and Component Supports	3-2.114
3-2.3-2	Allowable Displacements and Cycles for Vent Line Bellows	3-2.116
3-2.4-1	Vent System Frequency Analysis Results With Water Inside Downcomers, Based on Downcomers Braced Longitudinally	3-2.138
3-2.4-2	Vent System Frequency Analysis Results Without Water Inside Downcomers, Based on Downcomers Braced Longitudinally	3-2.139
3-2.4-3	Vent System Frequency Analysis Results with Water Inside Downcomers, Based on Downcomers Not Braced Longitudinally	3-2.142
3-2.4-4	Vent System Frequency Analysis Results without Water Inside Downcomers, Based on Downcomers Not Braced Longitudinally	3-2.144
3-2.5-1	Major Vent System Component Maximum Membrane Stresses for Governing Loads	3-2.182
3-2.5-2	Maximum Column Reactions for Governing Vent System Loads	3-2.183
3-2.5-3	Maximum Vent Line-Drywell Penetration Reactions for Governing Vent System Loads	3-2.184
3-2.5-4	Maximum Vent Line Bellows Displacements For Governing Vent System Loads	3-2.185
3-2.5-5	Maximum Vent System Stresses For Controlling Load Combinations	3-2.186
3-2.5-6	Maximum Vent Line Bellows Differential Displacements for Controlling Load Combinations	3-2.188
3-2.5-7	Maximum Fatigue Usage Factors For Vent System Components and Welds	3-2.189

LIST OF FIGURES

<u>Number</u>	<u>Title</u>	<u>Page</u>
3-2.1-1	Plan View of Containment	3-2.11
3-2.1-2	Elevation View of Containment	3-2.12
3-2.1-3	Suppression Chamber Section - Midbay Vent Line Bay	3-2.13
3-2.1-4	Suppression Chamber Section - Miter Joint	3-2.14
3-2.1-5	Suppression Chamber Section - Midbay Non-Vent Line Bay	3-2.15
3-2.1-6	Developed View of Suppression Chamber Segment	3-2.16
3-2.1-7	Vent Line Details - Upper End	3-2.17
3-2.1-8	Vent Line-Vent Header Spherical Junction	3-2.18
3-2.1-9	Vent Line Spherical Junction Drain	3-2.19
3-2.1-10	Developed View of Downcomer Longitudinal Bracing System	3-2.20
3-2.1-11	Downcomer-to-Vent Header Intersection Details - Dresden Unit 2	3-2.21
3-2.1-12	Downcomer-to-Vent Header Intersection Details - Dresden Unit 3	3-2.22
3-2.1-13	Downcomer Longitudinal Bracing System Configuration - Dresden Unit 2	3-2.23
3-2.1-14	Downcomer Longitudinal Bracing System Configuration - Dresden Unit 3	3-2.24
3-2.1-15	Vent Header Support Collar Plate Details	3-2.25
3-2.1-16	Vent System Support Column Details	3-2.26
3-2.1-17	Vacuum Breaker Locations	3-2.27
3-2.1-18	Vacuum Breaker Header Penetration Details	3-2.28

LIST OF FIGURES
(Continued)

<u>Number</u>	<u>Title</u>	<u>Page</u>
3-2.2-1	Vent System Internal Pressures For SBA Event	3-2.85
3-2.2-2	Vent System Internal Pressures for IBA Event	3-2.86
3-2.2-3	Vent System Internal Pressures for DBA Event	3-2.87
3-2.2-4	Vent System Temperatures for SBA Event	3-2.88
3-2.2-5	Vent System Temperatures for IBA Event	3-2.89
3-2.2-6	Vent System Temperatures for DBA Event	3-2.90
3-2.2-7	Downcomer Pool Swell Impact Loads	3-2.91
3-2.2-8	Pool Swell Impact Loads for Vent Header Deflectors at Selected Locations	3-2.92
3-2.2-9	Downcomer Longitudinal Bracing and Lateral Bracing	3-2.93
3-2.2-10	IBA and DBA Condensation Oscillation Downcomer Differential Pressure Load Distribution	3-2.94
3-2.2-11	Pool Acceleration Profile for Dominant Suppression Chamber Frequency at Midbay Location	3-2.95
3-2.2-12	Vent System SBA Event Sequence	3-2.108
3-2.2-13	Vent System IBA Event Sequence	3-2.109
3-2.2-14	Vent System DBA Event Sequence	3-2.110
3-2.4-1	Vent System 1/16 Segment Beam Model - Isometric View with Downcomer Longitudinal Bracing	3-2.146
3-2.4-2	Vent System 1/16 Segment Beam Model - Isometric View without Downcomer Longitudinal Bracing	3-2.147

LIST OF FIGURES
(Continued)

<u>Number</u>	<u>Title</u>	<u>Page</u>
3-2.4-3	Vent Line-Drywell Penetration Axisymmetric Finite Difference Model - View of Typical Meridian	3-2.148
3-2.4-4	Vent Line-Vent Header Spherical Junction Finite Element Model	3-2.149
3-2.4-5	Downcomer-Vent Header Intersection Finite Element Model - Isometric View	3-2.150
3-2.4-6	Harmonic Analysis Results for Support Column Submerged Structure Load Frequency Determination	3-2.151
3-2.4-7	Harmonic Analysis Results for Downcomer Submerged Structure Load Frequency Determination, Based on Downcomers Braced Longitudinally	3-2.152
3-2.4-8	Harmonic Analysis Results for Downcomer Submerged Structure Load Frequency Determination, Based on Downcomers Not Braced Longitudinally	3-2.153
3-2.4-9	Harmonic Analysis Results for Lateral Bracing Submerged Structure Load Frequency Determination	3-2.154
3-2.4-10	Harmonic Analysis Results for Longitudinal Bracing Horizontal Member Submerged Structure Load Frequency Determination	3-2.155
3-2.4-11	Harmonic Analysis Results for Longitudinal Bracing Diagonal Member Submerged Structure Load Frequency Determination	3-2.156
3-2.4-12	Harmonic Analysis Results for Condensation Oscillation Downcomer Load Frequency Determination	3-2.157
3-2.4-13	Harmonic Analysis Results for Condensation Oscillation Vent System Pressure Load Frequency Determination	3-2.158

LIST OF FIGURES
(Concluded)

<u>Number</u>	<u>Title</u>	<u>Page</u>
3-2.4-14	Harmonic Analysis Results for Chugging Downcomer Lateral Loads Frequency Determination, Based on Downcomers Braced Longitudinally	3-2.159
3-2.4-15	Harmonic Analysis Results for Chugging Downcomer Lateral Loads Frequency Determination, Based on Downcomers Not Braced Longitudinally	3-2.160
3-2.4-16	Harmonic Analysis Results for Chugging Vent System Pressure Load Frequency Determination	3-2.161
3-2.4-17	Vent System 180° Beam Model - Isometric View (Dresden Unit 2)	3-2.167
3-2.4-18	Vent System 180° Beam Model - Isometric View (Dresden Unit 3)	3-2.168
3-2.4-19	Allowable Number of Stress Cycles For Vent System Fatigue Evaluation	3-2.179
3-2.5-1	Vent System Support Column Response Due to Pool Swell Impact Loads - Outside Column	3-2.190
3-2.5-2	Vent System Support Column Response Due to Pool Swell Impact Loads - Inside Column	3-2.191

3-1.0 INTRODUCTION

In conjunction with Volume 1 of the PUAR, this volume documents the efforts undertaken to address the NUREG-0661 requirements which affect the Dresden Units 2 and 3 vent systems. The vent system PUAR is organized as follows:

- o INTRODUCTION
 - Scope of Analysis
 - Summary and Conclusions
- o VENT SYSTEM ANALYSIS
 - Component Description
 - Loads and Load Combinations
 - Acceptance Criteria
 - Methods of Analysis
 - Analysis Results

The INTRODUCTION section contains an overview of the scope of the vent system evaluation, as well as a summary of the conclusions derived from the comprehensive evaluation of the vent system. The VENT SYSTEM ANALYSIS section contains a comprehensive discussion of the vent system loads and load combinations and a description of the vent system components affected by these loads. This section also contains a discussion

of the methodology used to evaluate the effects of these loads, the associated evaluation results, and the acceptance limits to which the results are compared.

Relative to the methodology used to evaluate the effects of these loads, the associated evaluation results, and the acceptance limits to which the results are compared.

Relative to the methodology used to evaluate the effects of these loads, the associated evaluation results, and the acceptance limits to which the results are compared.

The criteria presented in Volume 1 are used as the basis for the Dresden Units 2 and 3 vent system evaluation. The modified vent system is evaluated for the effects of loss-of-coolant accident (LOCA)-related loads and safety relief valve (SRV) discharge-related loads defined by the Nuclear Regulatory Commission (NRC) Safety Evaluation Report NUREG-0661 (Reference 1) and the "Mark I Containment Program Load Definition Report" (LDR) (Reference 2).

The LOCA and SRV discharge loads used in this evaluation are formulated using the methodology discussed in Volume 1 of this report. The loads are developed using the plant unique geometry, operating parameters, and test results contained in the Plant Unique Load Definition (PULD) report (Reference 3). The effects of increased suppression pool temperatures which occur during SRV discharge events are also evaluated. These temperatures are taken from the plant's suppression pool temperature response analysis (Section 1-5.1). Other loads and methodology, such as the evaluation for seismic loads, are taken from the plant's design specification (Reference 4).

The evaluation includes performing a structural analysis of the vent system for the effects of LOCA-related and SRV discharge-related loads to confirm that the design of the vent system is adequate. Rigorous analytical techniques are used in this evaluation, including the use of detailed analytical models for computing the dynamic response of the vent system. Effects such as local penetration and intersection flexibilities are also considered in the vent system analysis.

The results of the structural evaluation for each load case are used to evaluate load combinations and fatigue effects for the vent system in accordance with the "Mark I Containment Program Structural Acceptance Criteria Plant Unique Analysis Applications Guide" (PUAAG) (Reference 5). The analysis results are compared with the acceptance limits specified by the PUAAG and the applicable sections of the American Society of Mechanical Engineers (ASME) Code (Reference 6).

3-1.2 Summary and Conclusions

The evaluation documented in this volume is based on the modified Dresden Units 2 and 3 vent systems described in Section 1-2.1. The overall load-carrying capacity of the modified vent system and its supports is substantially greater than the original design described in the plant's design specification.

The loads considered in the original design of the vent system and its supports include dead weight loads, operating basis earthquake (OBE) and design basis earthquake (DBE) loads, thrust loads, and pressure and temperature loads associated with normal operating conditions (NOC) and a postulated LOCA event. The additional loadings which affect the design of the vent system and supports are defined generically in NUREG-0661. These loads are postulated to occur during small break accident (SBA), intermediate break accident (IBA), or design basis accident (DBA) LOCA events and during SRV discharge events. These events result in impact and drag loads on vent system components above the suppression pool, in hydrodynamic internal pressure loadings on the vent system, in hydrodynamic drag loadings on the submerged vent system components, and in motion and reaction loadings caused by loads acting on structures attached to the vent system.

1850-1000 Section 1-4.0 discusses the methodology used to develop
each of the plant unique loadings for the vent system evaluation.
8500-1000 Applying this methodology results in conservative
01-0000 values for each of the significant loadings using
8000-1000 NUREG-0661 criteria and envelop those postulated to
1000-1000 occur during an actual LOCA or SRV discharge event.

The LOCA-related and SRV discharge-related loads are
1000-1000 grouped into event combinations using the NUREG-0661
0000-1000 criteria discussed in Section 1-3.2. The event
0000-1000 sequencing and event combinations specified and
0000-1000 evaluated envelop the actual events postulated to occur
0000-1000 throughout the life of the plant.

The loads contained in the postulated event combina-
0000-1000 tions which are major contributors to the total vent
1000-1000 system response include pressurization and thrust
0000-1000 loads, pool swell impact loads, condensation oscilla-
0000-1000 tion (CO) downcomer loads, and chugging downcomer
0000-1000 lateral loads. Although considered in the evaluation,
0000-1000 other loadings, such as internal pressure loads,
0000-1000 temperature loads, seismic loads, froth impingement and
0000-1000 fallback loads, submerged structure loads, and contain-
0000-1000 ment motion and reaction loads, have a lesser effect on
0000-1000 the total vent system response.

The vent system evaluation is based on the NUREG-0661 acceptance criteria discussed in Section 1-3.2. These acceptance limits are at least as restrictive as those used in the original vent system design documented in the plant's Safety Analysis Report (SAR). (Reference 7). Use of these criteria assures that the original vent system design margins have been restored.

The controlling event combinations for the vent system are those which include the loadings found to be major contributors to the vent system response. The evaluation results for these event combinations show that all of the vent system stresses and support reactions are within acceptable limits.

As a result, the modified vent systems described in Section 1-2.1 have been shown to fulfill the margins of safety inherent in the original vent system design documented in the plant's safety analysis report. The NUREG-0661 requirements are therefore considered to be met.

3-2.0 VENT SYSTEM ANALYSIS

Evaluations of each of the NUREG-0661 requirements which affect the design adequacy of the Dresden Units 2 and 3 vent systems are presented in the following sections. The criteria used in this evaluation are contained in Volume 1 of this report.

Section 3-2.1 describes the vent system components examined. Section 3-2.2 describes and presents the loads and load combinations for which the vent system is evaluated. The acceptance limits to which the analysis results are compared, discussed, and presented are in Section 3-2.3. Section 3-2.4 discusses the analysis methodology used to evaluate the effects of these loads and load combinations on the vent system. Section 3-2.5 presents the analysis results and the corresponding vent system design margins.

3-2.1 Component Description

The Dresden Units 2 and 3 vent systems are constructed from cylindrical shell segments joined together to form a manifold-like structure connecting the drywell to the suppression chamber. Figures 3-2.1-1 and 3-2.1-2 show the configuration of the vent system. The major components of the vent system include the vent lines (VL), vent line-vent header (VL/VH) spherical junctions, vent header (VH), and downcomers (DC). Figures 3-2.1-3 through 3-2.1-6 show the proximity of the vent system to other containment components.

The eight vent lines connect the drywell to the vent header in alternate mitered cylinders or bays of the suppression chamber. The vent lines are nominally 1/4" thick and have an inside diameter (ID) of 6'9". The upper ends of the vent lines include conical transition segments at the penetration to the drywell (Figure 3-2.1-7). The drywell insert plate around each vent line-drywell (VL/DW) penetration is 2-1/4" thick, with a 3-5/8" thick cylindrical nozzle. The vent lines are shielded from jet impingement loads at each vent line-drywell penetration location by jet deflectors which span the openings of the vent lines. The drywell/wet-well vacuum breakers are nominal 18" units. There are

two vacuum breakers in each vacuum breaker header. There are six vacuum breaker headers on the suppression chamber (Figure 3-2.1-17). The headers originate as a 30" outside diameter (OD) vertical penetration at the upper outside quadrant of six different vent line bays. This penetration is reinforced by a 1-1/2" thick insert plate at each location (Figure 3-2.1-18). The header then leaves the 30" penetration as two separate, horizontal 18" OD lines where the vacuum breakers are contained. After the two vacuum breakers, the two 18" OD lines come together again into a 24" OD line. A 24" diameter bellows assembly immediately follows this intersection. The header continues as a 24" diameter line from the bellows to the vent line-drywell penetration. This 24" diameter vent line penetration is reinforced with a 33" diameter by 3/4" thick insert plate (Figure 3-2.1-18). The eight vent line-vent header spherical junctions connect the vent lines and the vent header (Figure 3-2.1-8). Each spherical junction is constructed from six shell segments, with thicknesses varying from 1/4" to 3/4". The spherical junctions all have a 1" diameter drain line extending from the bottom of the spherical junction to below the pool surface. The drain lines are reinforced with a 4", Schedule 120 pipe sleeve that surrounds the drain line. The sleeve is attached to a 1" thick pad plate,

which is attached to the bottom of the spherical junction. The other end of the sleeve is attached to a 1/2" thick collar plate that keeps the drain line centered inside the sleeve (Figure 3-2.1-9).

The SRV piping is routed from the drywell through the vent line and penetrates the vent line inside the suppression chamber. Volume 5 of this report presents the analysis of the SRV piping and vent line penetration.

The vent header is a continuous assembly of mitered cylindrical shell segments joined together to form a ring header (Figure 3-2.1-1). The vent header is 1/4" thick and has an ID of 4'10".

Ninety-six downcomers penetrate the vent header in pairs (Figures 3-2.1-1 and 3.2.1-10). Two downcomer pairs are located in each vent line bay (VB); four pairs are located in each non-vent line bay (NVB). Each downcomer consists of an inclined segment which penetrates the vent header, and a vertical segment which terminates below the surface of the suppression pool (Figures 3-2.1-11 and 3-2.1-12). The inclined segment is 1/2" thick and the vertical segment is 1/4"

thick. The inside diameters of the inclined and vertical portions of the downcomer are 2'0".

Full penetration welds connect the vent lines to the drywell, the vent lines to the spherical junctions, the spherical junctions to the vent header, and the downcomers to the vent header. As such, the connections of the major vent system components are capable of developing the full capacity of the associated major components themselves.

The intersections of the downcomers and the vent header are reinforced with a system of stiffener plates and bracing members (Figures 3-2.1-10, 3-2.1-11, and 3-2.1-12). In the plane of the downcomer pairs, the intersections are stiffened by a pair of 1/2" stiffener plates located between each set of the downcomers and a pair of lateral bracing pipe members at the bottom of each set of two downcomers. The stiffener plates are welded both to the tangent points of the downcomer legs and to the vent header. The lateral bracings are welded to the downcomer rings near the tangent points. The system of stiffener plates is designed to reduce local intersection stresses caused by loads acting in the plane of the downcomers. The system of lateral

bracing ties the downcomer legs together in a pair; therefore, separation forces on the pair of downcomer legs will be taken as axial forces in the bracing.

In the direction normal to the plane of the downcomer pair, the downcomers are braced by a longitudinal bracing system. In Dresden Unit 2 these bracings are located in those vent line bays which house the SRV discharge line, and which extend to midlength of the neighboring non-vent bays (Figure 3-2.1-10). In this manner, 62% of all the downcomers are braced longitudinally. However, in Dresden Unit 3 all 96 downcomers are braced longitudinally. Figures 3-2.1-13 and 3-2.1-14 show the longitudinal bracing patterns for the two Dresden units. The ends of the horizontal pipe members near miter joints (MJ) and centerlines of the non-vent bays are welded to the downcomer rings. The 3" x 1" diagonal members and their adjacent horizontal pipe members are connected to lugs which are welded to the downcomers.

This bracing system provides an additional load path for the transfer of loads acting on the submerged portion of the downcomers and results in reduced local stresses in the downcomer-vent header intersection regions. The system of downcomer-vent header inter-

section stiffener plates and lateral bracings provides a redundant mechanism for the transfer of loads acting on the downcomers, thus reducing the magnitude of loads passing directly through the intersection. The longitudinal bracing also ties together several pairs of downcomers in the longitudinal direction, causing an increase in stiffness to the overall system. This stiffness increase minimizes the dynamic effect of several loads, including SRV loads on submerged structures. It also results in load sharing among the downcomers for SRV loads on submerged structures.

A bellows assembly is provided at the penetration of the vent line to the suppression chamber (Figure 3-2.1-7). The bellows allows differential movement of the vent system and suppression chamber to occur without developing significant interaction loads. Each bellows assembly consists of a stainless steel bellows unit connected to a 2-1/8" thick nozzle. The bellows unit has a 7'5" inside diameter and contains five convolutions which connect to a 1/2" thick cylindrical sleeve at the vent line end and a 1" thick cylindrical sleeve at the nozzle end. A 1-1/2" thick annular plate welded to the vent line connects to the upper end of the bellows assembly by full penetration welds. The lower end of the bellows assembly is a 2-1/8" thick

nozzle, already described, which is connected to the suppression chamber shell insert plate by full penetration welds. The overall length of the bellows assembly is 3'2-3/4".

Vent header deflectors are provided in both the vent line bays and the non-vent line bays (Figures 3-2.1-6 and 3-2.1-12). The deflectors shield the vent header from pool swell impact loads which occur during the initial phase of a DBA event. The vent header deflectors are constructed from 20" diameter, Schedule 100 pipe. The vent header deflectors are supported by 1" thick connection plates that are welded to the vent header support collar plates near each miter joint.

The vent system is supported vertically by two column members at each miter joint location (Figures 3-2.1-4, 3-2.1-15 and 3-2.1-16). The support column members are constructed from 6" diameter, Schedule 80 pipe. The upper ends of the support columns are connected to the 1" thick vent header support collar plates by 2-3/4" diameter pins. The support collar plates are attached to the vent header with 5/16" fillet welds. The support column loads are transferred at the upper pin locations by 3/4" thick pin plates. The lower ends of support columns are attached to 1" thick ring girder

pin plates with 2-3/4" diameter pins and 3/4" thick pin plates. The support column assemblies are designed to transfer vertical loads acting on the vent system to the suppression chamber ring girders, while simultaneously resisting drag loads on submerged structures.

The vent system is supported horizontally by the vent lines which transfer lateral loads acting on the vent system to the drywell at the vent line-drywell penetration locations. The vent lines also provide additional vertical support for the vent system, although the vent system support columns provide primary vertical support. The support provided by the vent line bellows is negligible since the relative stiffness of the bellows with respect to other vent system components is small.

The vent system also provides support for a portion of the SRV piping inside the vent line and suppression chamber (Figures 3-2.1-3 and 3-2.1-7). Loads acting on the SRV piping are transferred to the vent system by the penetration assembly and internal supports on the vent line. Conversely, loads acting on the vent system cause motions to be transferred to the SRV piping at the same support locations. Since the relative stiffness of the SRV discharge line is small with respect to other vent system components, the support

provided by the SRV discharge line to the vent system is negligible.

The overall load-carrying capacities of the vent system components described in the preceding paragraphs provide additional design margins for those components of the original vent system design described in the plant's safety analysis report.

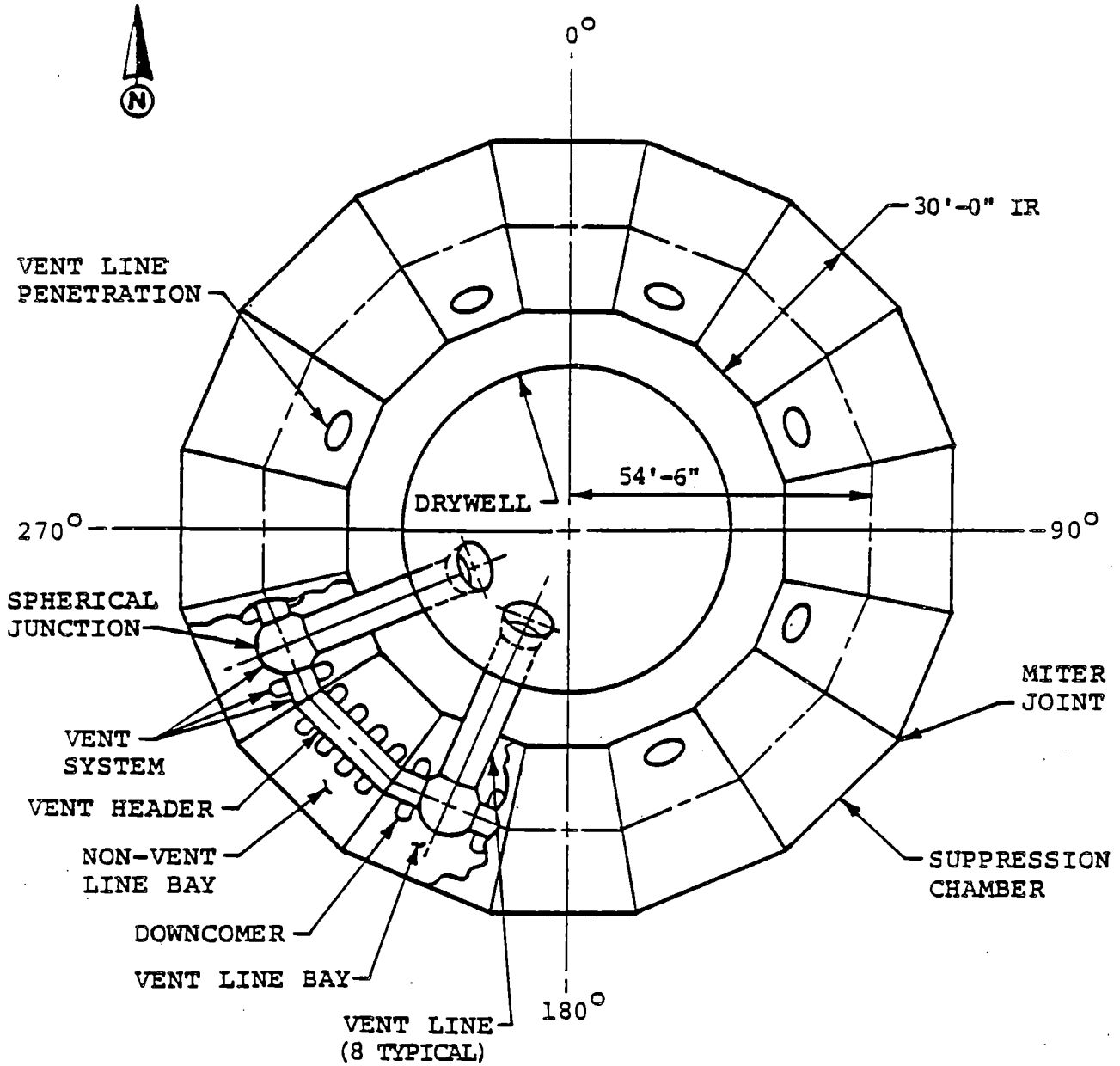


Figure 3-2.1-1

PLAN VIEW OF CONTAINMENT

COM-02-041-3
Revision 0

3-2.11

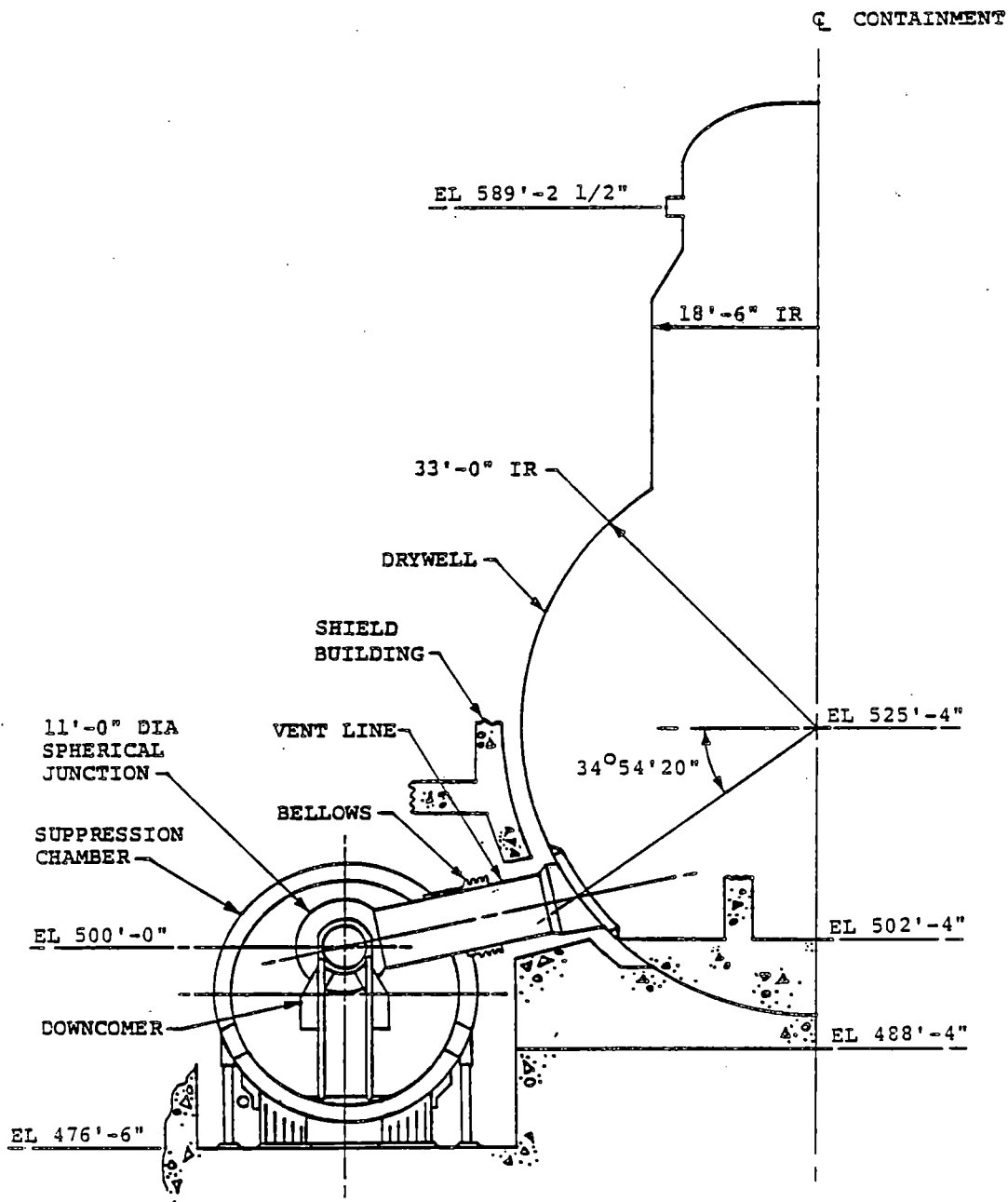


Figure 3-2.1-2

ELEVATION VIEW OF CONTAINMENT

COM-02-041-3
Revision 0

3-2.12

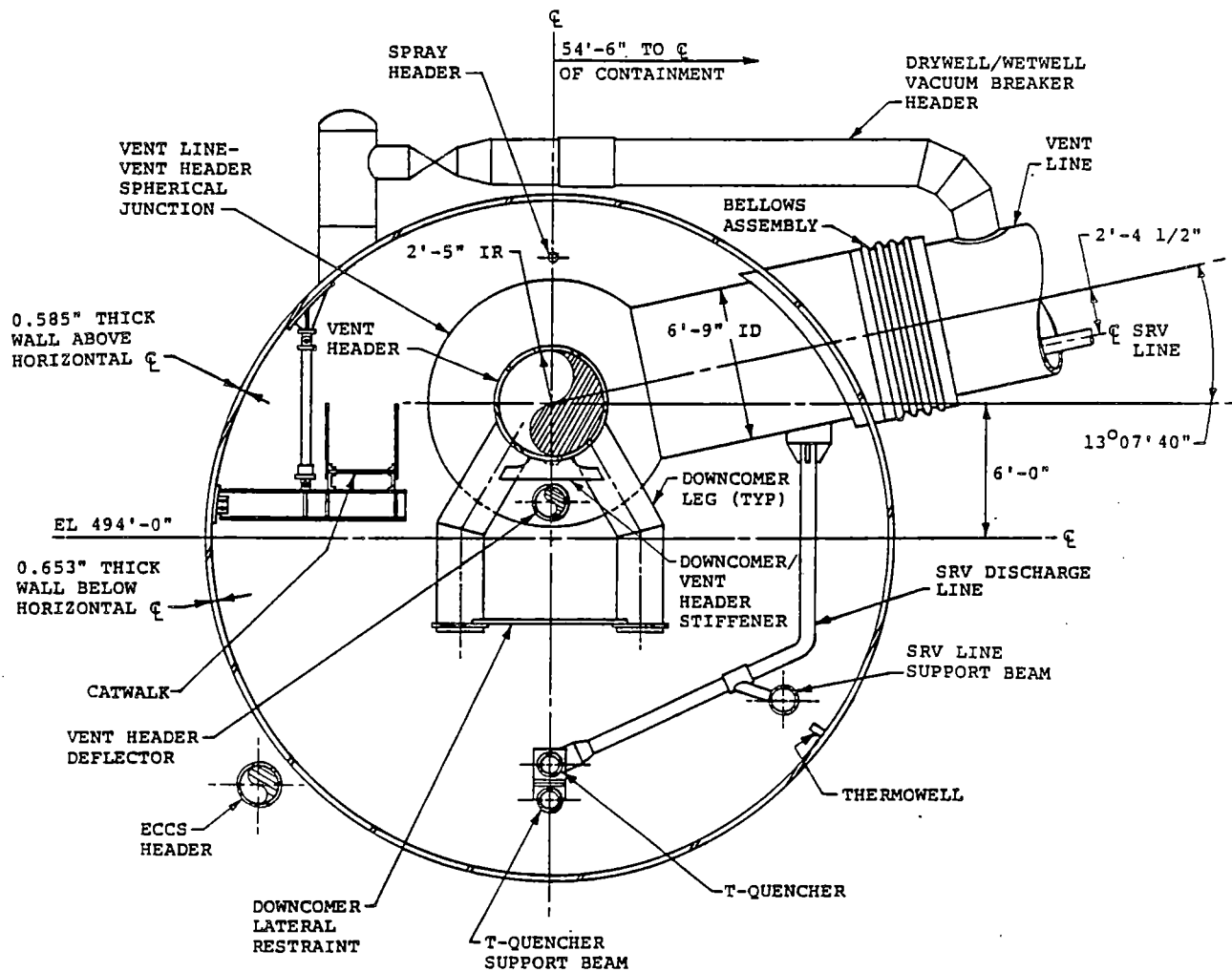


Figure 3-2.1-3

SUPPRESSION CHAMBER SECTION - MIDBAY
VENT LINE BAY

COM-02-041-3
Revision 0

3-2.13

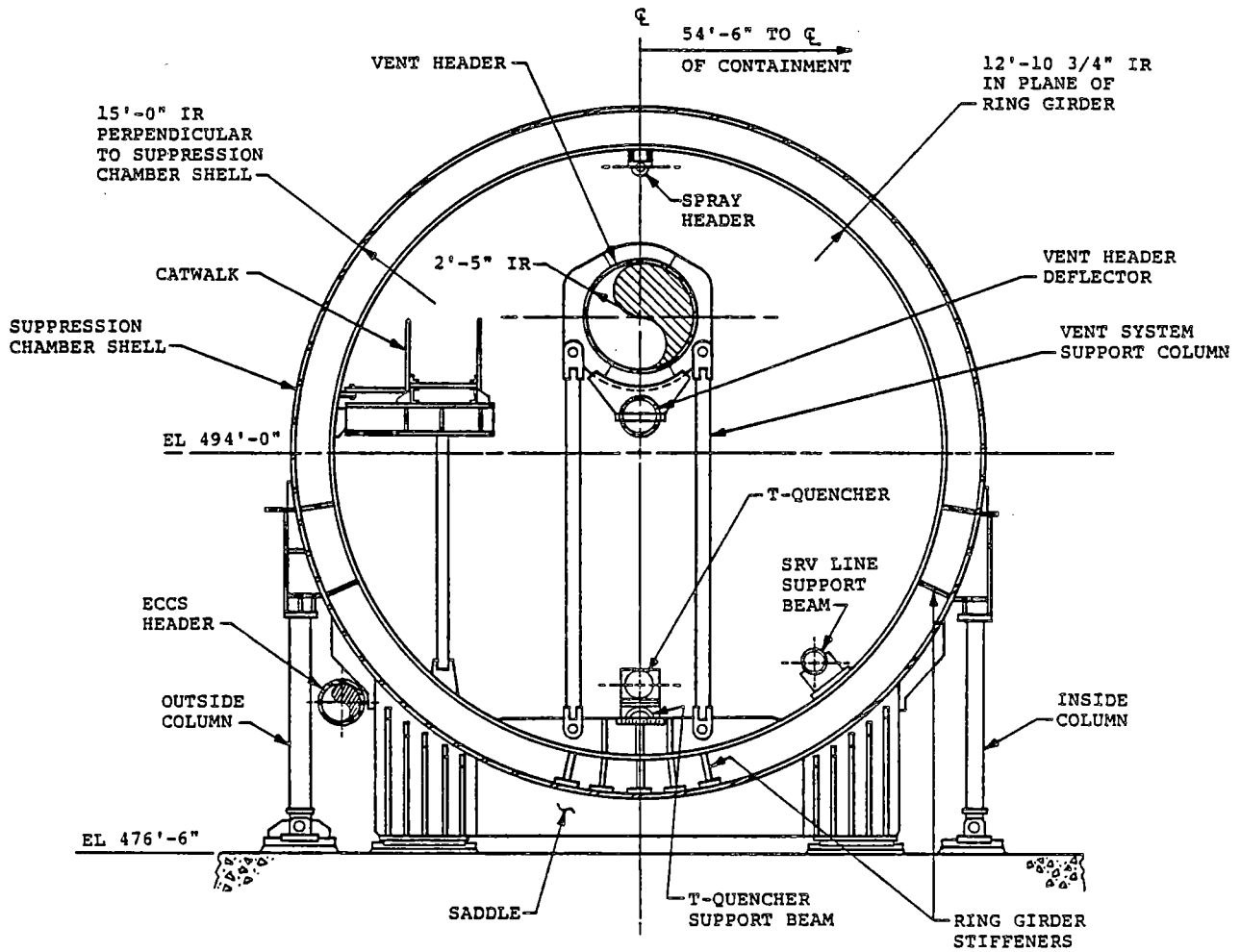


Figure 3-2.1-4
SUPPRESSION CHAMBER SECTION -
MITER JOINT

COM-02-041-3
 Revision 0

3-2.14

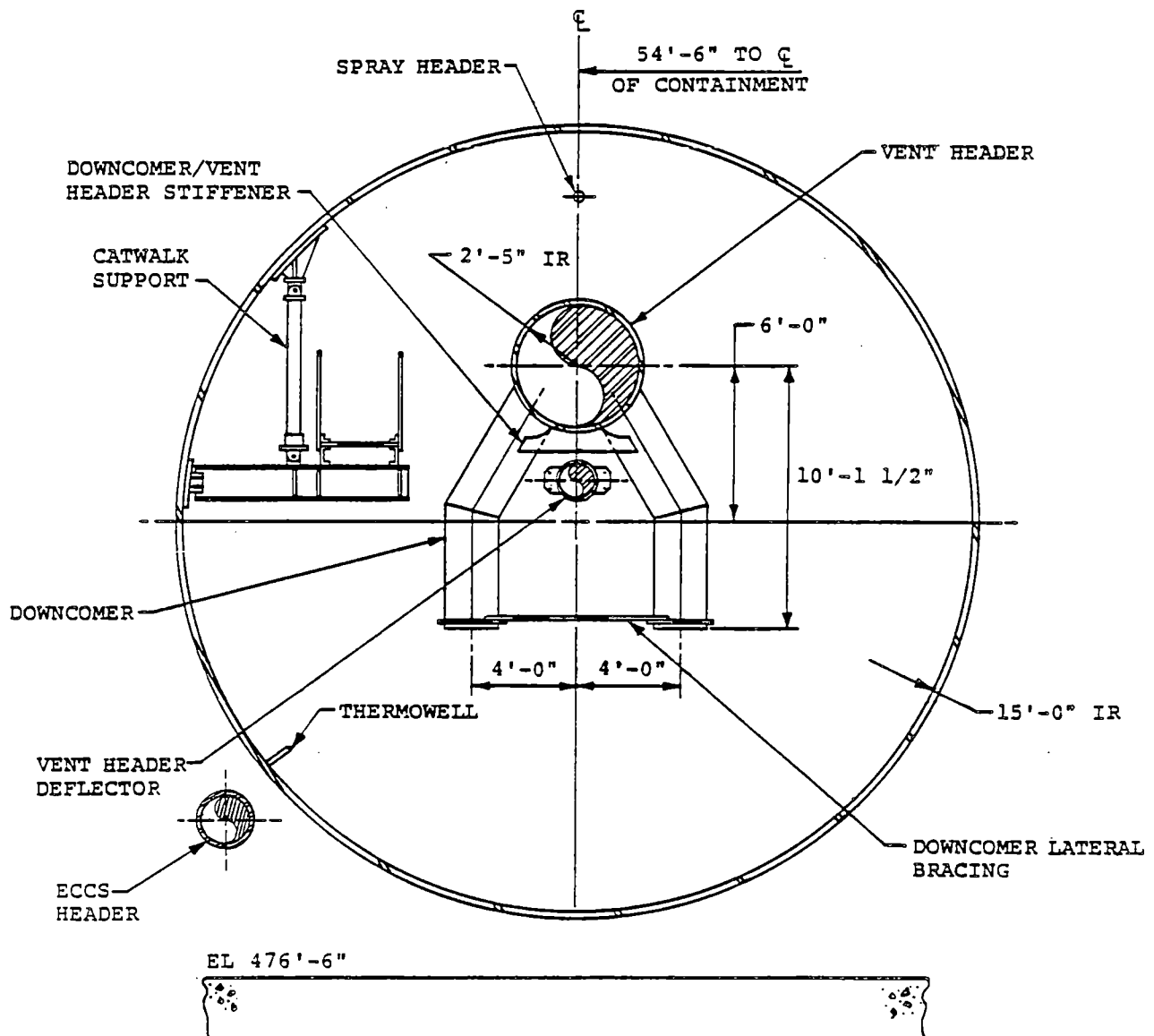


Figure 3-2.1-5
SUPPRESSION CHAMBER SECTION - MIDBAY
NON-VENT LINE BAY

COM-02-041-3
 Revision 0

3-2.15

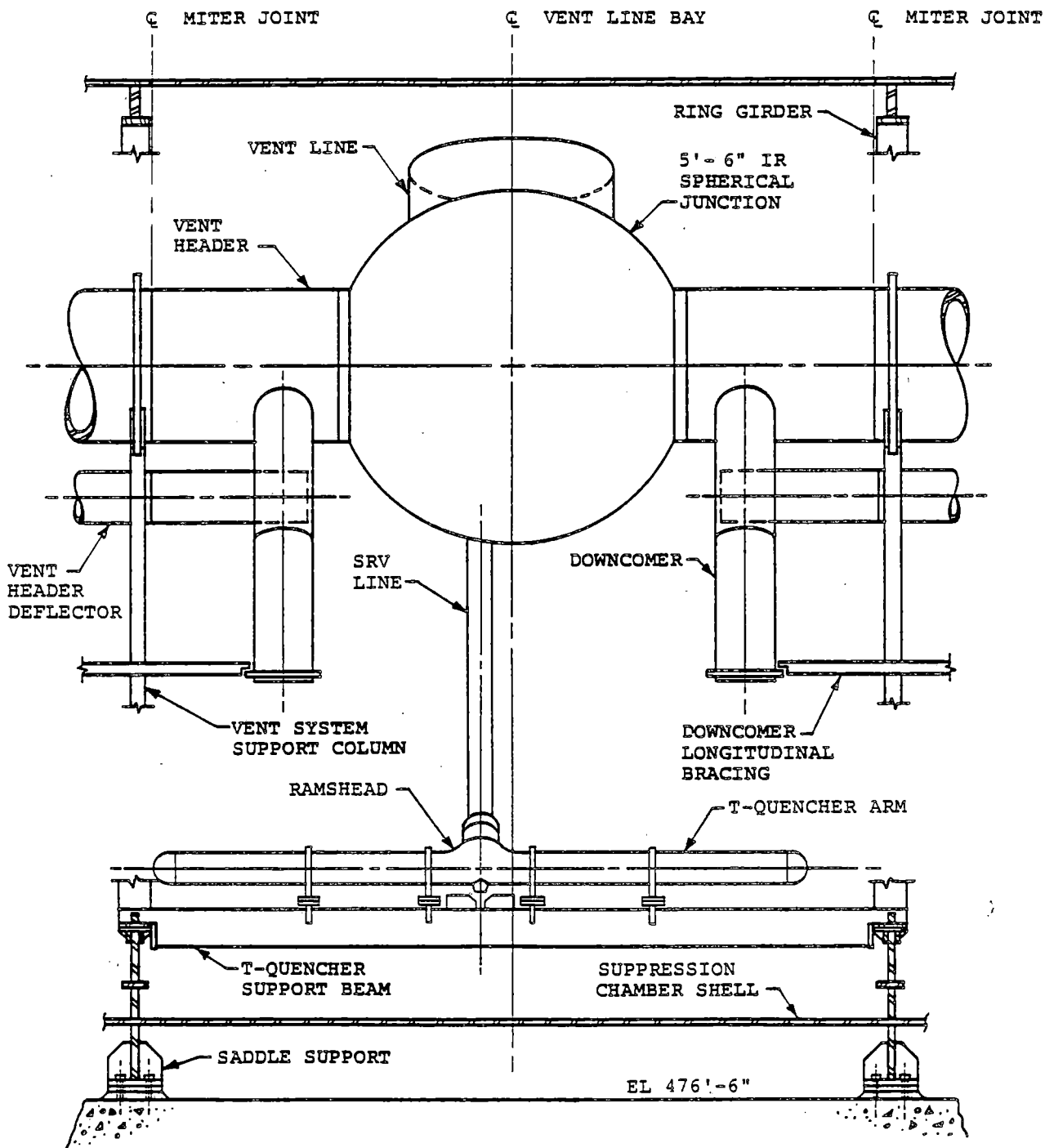


Figure 3-2.1-6

DEVELOPED VIEW OF SUPPRESSION CHAMBER SEGMENT

COM-02-041-3
Revision 0

3-2.16

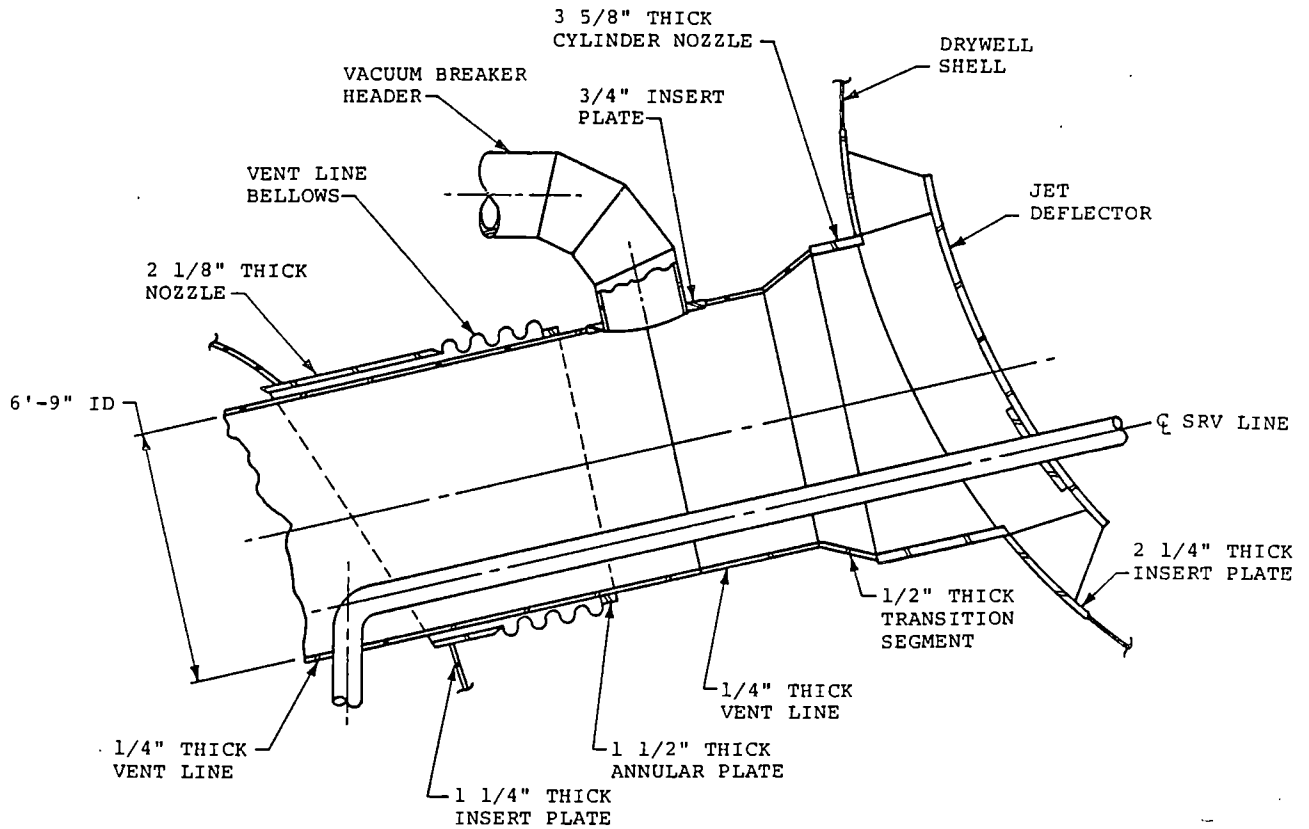


Figure 3-2.1-7

VENT LINE DETAILS - UPPER END

COM-02-041-3
Revision 0

3-2.17

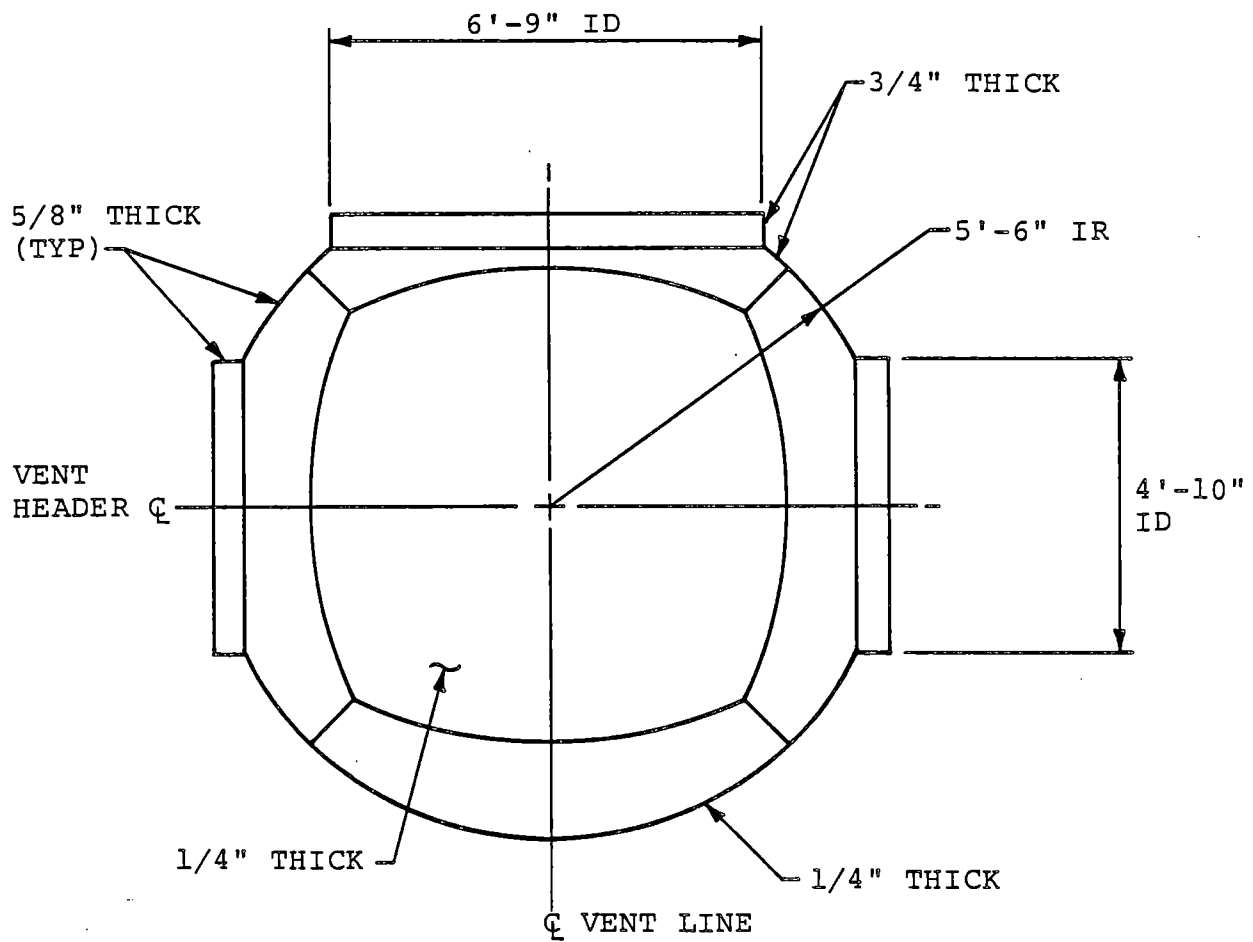


Figure 3-2.1-8

VENT LINE-VENT HEADER SPHERICAL JUNCTION

COM-02-041-3
Revision 0

3-2.18

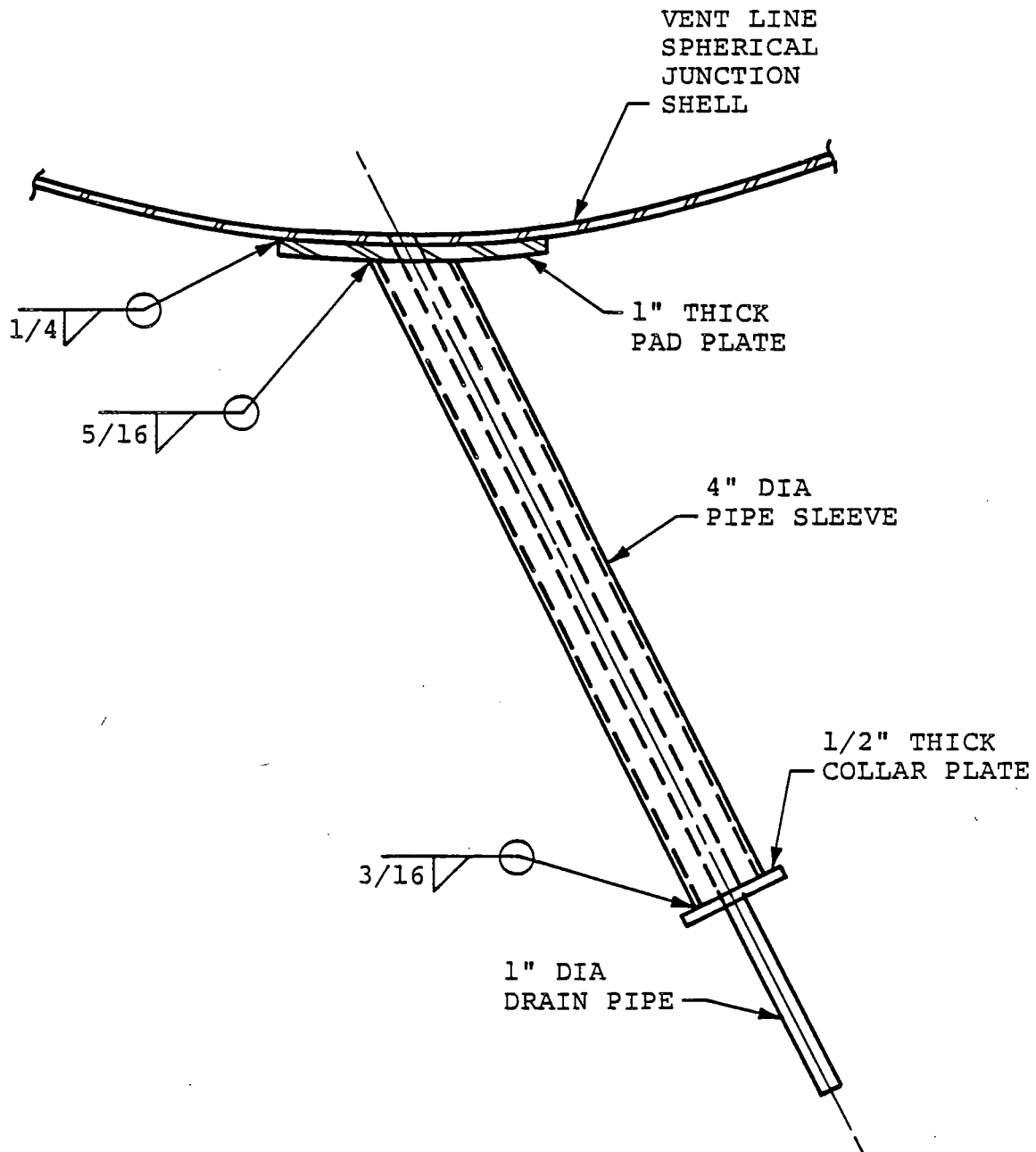
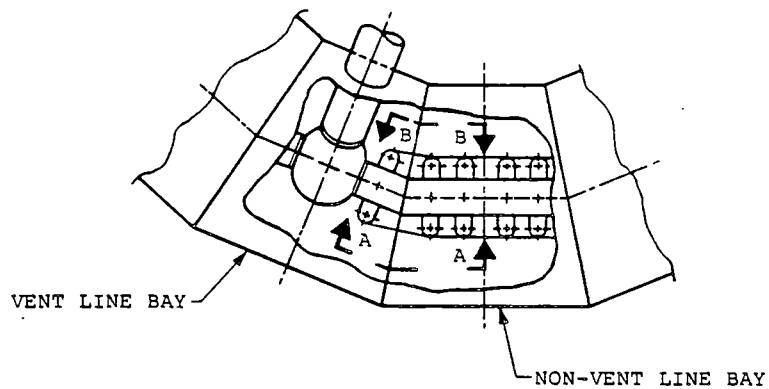
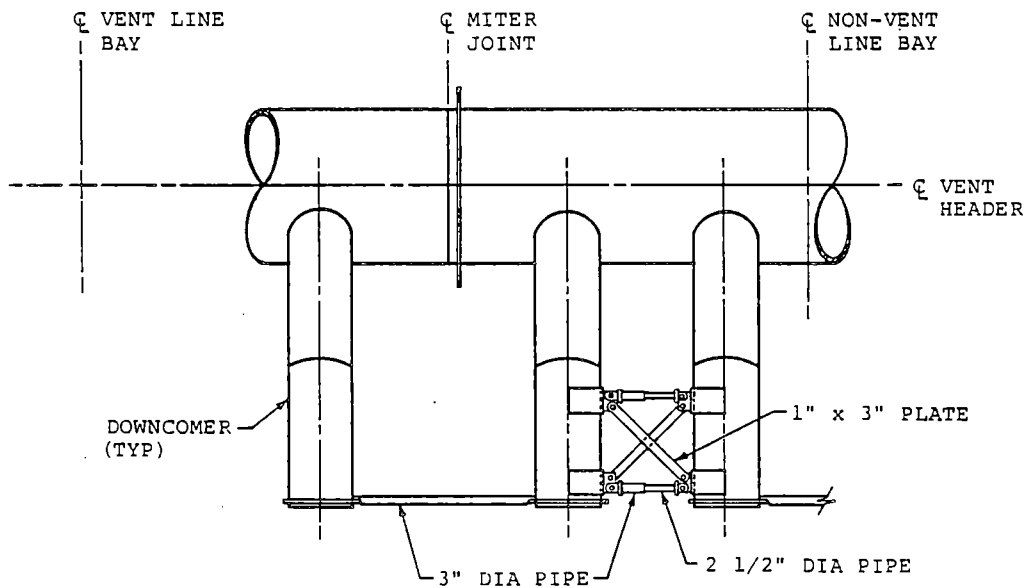


Figure 3-2.1-9
VENT LINE SPHERICAL JUNCTION DRAIN



PARTIAL PLAN VIEW OF SUPPRESSION CHAMBER



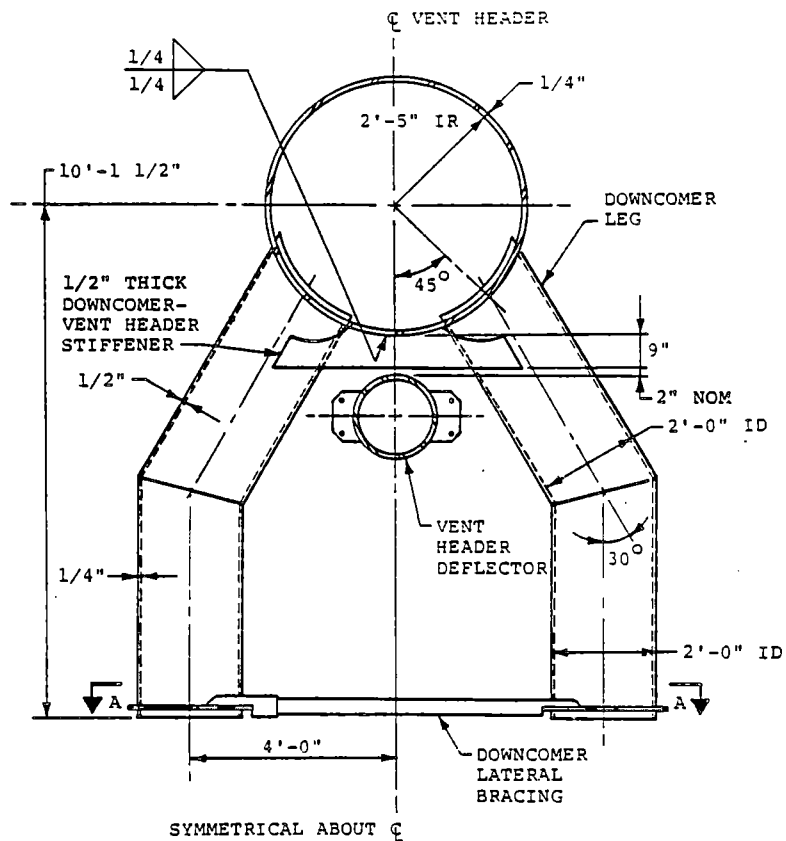
VIEW A-A

VIEW B-B (OPPOSITE HAND)

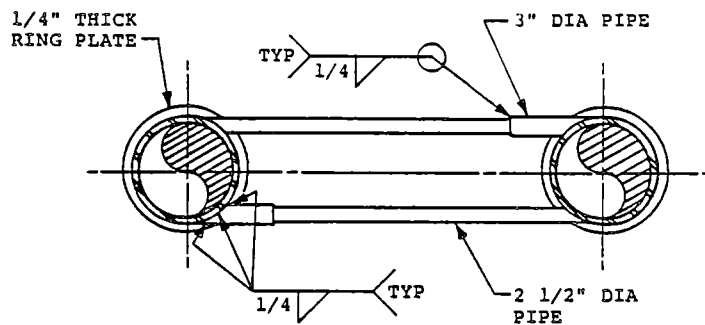
1. VENT HEADER DEFLECTOR AND VENT HEADER COLUMNS NOT SHOWN FOR CLARITY.

Figure 3-2.1-10

DEVELOPED VIEW OF DOWNCOMER
LONGITUDINAL BRACING SYSTEM



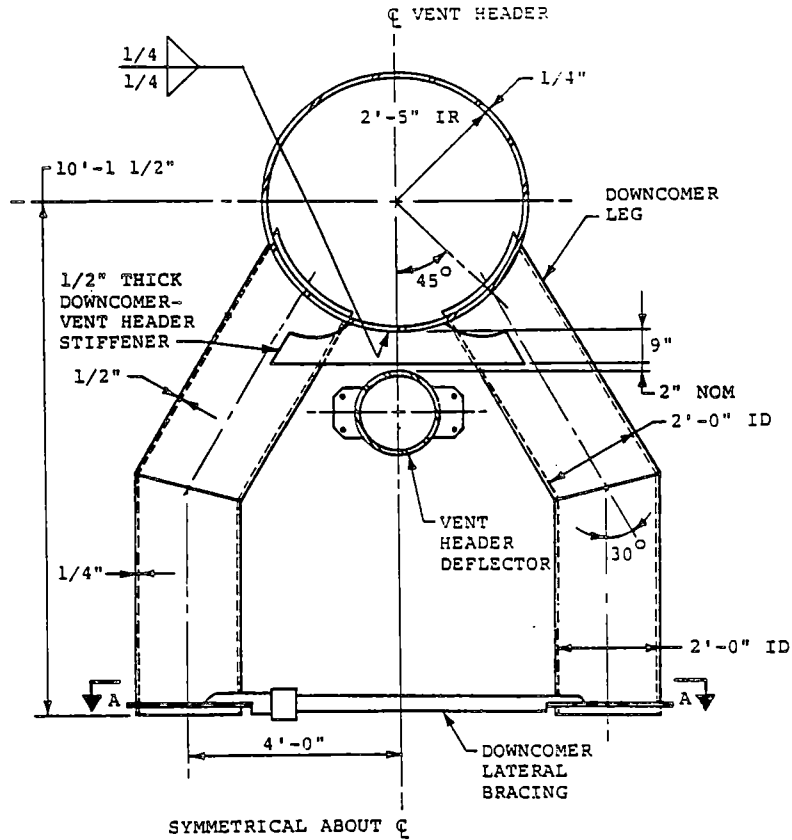
ELEVATION VIEW



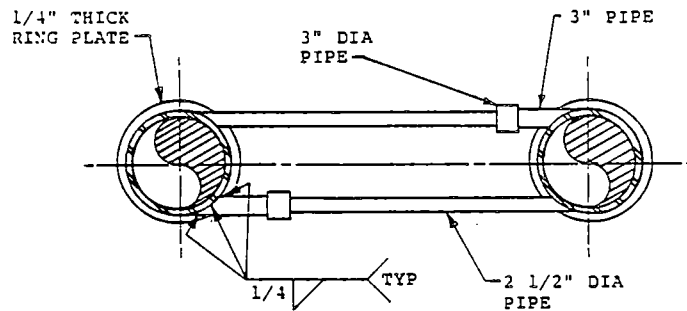
SECTION A-A

Figure 3-2.1-11

DOWNCOMER-TO-VENT HEADER INTERSECTION DETAILS -
DRESDEN UNIT 2



ELEVATION VIEW



SECTION A-A

Figure 3-2.1-12

DOWNCOMER-TO-VENT HEADER INTERSECTION DETAILS -
DRESDEN UNIT 3

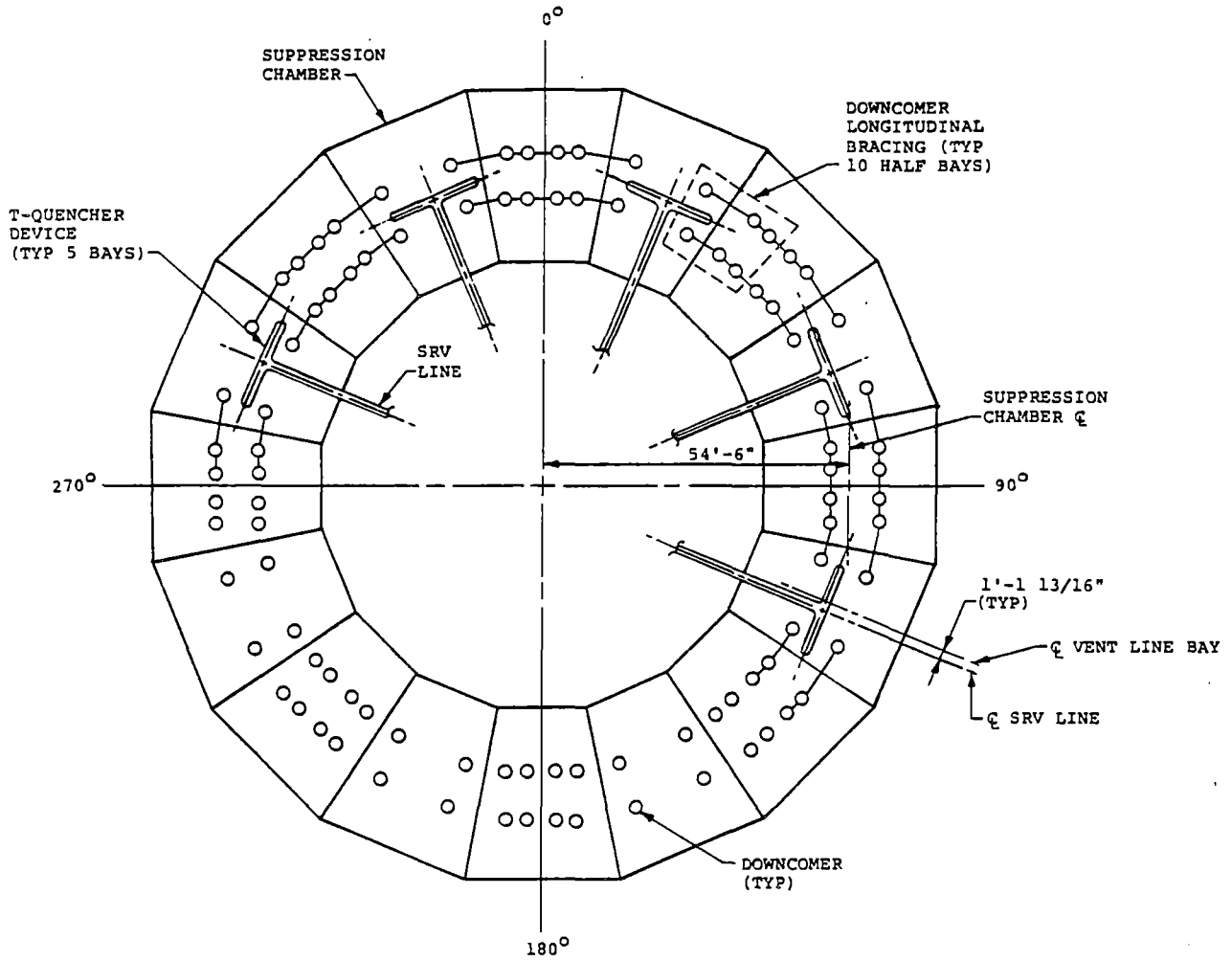


Figure 3-2.1-13

DOWNCOMER LONGITUDINAL BRACING SYSTEM CONFIGURATION -
DRESDEN UNIT 2

COM-02-041-3
Revision 0

3-2.23

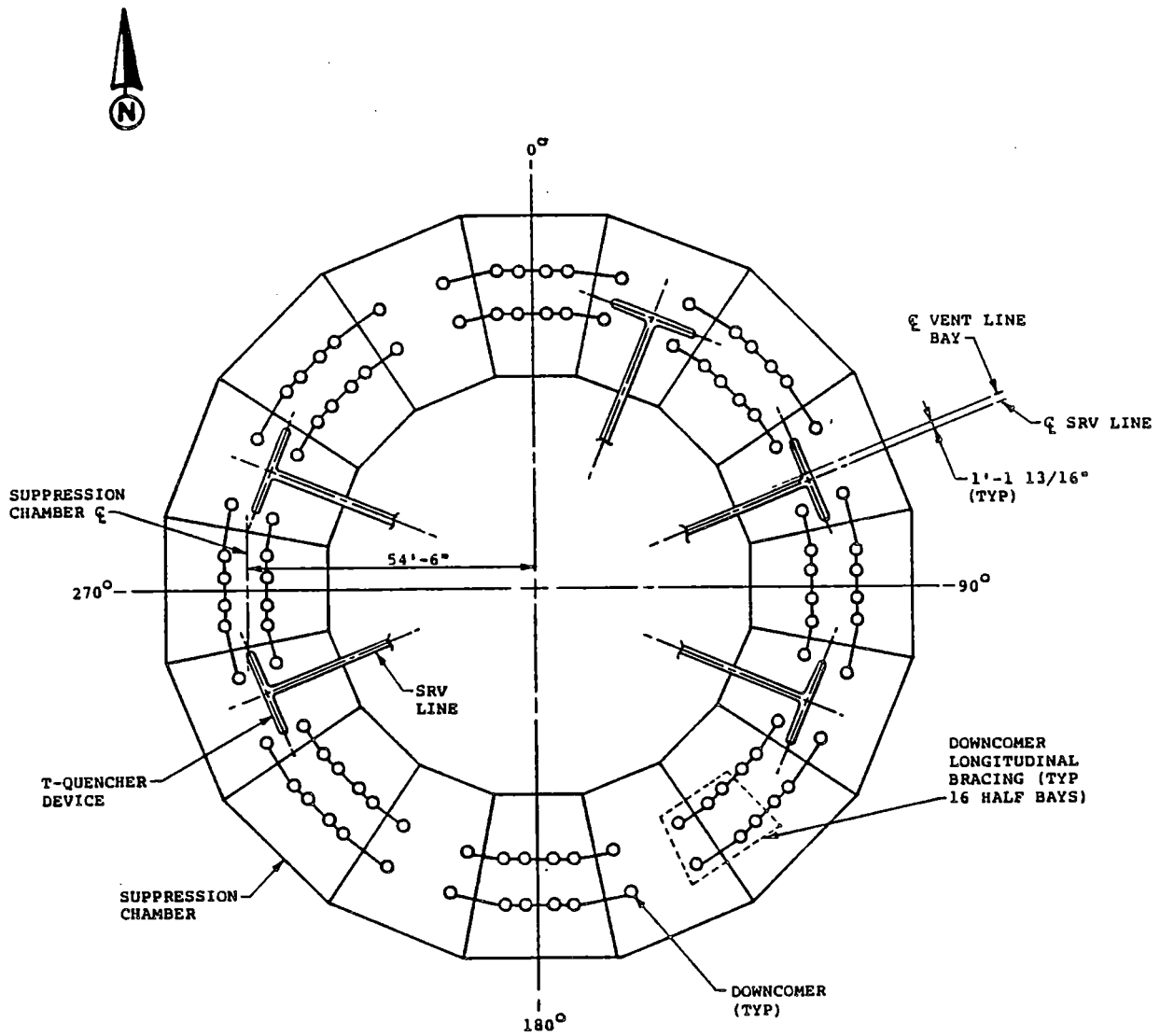
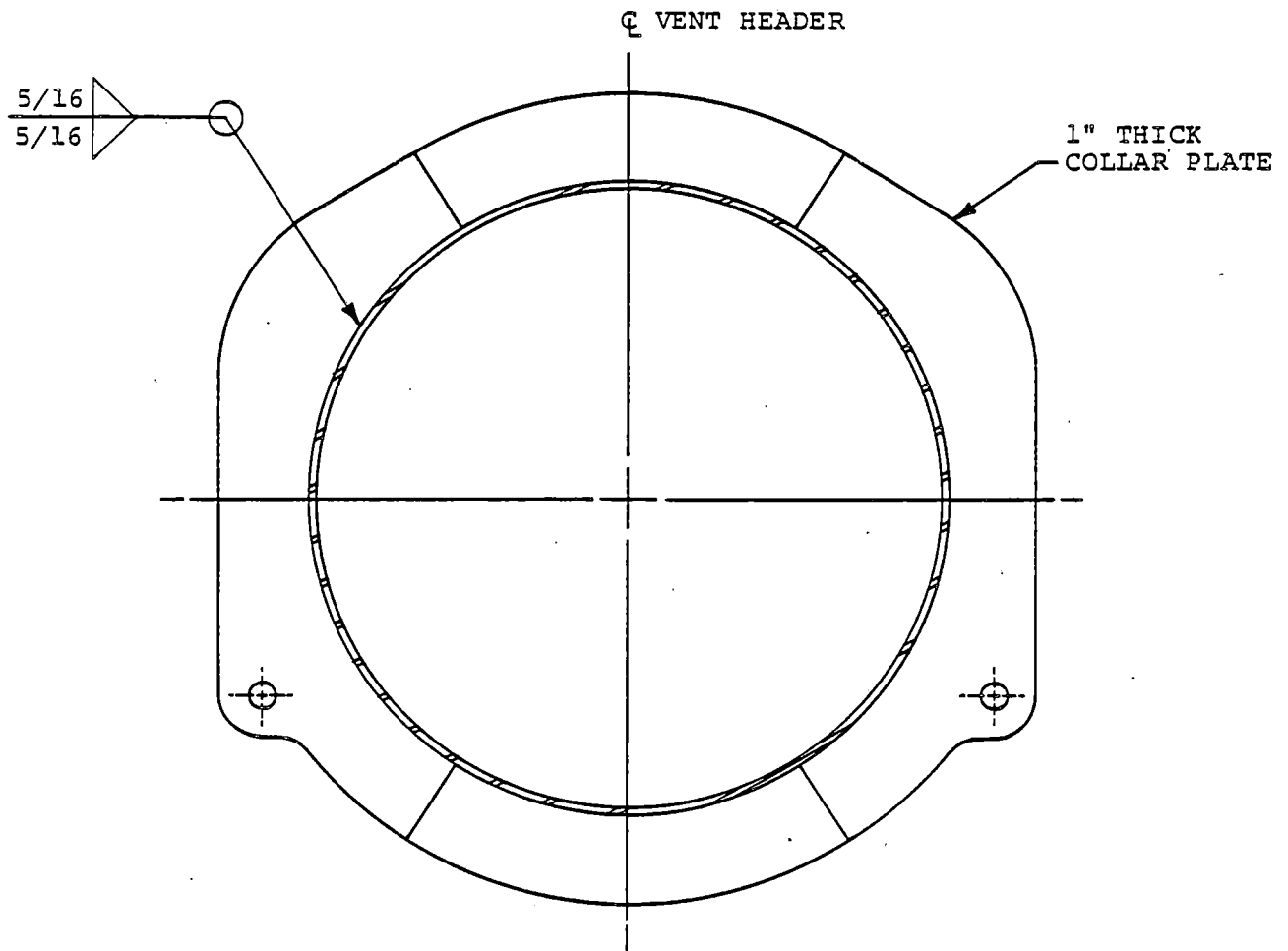


Figure 3-2.1-14

DOWNCOMER LONGITUDINAL BRACING SYSTEM CONFIGURATION -
DRESDEN UNIT 3

COM-02-041-3
 Revision 0

3-2.24



SECTION THROUGH VENT HEADER
SUPPORT COLLAR

Figure 3-2.1-15

VENT HEADER SUPPORT COLLAR PLATE DETAILS

COM-02-041-3
Revision 0

3-2.25

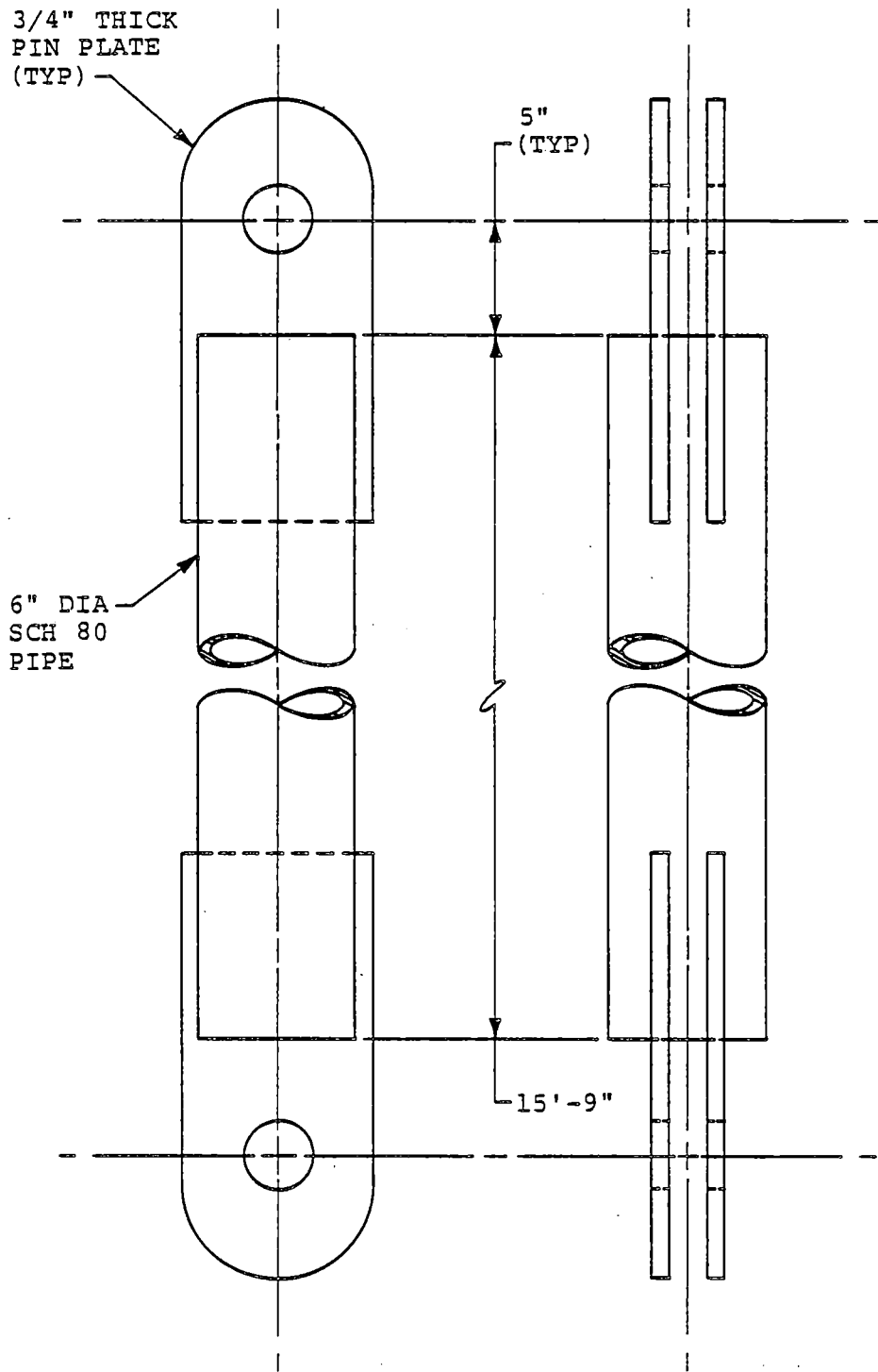


Figure 3-2.1-16

VENT SYSTEM SUPPORT COLUMN DETAILS

COM-02-041-3
Revision 0

3-2.26

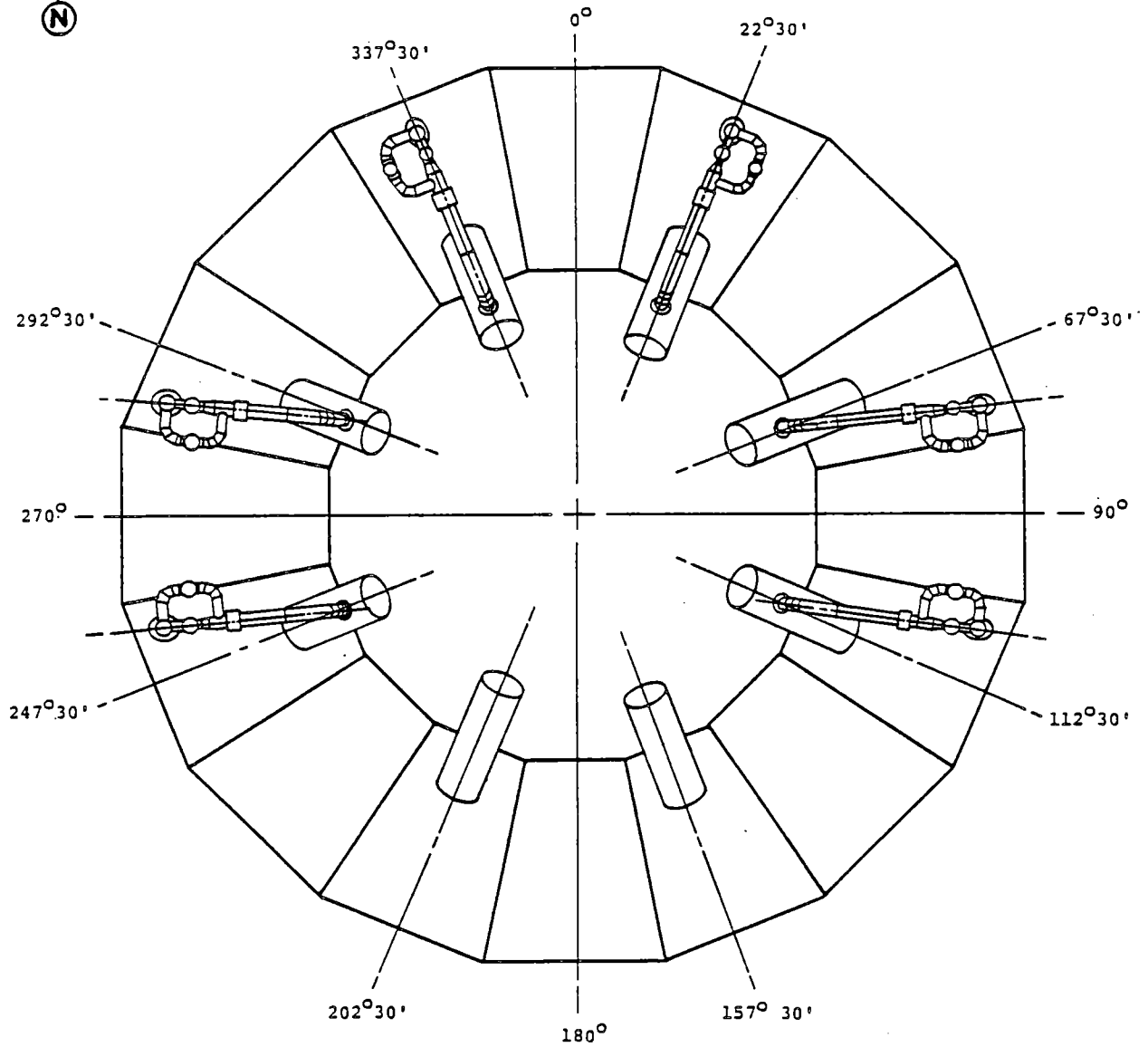
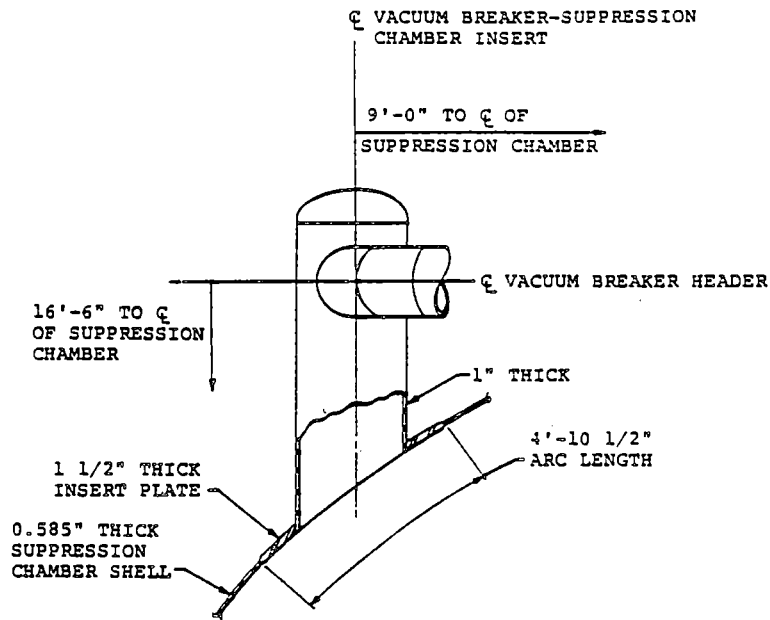


Figure 3-2.1-17

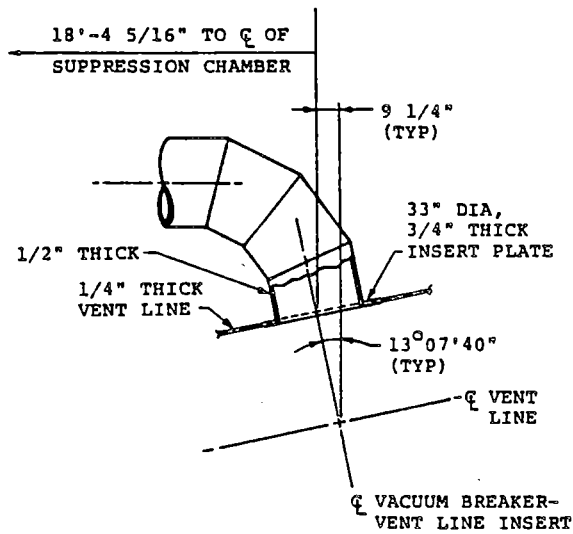
VACUUM BREAKER LOCATIONS

COM-02-041-3
Revision 0

3-2.27



SUPPRESSION CHAMBER PENETRATION



VENT LINE PENETRATION

Figure 3-2.1-18

VACUUM BREAKER HEADER PENETRATION DETAILS

3-2.2 Loads and Load Combinations

The loads for which the Dresden Units 2 and 3 vent systems are evaluated are defined in NUREG-0661 on a generic basis for all Mark I plants. Section 1-4.0 discusses the methodology used to develop plant unique vent system loads for each load defined in NUREG-0661. The results of applying the methodology to develop specific values for each of the governing loads which act on the vent system are discussed and presented in Section 3-2.2.1.

Using the event combinations and event sequencing defined in NUREG-0661 and discussed in Sections 1-3.2 and 1-4.3, the controlling load combinations which affect the vent system are formulated. The controlling vent system load combinations are discussed and presented in Section 3-2.2.2.

3-2.2.1 Loads

The loads acting on the vent system are categorized as follows:

1. Dead Weight Loads
2. Seismic Loads
3. Pressure and Temperature Loads
4. Vent System Discharge Loads
5. Pool Swell Loads
6. Condensation Oscillation Loads
7. Chugging Loads
8. Safety Relief Valve Discharge Loads
9. Piping Reaction Loads
10. Containment Interaction Loads

Loads in Categories 1 through 3 were considered in the original containment design as documented in the plant's containment data specifications (References 8 and 9). Additional Category 3 pressure and temperature loads result from postulated LOCA and SRV discharge events. Loads in Categories 4 through 7 result from postulated LOCA events; loads in Category 8 result from SRV discharge events; loads in Category 9 are reactions which result from loads acting on SRV piping systems; loads in Category 10 are motions which result from loads acting on other containment-related structures.

Not all of the loads defined in NUREG-0661 are evaluated in detail since some are enveloped by others or have a negligible effect on the vent system. Only those loads which maximize the vent system response and lead to controlling stresses are fully evaluated and discussed. These loads are referred to as governing loads in subsequent discussions.

Table 3-2.2-1 shows the specific vent system components affected by each of the loadings defined in NUREG-0661. The table also lists the section in Volume 1 in which the methodology for developing values for each loading is discussed. The magnitudes and characteristics of each governing vent system load in each load category are identified and presented in the following paragraphs.

1. Dead Weight Loads

- a. Dead Weight of Steel: The weight of steel used to construct the modified vent system and its supports is considered. The nominal component dimensions and a density of steel of 490 lb/ft^3 are used in this calculation.

2. Seismic Loads

a. OBE Loads: The vent system is subjected to horizontal and vertical accelerations during an operating basis earthquake (OBE). This loading is taken from the original design basis for the containment documented in the plant's design specification. The OBE loads have a maximum horizontal acceleration of 0.25g and a maximum vertical acceleration of 0.067g.

b. SSE Loads: The vent system is subjected to horizontal and vertical accelerations during a safe shutdown earthquake (SSE). This loading is taken from the original design basis for the containment documented in the plant's SAR, termed a DBE (Reference 4). The SSE loads have a maximum horizontal acceleration of 0.50g and a maximum vertical acceleration of 0.134g.

3. Pressure and Temperature Loads

a. Normal Operating Internal Pressure Loads: The vent system is subjected to internal pressure loads during normal operating conditions. This loading is taken from the

original design basis for the containment documented in the plants' containment data specifications (References 8 and 9). The range of normal operating internal pressures specified is -0.2 to 1.0 psi.

- b. LOCA Internal Pressure Loads: The vent system is subjected to internal pressure loads during a SBA, an IBA, and a DBA event. The procedure used to develop LOCA internal pressures for the containment is discussed in Section 1-4.1.1. Figures 3-2.2-1 through 3-2.2-3 present the resulting vent system internal pressure transients and pressure magnitudes at key times during the SBA, IBA, and DBA events.

The vent system internal pressures for each event are conservatively assumed equal to the corresponding drywell internal pressures; reductions due to losses are negligible. The net internal pressures acting on the vent system components inside the suppression chamber are extracted as the difference in pressures between the vent system and suppression chamber.

The pressures specified are assumed to act uniformly over the vent line, vent header, and downcomer shell surfaces. The external or secondary containment pressure for the vent system components outside the suppression chamber for all events is assumed to be zero. The effects of internal pressure on the vent system for the DBA event are included in the pressurization and thrust loads discussed in Load Case 4a.

- c. Normal Operating Temperature Loads: The vent system is subjected to the thermal expansion loads associated with normal operating conditions. This loading is taken from the original design basis for the containment documented in the plant's containment data specifications (References 8 and 9). The range of normal operating temperatures for the vent system with a concurrent SRV discharge event is 70° to 131°F (Table 3-2.2-2).

Additional normal operating temperatures for the vent system inside the suppression chamber are taken from the suppression pool

temperature response analysis (Reference 10). Table 3-2.2-2 provides a summary of the resulting vent system temperatures.

- d. LOCA Temperature Loads: The vent system is subjected to thermal expansion loads associated with the SBA, IBA, and DBA events. The procedure used to develop LOCA containment temperatures is discussed in Section 1-4.1.1. Figures 3-2.2-4 through 3-2.2-6 present the resulting vent system temperature transients and temperature magnitudes at key times during the SBA, IBA, and DBA events.

Additional vent system SBA event temperatures are taken from the suppression pool temperature response analysis. Table 3-2.2-2 summarizes the resulting vent system temperatures. The greater of the temperatures specified in Figure 3-2.2-4 and Table 3-2.2-2 is used in evaluating the effects of SBA event temperatures.

The temperatures of the major vent system components, such as the vent line, vent header, spherical junction, and downcomers,

are conservatively assumed equal to the corresponding drywell temperatures for the IBA and DBA events. For the SBA event, the temperature of the major vent system components is assumed equal to the maximum saturation temperature of the drywell, which is 273°F.

The temperatures of the external vent system components, such as the support columns, vent header support collars, downcomer lateral bracings, downcomer longitudinal bracings, vent header deflectors, and downcomer rings and downcomer stiffener plates, are assumed equal to the corresponding suppression chamber temperatures for each event.

The temperatures specified are assumed to be representative of the major component and external component metal temperatures throughout the vent system. The ambient or initial temperature of the vent system for all events is assumed equal to the arithmetic mean of the minimum and maximum vent system operating temperatures.

4. Vent System Discharge Loads

- a. Pressurization and Thrust Loads: The vent system is subjected to dynamic pressurization and thrust loads during a DBA event. The procedure used to develop vent system reaction loads due to pressure imbalances and to changes in linear momentum is discussed in Section 1-4.1.2. Table 3-2.2-3 shows the resulting maximum forces for each of the major component unreacted areas at key times during the DBA event.

The vent system discharge loads shown include the effects of the zero drywell/wetwell and the operating drywell/wetwell pressure differential. The vent system discharge loads specified for the DBA event include the effects of DBA internal pressure loads discussed in Load Case 3a. The vent system discharge loads which occur during the SBA or IBA events are negligible.

5. Pool Swell-Related Loads

- a. Vent System Impact and Drag Loads: During the initial phase of a DBA event, transient impact and drag pressures are postulated to

act on major vent system components above the suppression pool. The major components affected are the vent line inside the suppression chamber below the maximum bulk pool height, the spherical junction, the unprotected vent header, and the inclined portion of the downcomers. The major part of the vent header is shielded by the vent header deflectors and receives a relatively small amount of the pool swell impact and drag loads. The loads are developed based on the operating drywell/wetwell pressure differential condition except those applied to the vent header deflectors. These loads are defined in the plant's PULD for a zero drywell/wetwell pressure differential condition. Multiplication factors are developed to adjust operating ΔP condition loads to the zero drywell/wetwell pressure differential condition.

The procedure used to develop the transient forces and the spatial distribution of pool swell impact loads on these components is discussed in Section 1-4.1.4. Table 3-2.2-4 and Figures 3-2.2-7 and 3-2.2-8 summarize the

resulting magnitudes and distribution of pool swell impact loads on the vent line, the unprotected portion of the vent header, the spherical junction, downcomers, and the vent header deflector. The results shown are based on plant unique Quarter-Scale Test Facility (QSTF) test data contained in the PULD (Reference 3) and include the effects of the main vent orifice tests. Pool swell loads are considered negligible during the SBA and IBA events.

- b. Pool Swell Drag Loads on Other Structures: During the initial phase of a DBA event, transient drag pressures are postulated to act on submerged components of the vent system. The components affected are the downcomer longitudinal bracing members, and the SRV piping and supports.

The procedure used to develop the transient forces and the spatial distribution of pool swell drag loads on these components is discussed in Section 1-4.1.4. Table 3-2.2-5 and Figure 3-2.2-9 summarize the resulting

magnitudes and distribution of pool swell drag pressures on the downcomer longitudinal bracing. The pool swell drag loads on the SRV piping and supports located beneath the level of the vent line are presented in Volume 5 of this report. The results shown are based on plant unique QSTF test data contained in the PULD, which are used to determine the impact velocities and arrival times. Pool swell loads are considered negligible during the SBA and IBA events.

- c. Froth Impingement and Fallback Loads: During the initial phase of a DBA event, transient impingement pressures are postulated to act on vent system components located in specified regions above the rising suppression pool. The impacted components located in Region I include the vent line and the vent header. The impacted components located in Region II include the spherical junction and the vent line.

The procedure used to develop the transient forces and spatial distribution of froth impingement and fallback loads on these components is discussed in Section 1-4.1.4. Froth impingement and fallback loads do not occur during the SBA and IBA events.

- d. Pool Fallback Loads: During the later portion of the pool swell event, transient drag pressures are postulated to act on selected vent system components located between the maximum bulk pool height and the downcomer exit. The components affected are the vacuum breaker, the downcomer rings, the downcomer lateral bracings, the downcomer longitudinal bracing, and the SRV piping and supports located beneath the level of the vent line. The procedure used to develop transient drag pressures and spatial distribution of pool fallback loads on these components is discussed in Section 1-4.1.4.

Table 3-2.2-5 summarizes the resulting magnitudes and distribution of pool fallback loads on the downcomer rings, the downcomer lateral bracings, and the downcomer longitudinal

bracing members. The pool fallback loads on the SRV piping and supports located beneath the level of the vent line are presented in Volume 5 of this report. The results shown include the effects of maximum pool displacements measured in plant unique OSTF tests. Pool fallback loads do not occur during the SBA and IBA events.

- e. LOCA Water Jet Loads: Water jet loads are postulated to act on the submerged vent system components during the water clearing phase of a DBA event. The components affected are the vent system support columns. The procedure used to develop the transient forces and spatial distribution of LOCA water clearing loads on these components is discussed in Section 1-4.1.5. Table 3-2.2-6 shows the resulting magnitudes and distribution of LOCA water jet loads acting on the support columns.

- f. LOCA Bubble-Induced Loads: Transient drag pressures are postulated to act on the submerged vent system components during the air clearing phase of a DBA event. The

components affected are the downcomers, the downcomer lateral bracings, the downcomer rings, the downcomer longitudinal bracing members, the support columns, and the submerged portion of the SRV piping. The procedure used to develop the transient forces and spatial distribution of DBA air bubble-induced drag loads on these components is discussed in Section 1-4.1.6.

Tables 3-2.2-6, 3-2.2-7, and 3-2.2-8 show the resulting magnitudes and distribution of drag pressures acting on the vent system support columns, the downcomers, the downcomer lateral bracings, the downcomer rings, and the downcomer longitudinal bracing members for the controlling DBA air clearing load case. The controlling DBA air clearing loads on the submerged portion of the SRV piping are presented in Volume 5 of this report. The results shown include the effects of velocity drag, acceleration drag, and interference effects. The LOCA air bubble-induced drag loads which occur during a SBA or an IBA event are negligible.

6. Condensation Oscillation Loads

- a. IBA CO Downcomer Loads: Harmonic internal pressure loads are postulated to act on the downcomers during the CO phase of an IBA event. The procedure used to develop the harmonic pressures and spatial distribution of IBA CO downcomer loads is discussed in Section 1-4.1.7. The loading consists of a uniform internal pressure component acting on all downcomers and a differential internal pressure component acting on one downcomer in a downcomer pair. Table 3-2.2-9 shows the resulting pressure amplitudes and associated frequency range for each of the three harmonics in the IBA CO downcomer loading. Figure 3-2.2-10 shows the corresponding distribution of differential downcomer internal pressure loadings.

The IBA CO downcomer load harmonic in the range of the dominant downcomer frequency for the uniform and the differential pressure components is applied at the dominant downcomer frequency. The remaining two downcomer load harmonics are applied at

frequencies which are multiples of the dominant frequency. The results of the three harmonics for the uniform and differential IBA CO downcomer load components are combined by absolute sum.

b. DBA CO Downcomer Loads: Harmonic internal pressure loads are postulated to act on the downcomers during the CO phase of a DBA event. The procedure used to develop the harmonic pressures and spatial distribution of DBA CO downcomer loads is the same as that discussed for IBA CO downcomer loads in Load Case 6a. Table 3-2.2-10 shows the resulting pressure amplitudes and associated frequency range for each of the three harmonics in the DBA CO downcomer loading. Figure 3-2.2-10 shows the corresponding distribution of differential downcomer internal pressure loadings.

c. IBA CO Vent System Pressure Loads: Harmonic internal pressure loads are postulated to act on the vent system during the CO phase of an IBA event. The components affected are the vent line, the spherical junction, the vent

header, and the downcomers. The procedure used to develop the harmonic pressures and the spatial distribution of IBA CO vent system pressures is discussed in Section 1-4.1.7. Table 3-2.2-11 shows the resulting pressure amplitudes and associated frequency range for the vent line and vent header. The loading is applied at the frequency within a specified range which maximizes the vent system response.

The effects of IBA CO vent system pressures on the downcomers are included in the IBA CO downcomer loads discussed in Load Case 6a. An additional static internal pressure of 1.7 psi is applied uniformly to the vent line, vent header, and downcomers to account for the effects of downcomer submergence. The IBA CO vent system pressures act in conjunction with the IBA containment internal pressures discussed in Load Case 3a.

- d. DBA CO Vent System Pressure Loads: Harmonic internal pressure loads are postulated to act on the vent system during the CO phase of a DBA event. The components affected are the

vent line, the spherical junction, the vent header, and downcomers. The procedure used to develop the harmonic pressures and the spatial distribution of the DBA CO vent system pressures is the same as that discussed for the IBA in Load Case 6c. Table 3-2.2-11 shows the resulting pressure amplitudes and associated frequency range for the vent line and vent header. The effects of DBA CO vent system pressures on the downcomers are included in the DBA CO downcomer loads discussed in Load Case 6b. The DBA CO vent system pressures act in addition to the DBA vent system pressurization and thrust loads discussed in Load Case 4a.

- e. IBA CO Submerged Structure Loads: Harmonic pressure loads are postulated to act on the submerged vent system components during the CO phase of an IBA event. In accordance with NUREG-0661, the loads on submerged structures specified for pre-chug are used in lieu of IBA CO loads on submerged structures. Pre-chug submerged structure loads are discussed in Load Case 7c.

f. DBA CO Submerged Structure Loads: Harmonic drag pressures are postulated to act on the submerged vent system components during the CO phase of a DBA event. The components affected are the downcomer lateral bracings, the downcomer rings, the downcomer longitudinal bracing members, the support columns, and the submerged portions of the SRV piping. The procedure used to develop the harmonic forces and spatial distribution of DBA CO drag loads on these components is discussed in Section 1-4.1.7.

Loads are developed for the case with the average source strength at all downcomers and the case with twice the average source strength at the nearest downcomer. The results of these two cases are evaluated to determine the controlling loads.

Tables 3-2.2-12 and 3-2.2-13 show the resulting magnitudes and distribution of drag pressures acting on the support columns, the downcomer lateral bracings, the downcomer rings, and the downcomer longitudinal bracing

members for the controlling DBA CO drag load case. The controlling DBA CO drag loads on the submerged portion of the SRV piping are presented in Volume 5 of this report. The effects of DBA CO submerged structure loads on the downcomers are included in the loads discussed in Load Case 6b.

The results in Tables 3-2.2-12 and 3-2.2-13 include the effects of velocity drag, acceleration drag, torus shell FSI acceleration drag, interference effects, and acceleration drag volumes. Figure 3-2.2-11 shows a typical pool acceleration profile from which the FSI accelerations are derived. The results of each harmonic in the loading are combined using the methodology discussed in Section 1-4.1.7.

7. Chugging Loads

- a. Chugging Downcomer Lateral Loads: Lateral loads are postulated to act on the downcomers during the chugging phase of a SBA, an IBA, and a DBA event. The procedure used to develop chugging downcomer lateral loads is discussed in Section 1-4.1.8. The maximum

lateral load acting on any one downcomer in any direction is obtained using the maximum downcomer lateral load and chugging pulse duration measured at the Full-Scale Test Facility (FSTF), the frequency of the tied downcomers for the FSTF, and the plant unique downcomer frequency calculated for both longitudinally braced and unbraced conditions. Table 3-2.2-14 summarizes this information. The resulting ratios of Dresden Units 2 and 3 to the FSTF dynamic load factors (DLF) are used in subsequent calculations to determine the magnitude of multiple downcomer loads and to determine the load magnitude used for evaluating fatigue. Section 3-2.4.1 discusses the methodology used to determine the plant unique downcomer frequency.

The magnitude of chugging lateral loads acting on multiple downcomers simultaneously is determined using the methodology described in Section 1-4.1.8. The methodology uses the value of 10^{-4} as the probability of exceeding a given downcomer load magnitude once per LOCA. The chugging load magnitudes (Table

3-2.2-15) are determined using the above value of non-exceedance probability (NEP) and the ratio of the DLF's from the maximum downcomer load calculation. The distributions of chugging downcomer lateral loads considered are those cases which maximize overall effects in the vent system. Table 3-2.2-16 summarizes these distributions. The maximum downcomer lateral load magnitude used for evaluating the local effect on the downcomer-vent header intersection is obtained using both the maximum downcomer lateral load measured at the FSTF and the ratio of DLF's from the maximum downcomer load calculation.

The maximum downcomer lateral load magnitude used for evaluating fatigue is obtained using both the maximum downcomer lateral load measured at the FSTF with a 95% NEP and the ratio of DLF's from maximum downcomer load calculations. The stress reversal histograms provided for FSTF are converted to plant unique stress reversal histograms using the postulated plant unique chugging duration (Table 3-2.2-17).

b. Chugging Vent System Pressures: Transient and harmonic internal pressures are postulated to act on the vent system during the chugging phase of a SBA, an IBA, and a DBA event. The components affected are the vent line, the spherical junction, the vent header, and the downcomers. The procedure used to develop chugging vent system pressures is discussed in Section 1-4.1.8. The load consists of a gross vent system pressure oscillation component, an acoustic vent system pressure oscillation component, and an acoustic downcomer pressure oscillation component. Table 3-2.2-18 shows the resulting pressure magnitudes and characteristics of the chugging vent system pressure loading. The three load components are evaluated individually and are not combined with each other.

The overall effects of chugging vent system pressures on the downcomers are included in the loads discussed in Load Case 7a. The downcomer pressures (Table 3-2.2-18) are used to evaluate downcomer hoop stresses. The chugging vent system pressures act in

addition to the SBA and IBA containment internal pressures discussed in Load Case 3a and the DBA pressurization and thrust loads discussed in Load Case 4a.

- c. Pre-Chug Submerged Structure Loads: During the chugging phase of a SBA, an IBA, or a DBA event, harmonic drag pressures associated with the pre-chug portion of a chugging cycle are postulated to act on the submerged vent system components. The components affected are the downcomer lateral bracings, the downcomer rings, the downcomer longitudinal bracing members, the support columns, and the submerged portion of the SRV piping. The procedure used to develop the harmonic forces and spatial distribution of pre-chug drag loads on these components is discussed in Section 1-4.1.8.

Loads are developed for the case with the average source strength at all downcomers and the case with twice the average source strength at the nearest downcomer. The results of these two cases are evaluated to determine the controlling loads. Tables

3-2.2-19 and 3-2.2-20 show the resulting magnitudes and distribution of drag pressures acting on the support columns, the downcomer lateral bracings, the downcomer rings, and the downcomer longitudinal bracing members for the controlling pre-chug drag load case. The controlling pre-chug drag loads on the submerged portion of the SRV piping are presented in Volume 5 of this report. The effects of pre-chug submerged structure loads on the downcomers are included in the loads discussed in Load Case 7a.

The results shown include the effects of velocity drag, acceleration drag, torus shell fluid-structure interaction (FSI) acceleration drag, interference effects, and acceleration drag volumes. Figure 3-2.2-11 shows a typical pool acceleration profile from which the FSI accelerations are derived.

- d. Post-Chug Submerged Structure Loads: During the chugging phase of a SBA, an IBA, or a DBA event, harmonic drag pressures associated with the post-chug portion of a chug cycle are postulated to act on the submerged vent

system components. The components affected are the downcomer lateral bracings, the downcomer rings, the downcomer longitudinal bracing members, the support columns, and the submerged portion of the SRV piping. Section 1-4.1.8 discusses the procedure used to develop the harmonic forces and spatial distribution of post-chug drag loads on these components.

Loads are developed for the cases with the maximum source strength at the nearest two downcomers acting both in phase and out of phase. The results of these cases are evaluated to determine the controlling loads. Tables 3-2.2-21 and 3-2.2-22 shows the resulting magnitudes and distribution of drag pressures acting on the support columns, the downcomer lateral bracings, the downcomer rings, and the downcomer longitudinal bracing members for the controlling post-chug drag load case. The controlling post-chug drag loads on the submerged portion of the SRV piping are presented in Volume 5 of this report. The effects of post-chug submerged structure loads acting on the downcomers are

included in the chugging downcomer lateral loads discussed in Load Case 7a.

The results shown include the effects of velocity drag, acceleration drag, torus shell FSI acceleration drag, interference effects, and acceleration drag volumes. Figure 3-2.2-11 shows a typical pool acceleration profile from which the FSI accelerations are derived. The results of each harmonic are combined using the methodology described in Section 1-4.1.8.

8. Safety Relief Valve Discharge Loads

- a. T-quencher Water Jet Loads: Water jet loads from the quencher arm holes are postulated to act on the submerged vent system components during the water clearing phase of a SRV discharge event. The quencher water jet does not reach the downcomer and the downcomer bracings. The components affected are the vent system support columns. The procedure used to develop the transient forces and spatial distribution of the SRV discharge water jet loads on these components is discussed in Section 1-4.2.4. Table 3-2.2-23

provides the resulting magnitudes and distribution of SRV water jet loads acting on the support columns.

- b. SRV Bubble-Induced Drag Loads: Transient drag pressures are postulated to act on the submerged vent system components during the air clearing phase of a SRV discharge event. The components affected are the downcomers, the downcomer lateral bracings, the downcomer rings, the downcomer longitudinal bracing members, support columns, and the submerged portion of the SRV piping. The procedure used to develop the transient forces and spatial distribution of the SRV discharge air bubble-induced drag loads on these components is discussed in Section 1-4.2.4.

Loads are developed for the case with four bubbles from quenchers located in the bay containing the structure or in either of the adjacent bays. A calibration factor is applied to the resulting downcomer loads developed using the methodology discussed in Section 1-4.2.2. Tables 3-2.2-23, 3-2.2-24,

and 3-2.2-25 show the magnitudes and distribution of drag pressures acting on the support columns, the downcomers, the downcomer lateral bracings, the downcomer rings, and the downcomer longitudinal bracings for the controlling SRV discharge drag load case.

These results include the effects of velocity drag, acceleration drag, interference effects, and acceleration drag volumes.

9. Piping Reaction Loads

- a. SRV Piping Reaction Loads: Reaction loads impact the vent system because of loads acting on the drywell and wetwell SRV piping systems. These reaction loads occur at the vent line-SRV piping penetration and at the safety relief valve discharge line (SRVDL) supports inside the vent line. The SRV piping reaction loads consist of those caused by motions of the suppression chamber and loads acting on the drywell and wetwell portions of the SRV piping systems. Loads acting on the SRV piping systems are pressurization loads, thrust loads, and other operating or design basis loads.

The effects of the SRV piping reaction loads on the vent system are included in the vent system analysis. These reaction loads were taken from the analysis of the SRV piping system described in Volume 5 of this report.

10. Containment Interaction Loads

- a. Containment Structure Motions: Loads acting on the drywell, suppression chamber, and vent system cause interaction effects between these structures. The interaction effects result in vent system motions applied at the attachment points of the vent system to the drywell and the suppression chamber. The effects of these motions on the vent system are considered in the vent system analysis.

The values of the loads presented in the preceding paragraphs envelop those which could occur during the LOCA and SRV discharge events postulated. An evaluation for the effects of the above loads results in conservative estimates of the vent system responses and leads to bounding values of vent system stresses.

Table 3-2.2-1

VENT SYSTEM COMPONENT LOADING INFORMATION

VOLUME 3 LOAD DESIGNATION			PUAR SECTION REFERENCE	COMPONENT PART LOADED													REMARKS
CATEGORY LOADS	LOAD TYPE	CASE NUMBER		DRYWELL- PENETRA- TION	VENT LINE	VENT LINE BELLOWS	V/V/S SPHERICAL JUNCTION	VENT HEADER	VENT HEADER DEFLECTOR	DOWN- COMER	DOWNCOMER LATERAL BRACING	DOWNCOMER LONGITU- DINAL BRACING	SUPPORT COLUMNS				
DEAD WEIGHT	DEAD WEIGHT OF STEEL	1a	1-3.1	X	X	X	X	X	X	X	X	X	X	AS-MODIFIED GEOMETRY			
SEISMIC	OBE	2a	1-3.1	X	X	X	X	X	X	X	X	X	X	HORIZONTAL, VERTICAL			
	SSE	2b	1-3.1	X	X	X	X	X	X	X	X	X	X	HORIZONTAL, VERTICAL			
PRESSURE AND TEMPERATURE	NORMAL OPERATING INTERNAL PRESSURE	3a	1-3.1	X	X	X	X	X		X				0.0 TO 2.0 psi			
	LOCA INTERNAL PRESSURE	3b	1-4.1.1	X	X	X	X	X		X				SDA, IBA, & DBA PRESSURES			
	NORMAL OPERATING TEMPERATURE	3c	1-3.1	X	X	X	X	X	X	X	X	X	X	70° TO 131°F			
	LOCA TEMPERATURE	3d	1-4.1.1	X	X	X	X	X	X	X	X	X	X	SDA, IBA, & DBA TEMPERATURES			
VENT SYSTEM DISCHARGE	PRESSURIZATION AND THRUST	4a	1-4.1.2	X	X		X	X		X				FORCES ON UNREACTED AREAS			
POOL SHELL	VENT SYSTEM IMPACT AND DRAG	5a	1-4.1.4.1		X		X		X	X				HEADER SHIELDED BY DEFLECTORS			
	IMPACT AND DRAG LOADS ON OTHER STRUCTURES	5b	1-4.1.4.2				X					X		COMPONENTS BELOW MAXIMUM POOL HEIGHT			
	FROTH IMPINGEMENT & FALLBACK	5c	1-4.1.4.3				X							TWO REGIONS SPECIFIED			
	POOL FALLBACK	5d	1-4.1.4.4								X	X		MAJOR COMPONENTS NOT AFFECTED			
	LOCA WATER JET	N/A	1-4.1.5										X	EFFECTS NEGLIGIBLE			
	LOCA AIR BUBBLE-INDUCED DRAG	5f	1-4.1.6							X	X	X	X	PRIMARILY LOCAL EFFECTS			
CONDENSATION OSCILLATION	IBA CO, DOWNCOMER	6a	1-4.1.7.2							X				UNIFORM & DIFFERENTIAL COMPONENTS			
	DBA CO, DOWNCOMER	6b	1-4.1.7.2							X				UNIFORM & DIFFERENTIAL COMPONENTS			
	IBA CO, VENT SYSTEM PRESSURE	6c	1-4.1.7.2	X	X			X						DOWNCOMER PRESSURES INCLUDED IN 6a			
	DBA CO, VENT SYSTEM PRESSURE	6d	1-4.1.7.2	X	X			X						DOWNCOMER PRESSURES INCLUDED IN 6b			
	IBA CO, SUBMERGED STRUCTURE	6e	1-4.1.7.3							X	X	X		DOWNCOMER LOADS INCLUDED IN 6a			
	DBA CO, SUBMERGED STRUCTURE	6f	1-4.1.7.3							X	X	X		DOWNCOMER LOADS INCLUDED IN 6b			
CHUGGING	CHUGGING, DOWNCOMER LATERAL	7a	1-4.1.8.2							X				RSEL BASED ON FSTP			
	CHUGGING, VENT SYSTEM PRESSURES	7b	1-4.1.8.2	X	X			X		X				THREE LOADING ALTERNATES			
	PRE-CHUG, SUBMERGED STRUCTURE	7c	1-4.1.8.3							X	X	X		DOWNCOMER LOADS INCLUDED IN 7a			
	POST-CHUG, SUBMERGED STRUCTURE	7d	1-4.1.8.3							X	X	X		DOWNCOMER LOADS INCLUDED IN 7a			
SRV DISCHARGE	T-QUENCHER WATER JET	8a	1-4.2.4										X	EFFECTS NEGLIGIBLE			
	T-QUENCHER BUBBLE-INDUCED DRAG	8b	1-4.2.4							X	X	X	X	PRIMARILY LOCAL EFFECTS			
PIPING REACTION	SRV PIPING REACTION	9a	VOLUME 5		X			X						REACTIONS ON VENT LINE AND HEADER			
CONTAINMENT INTERACTION	CONTAINMENT STRUCTURE MOTIONS	10a	VOLUME 2	X		X							X	DRYWELL AND TORUS MOTIONS			

COM-02-041-3
Revision 0

3-2.60

Table 3-2.2-2

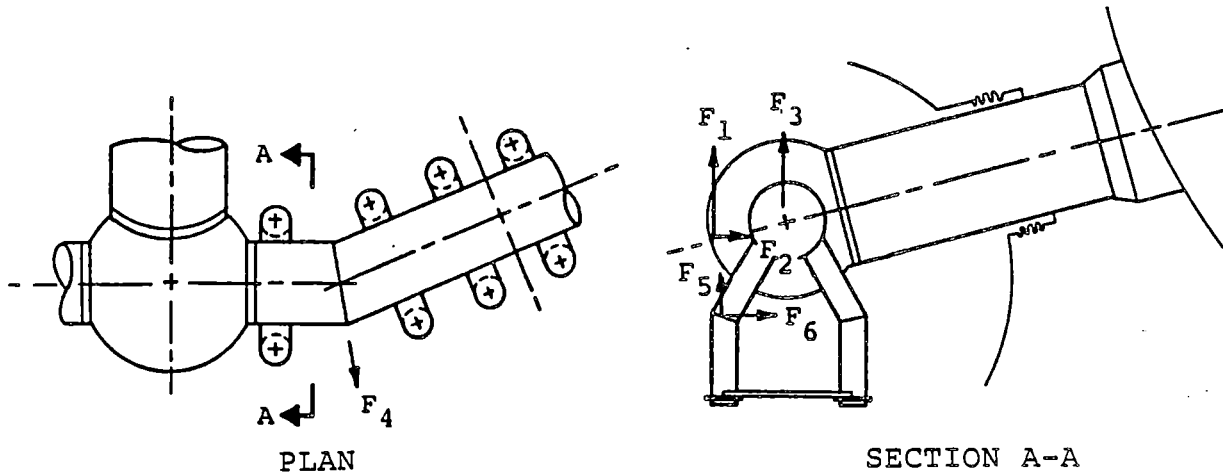
SUPPRESSION POOL TEMPERATURE RESPONSE
ANALYSIS RESULTS - MAXIMUM TEMPERATURES

CONDITION	CASE (1) NUMBER	NUMBER OF SRV'S ACTUATED	MAXIMUM BULK POOL TEMPERATURE (°F)
NORMAL OPERATING	1A	0	131
	1B	0	129
	2A	1	113
	2B	1	122
	2C	2	115
SBA EVENT	3A	5	154
	3B	5	147

(1) SEE SECTION 1-5.1 FOR A DESCRIPTION OF SRV DISCHARGE EVENTS.

Table 3-2.2-3

VENT SYSTEM PRESSURIZATION AND THRUST LOADS
FOR DBA EVENT



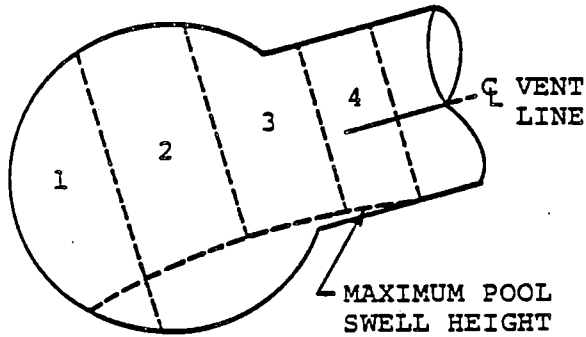
KEY DIAGRAM

TIME DURING DBA EVENT (sec)	MAXIMUM COMPONENT FORCE MAGNITUDE (kips)					
	F ₁	F ₂	F ₃	F ₄	F ₅	F ₆
POOL SWELL 0.0 TO 5.0	-171.10	-39.10	63.80	25.70	1.30	-4.70
CONDENSATION OSCILLATION 5.0 TO 35.0	-97.29	-22.23	33.39	14.61	0.61	-2.24
CHUGGING 35.0 TO 65.0	-18.53	-4.24	6.78	5.36	0.15	-0.56

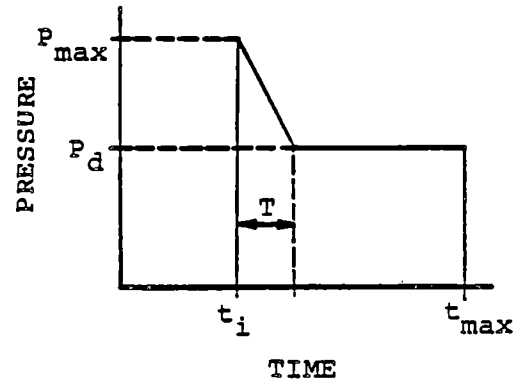
1. LOADS SHOWN INCLUDE THE EFFECTS OF THE DBA INTERNAL PRESSURES IN FIGURE 3-2.2-3.
2. LOADS SHOWN INCLUDE A DLF OF 1.1.

Table 3-2.2-4

POOL SWELL IMPACT LOADS FOR VENT LINE
AND SPHERICAL JUNCTION



KEY DIAGRAM



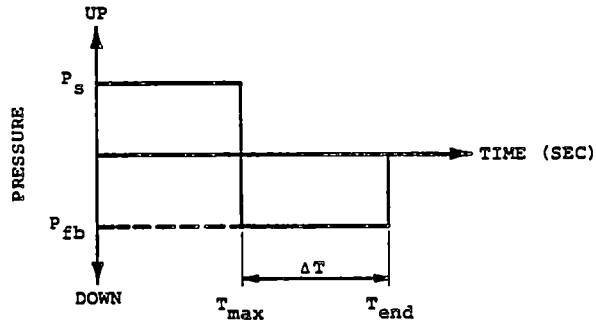
PRESSURE TRANSIENT

SEGMENT NUMBER	TIME (sec)			PRESSURE (psi)	
	IMPACT (t_i)	IMPACT DURATION (T)	MAXIMUM POOL HEIGHT (t_{max})	IMPACT (P_{max})	DRAG (P_d)
1	0.2198	0.1970	0.5210	27.81	5.11
2	0.2707	0.1461	0.5210	22.38	5.60
3	0.3581	0.1108	0.5210	14.23	5.92
4	0.5130	0.0400	0.5430	10.06	0.00

1. SEE FIGURE 3-2.1-8 FOR STRUCTURE GEOMETRY.
2. PRESSURES SHOWN ARE APPLIED TO VERTICAL PROJECTED AREAS IN A DIRECTION NORMAL TO VENT LINE AXIS.
3. LOADS ARE SYMMETRIC WITH RESPECT TO VERTICAL CENTERLINE OF VENT LINE.

Table 3-2.2-5

DOWNCOMER LONGITUDINAL BRACING AND LATERAL BRACING
POOL SWELL DRAG AND FALLBACK SUBMERGED STRUCTURE
LOAD DISTRIBUTION



LONGITUDINAL BRACING MEMBER	OPERATING ΔP				ZERO ΔP			
	TIME (sec)		MAXIMUM PRESSURE MAGNITUDE (psi)		TIME (sec)		MAXIMUM PRESSURE MAGNITUDE (psi)	
	T _{max}	T _{end}	P _s	P _{fb}	T _{max}	T _{end}	P _s	P _{fb}
①	0.521	1.341	7.4	5.4	0.577	1.387	5.4	5.3
②	0.521	1.341	9.3	5.8	0.577	1.387	6.8	5.7
③	0.521	1.341	11.0	5.8	0.577	1.387	8.0	5.7
④	0.521	1.341	9.3	4.5	0.577	1.387	6.8	4.3
⑤	0.521	1.341	6.2	3.5	0.577	1.387	4.5	3.5
⑥	0.521	1.341	6.2	3.5	0.577	1.387	4.5	3.5
LATERAL BRACING MEMBER ⑦	0.521	1.209	N/A	4.9	0.596	1.336	N/A	4.4
STIFFENER RINGS ⑧	0.521	1.232	N/A	4.5	0.596	1.336	N/A	4.2

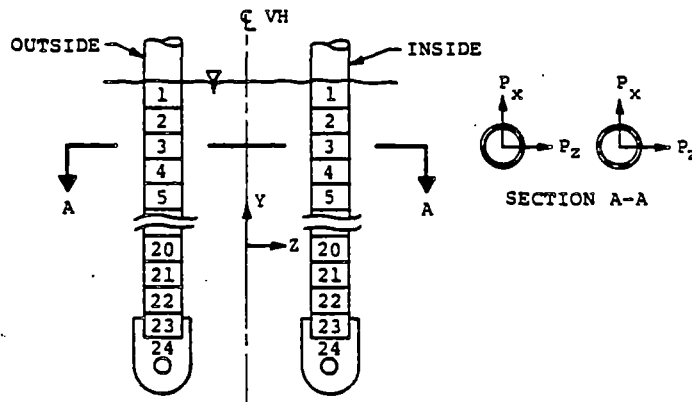
1. SEE FIGURE 3-2.2-9 FOR BRACING MEMBER DESIGNATION.
2. PRESSURES SHOWN ARE APPLIED TO VERTICAL PROJECTED AREAS IN THE DIRECTION NORMAL TO THE STRUCTURE.
3. PRESSURES SHOWN ARE SYMMETRICAL WITH RESPECT TO VERTICAL CENTERLINE OF VENT HEADER.
4. AVERAGE PRESSURE ON STIFFENER RING IS USED.
5. T_{end} BASED ON MAXIMUM ΔT VALUES.

COM-02-041-3
Revision 0

3-2.64

Table 3-2.2-6

SUPPORT COLUMN LOCA WATER JET AND BUBBLE-INDUCED
DRAG LOAD DISTRIBUTION



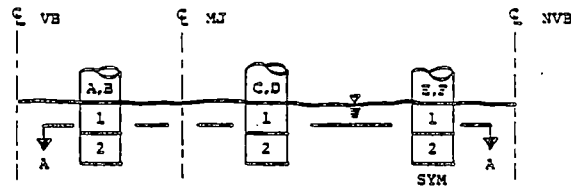
ELEVATION VIEW - MITERED JOINT

SEGMENT NUMBER	LOCAFOR (OPERATING ΔP) (1)				LOCA JET (OPERATING ΔP) (1)			
	AVERAGE PRESSURE (psi)				AVERAGE PRESSURE (psi)			
	INSIDE COLUMN		OUTSIDE COLUMN		INSIDE COLUMN		OUTSIDE COLUMN	
	P_x	P_z	P_x	P_z	P_x	P_z	P_x	P_z
1	0.02	-0.05	0.02	-0.03	0.00	0.00	0.00	0.00
2	0.05	-0.14	0.05	-0.08	0.00	0.00	0.00	0.00
3	0.08	-0.25	0.09	-0.12	0.00	0.00	0.00	0.00
4	0.12	-0.40	0.14	-0.17	0.00	0.00	0.00	0.00
5	0.17	-0.60	0.20	-0.21	0.00	0.00	0.00	0.00
6	0.24	-0.87	0.26	-0.24	0.00	0.00	0.00	0.00
7	0.34	-1.20	0.35	-0.27	0.00	0.00	0.00	0.00
8	0.47	-1.60	0.43	-0.28	0.00	0.00	0.00	0.00
9	0.62	-2.01	0.51	-0.30	1.45	2.38	0.59	0.12
10	0.75	-2.30	0.56	-0.32	1.82	2.93	0.70	0.12
11	0.78	-2.37	0.58	-0.34	1.82	2.81	0.64	0.12
12	0.73	-2.17	0.56	-0.36	0.85	1.47	0.40	0.12
13	0.61	-1.78	0.52	-0.38	0.79	1.22	0.27	0.12
14	0.49	-1.37	0.45	-0.40	0.92	1.45	0.31	0.12
15	0.40	-0.99	0.39	-0.42	0.99	1.67	0.36	0.12
16	0.34	-0.68	0.34	-0.43	0.80	1.58	0.40	0.12
17	0.30	-0.45	0.29	-0.43	0.57	1.31	0.38	0.11
18	0.28	-0.28	0.26	-0.43	0.38	1.01	0.32	0.11
19	0.27	-0.17	0.24	-0.43	0.26	0.74	0.26	0.10
20	0.27	-0.08	0.22	-0.42	0.18	0.54	0.21	0.10
21	0.27	-0.03	0.21	-0.40	0.14	0.38	0.17	0.09
22	0.26	0.00	0.21	-0.39	0.37	0.86	0.44	0.27
23	0.84	0.05	0.64	-1.20	0.33	0.60	0.36	0.27
24	0.83	0.08	0.62	-1.15	0.30	0.40	0.31	0.29

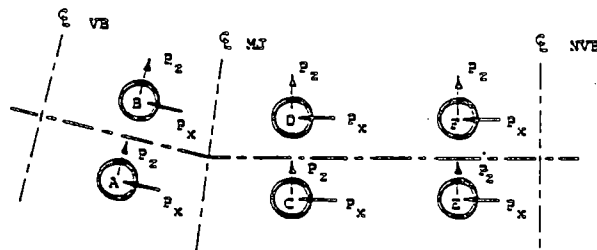
(1) LOADS SHOWN INCLUDE A DLF OF 2.0.

Table 3-2.2-7

DOWNCOMER LOCA BUBBLE-INDUCED DRAG
LOAD DISTRIBUTION



ELEVATION VIEW-DOWNCOMERS



SECTION A-A

ITEM	SEGMENT NUMBER	PRESSURE MAGNITUDE (psi) ⁽¹⁾ (OPERATING ΔP)		
		P _x	P _z	
DOWNCOMER	A	1	0.27	-0.44
		2	0.82	-1.34
	B	1	0.69	0.24
		2	2.21	0.72
	C	1	0.48	-0.49
		2	1.46	-1.62
	D	1	0.31	0.07
		2	0.90	0.23
	E	1	0.04	-0.48
		2	0.09	-1.44
	F	1	0.02	0.44
		2	0.05	1.34

(1) LOADS SHOWN INCLUDE A DLF OF 2.0.

Table 3-2.2-8

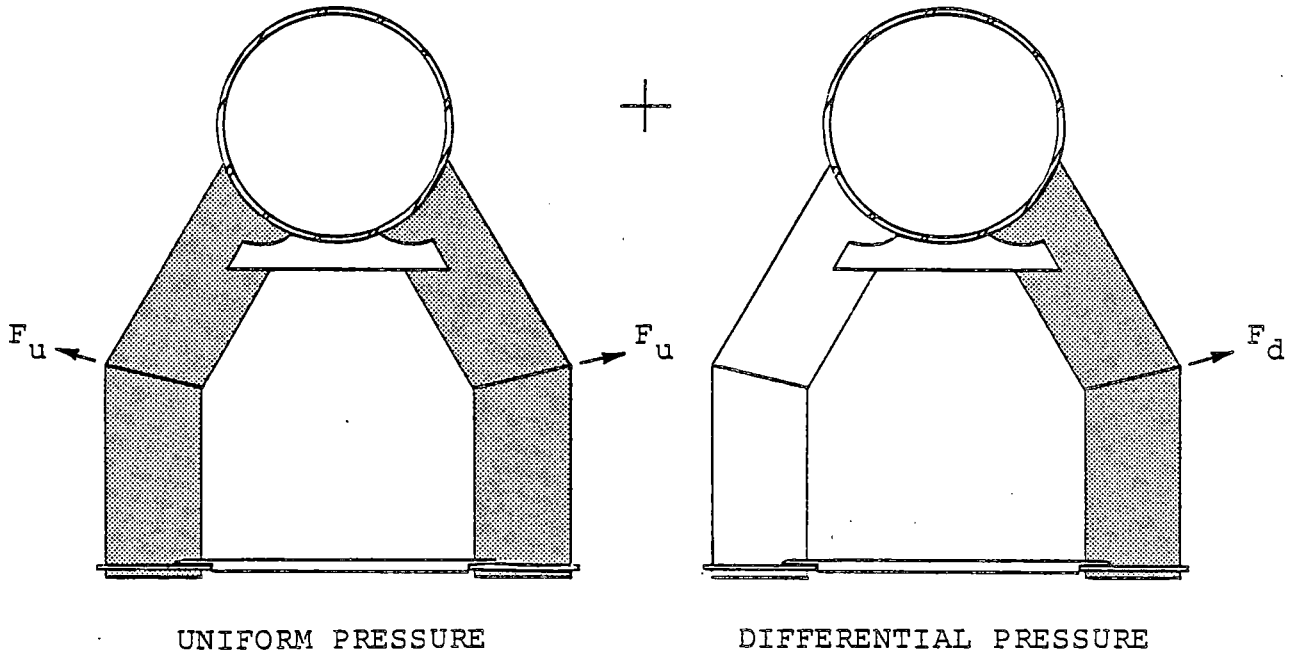
DOWNCOMER LONGITUDINAL BRACING AND LATERAL BRACING
LOCA BUBBLE - INDUCED DRAG LOAD DISTRIBUTION

ITEM ⁽¹⁾		AVERAGE PRESSURE (psi) ⁽²⁾					
		OPERATING ΔP			ZERO ΔP		
		P _x	P _y	P _z	P _x	P _y	P _z
LONGITUDINAL BRACING MEMBER	① ⁽³⁾	0.00	3.14	-0.45	0.00	3.95	-0.56
	② ⁽³⁾	0.00	6.13	-2.34	0.00	7.72	-2.94
	③ ⁽³⁾	0.00	4.81	-3.76	0.00	6.01	-4.70
	④ ⁽³⁾	0.00	4.33	-0.35	0.00	5.46	-0.44
	⑤	8.82	12.59	-1.48	11.13	15.89	-1.86
	⑥	10.13	12.25	-1.86	12.77	15.44	-2.34
LATERAL BRACING MEMBER	⑦ ⁽³⁾	1.56	3.96	0.00	1.97	4.98	0.00
STIFFENER RINGS	⑧	0.00	21.90	0.00	0.00	27.60	0.00

- (1) SEE FIGURE 3-2.2-9 FOR BRACINGS IDENTIFICATIONS.
(2) LOADS SHOWN INCLUDE A DLF OF 2.0.
(3) AVERAGE PRESSURE MAGNITUDES EXCLUDE PRESSURE OVER END CONNECTIONS.

Table 3-2.2-9

IBA CONDENSATION OSCILLATION
DOWNCOMER LOADS



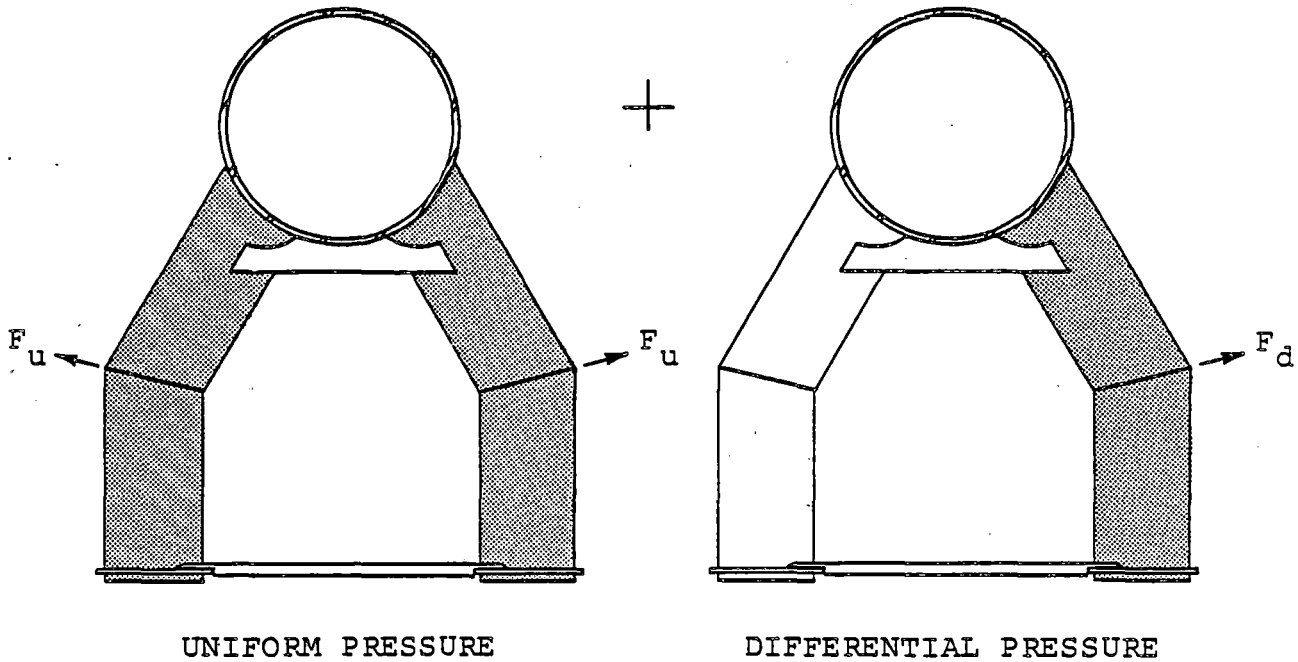
FREQUENCY INTERVAL (Hz)	DOWNCOMER LOAD AMPLITUDES ⁽¹⁾			
	UNIFORM (F_u)		DIFFERENTIAL (F_d) ⁽²⁾	
	PRESSURE (psi)	FORCE (lb)	PRESSURE (psi)	FORCE (lb)
6.0 - 10.0	1.10	218.00	0.20	40.00
12.0 - 20.0	0.80	159.00	0.20	40.00
18.0 - 30.0	0.20	40.00	0.20	40.00

(1) EFFECTS OF UNIFORM AND DIFFERENTIAL PRESSURES SUMMED TO OBTAIN TOTAL LOAD.

(2) SEE FIGURE 3-2.2-10 FOR DOWNCOMER DIFFERENTIAL PRESSURE LOAD DISTRIBUTION.

Table 3-2.2-10

DBA CONDENSATION OSCILLATION
DOWNCOMER LOADS



FREQUENCY INTERVAL (Hz)	DOWNCOMER LOAD AMPLITUDES ⁽¹⁾			
	UNIFORM (F_u)		DIFFERENTIAL (F_d) ⁽²⁾	
	PRESSURE (psi)	FORCE (lb)	PRESSURE (psi)	FORCE (lb)
4.0 - 8.0	3.60	714.00	2.85	566.00
8.0 - 16.0	1.30	258.00	2.60	516.00
12.0 - 24.0	0.60	119.00	1.20	238.00

(1) EFFECTS OF UNIFORM AND DIFFERENTIAL PRESSURES SUMMED TO OBTAIN TOTAL LOAD.

(2) SEE FIGURE 3-2.2-10 FOR DOWNCOMER DIFFERENTIAL PRESSURE LOAD DISTRIBUTION.

Table 3-2.2-11

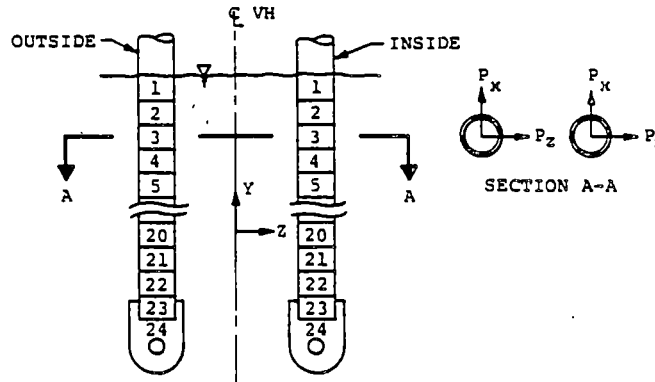
IBA AND DBA CONDENSATION OSCILLATION
VENT SYSTEM INTERNAL PRESSURES

LOAD CHARACTERISTICS	COMPONENT LOAD			
	VENT LINE		VENT HEADER	
	IBA	DBA	IBA	DBA
TYPE	SINGLE HARMONIC	SINGLE HARMONIC	SINGLE HARMONIC	SINGLE HARMONIC
MAGNITUDE (psi)	±2.5	±2.5	±2.5	±2.5
DISTRIBUTION	UNIFORM	UNIFORM	UNIFORM	UNIFORM
FREQUENCY RANGE (Hz)	6 - 10	4 - 8	6 - 10	4 - 8

1. DOWNCOMER CO INTERNAL PRESSURE LOADS ARE INCLUDED IN LOADS SHOWN IN TABLES 3-2.2.10 AND 3-2.2-11.
2. LOADS SHOWN ACT IN ADDITION TO VENT SYSTEM INTERNAL PRESSURES IN FIGURES 3-2.2-2 AND 3-2.2-3.
3. ADDITIONAL STATIC INTERNAL PRESSURE OF 1.7 PSI APPLIED TO THE ENTIRE VENT SYSTEM TO ACCOUNT FOR NOMINAL SUBMERGENCE OF DOWNCOMERS.

Table 3-2.2-12

SUPPORT COLUMN DBA CONDENSATION OSCILLATION
SUBMERGED STRUCTURE LOAD DISTRIBUTION



ELEVATION VIEW - MITERED JOINT

SEGMENT NUMBER	AVERAGE PRESSURE (psi)(1)			
	INSIDE COLUMN		OUTSIDE COLUMN	
	P_x	P_z	P_x	P_z
1	0.20	0.17	0.20	0.21
2	0.63	0.52	0.58	0.47
3	1.10	0.91	0.96	0.65
4	1.66	1.36	1.35	0.78
5	2.31	1.89	1.72	0.86
6	3.00	2.47	2.07	0.90
7	3.67	3.02	2.36	0.93
8	4.13	3.40	2.55	0.93
9	4.23	3.51	2.60	0.92
10	3.96	3.30	2.52	0.92
11	3.41	2.88	2.32	0.94
12	2.77	2.38	2.05	0.96
13	2.18	1.92	1.76	0.98
14	1.69	1.54	1.48	1.00
15	1.30	1.24	1.23	1.01
16	1.01	1.03	1.02	1.02
17	0.79	0.86	0.84	1.02
18	0.63	0.75	0.70	1.02
19	0.51	0.64	0.58	1.01
20	0.42	0.61	0.49	1.01
21	0.38	0.56	0.42	1.00
22	0.36	0.53	0.36	1.00
23	1.06	0.97	0.94	1.76
24	1.03	0.89	0.83	1.73

(1) LOADS SHOWN INCLUDE FSI EFFECTS AND DLF'S.

Table 3-2.2-13

DOWNCOMER LONGITUDINAL BRACING AND LATERAL BRACING
DBA CONDENSATION OSCILLATION SUBMERGED STRUCTURE
LOAD DISTRIBUTION

ITEM ⁽¹⁾		AVERAGE PRESSURE (psi) ⁽²⁾		
		P _x	P _y	P _z
LONGITUDINAL BRACING MEMBER	① ⁽³⁾	0.00	1.46	1.30
	② ⁽³⁾	0.00	3.03	1.14
	③ ⁽³⁾	0.00	2.48	1.28
	④ ⁽³⁾	0.00	4.41	0.56
	⑤	6.58	10.57	2.41
	⑥	4.80	6.84	2.40
LATERAL BRACING MEMBER	⑦ ⁽³⁾	2.31	2.19	0.00
STIFFENER RINGS	⑧	0.00	3.88	0.00

- (1) SEE FIGURE 3-2.2-9 FOR BRACING IDENTIFICATIONS.
(2) LOADS SHOWN INCLUDE FSI AND DLF'S.
(3) AVERAGE PRESSURE MAGNITUDES DO NOT INCLUDE PRESSURE OVER END CONNECTIONS.

Table 3-2.2-14

MAXIMUM DOWNCOMER CHUGGING LOAD DETERMINATION

MAXIMUM CHUGGING LOAD FOR SINGLE DOWNCOMER

FSTF

MAXIMUM LOAD MAGNITUDE: $P_1 = 3.046$ kips

TIED DOWNCOMER FREQUENCY: $f_1 = 2.9$ Hz

PULSE DURATION: $t_d = 0.003$ sec

DYNAMIC LOAD FACTOR: $DLF_1 = \pi f_1 t_d = 0.027$

DRESDEN UNITS 2 AND 3 (DOWNCOMER BRACED LONGITUDINALLY)

DOWNCOMER FREQUENCY: $f = 9.277$ Hz⁽¹⁾

DYNAMIC LOAD FACTOR: $DLF = \pi f t_d = 0.0874$

MAXIMUM LOAD MAGNITUDE (IN ANY DIRECTION):

$$P_{\max} = P_1 \left(\frac{DLF}{DLF_1} \right) = 3.046 \left(\frac{0.0874}{0.027} \right) = 9.86 \text{ kips}$$

DRESDEN UNITS 2 AND 3 (DOWNCOMERS NOT BRACED LONGITUDINALLY)

DOWNCOMER FREQUENCY: $f = 9.170$ ⁽²⁾

DYNAMIC LOAD FACTOR: $DLF = \pi f t_d = 0.0864$

MAXIMUM LOAD MAGNITUDE (IN ANY DIRECTION):

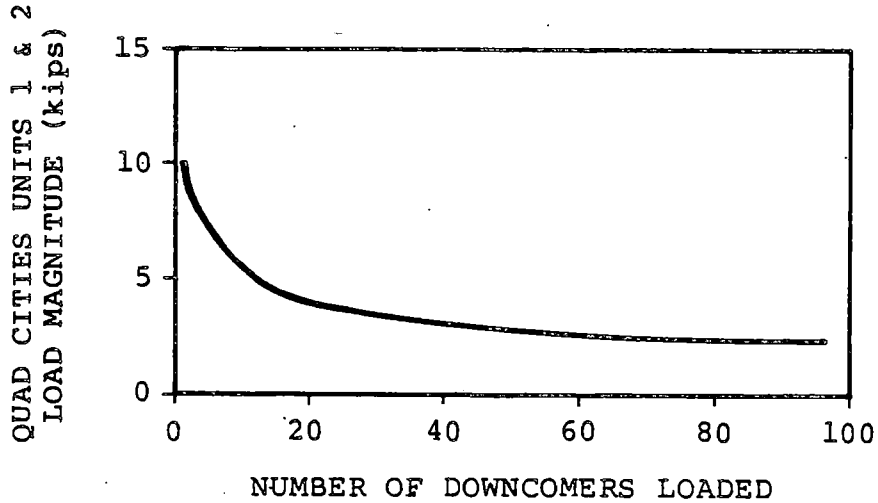
$$P_{\max} = P_1 \left(\frac{DLF}{DLF_1} \right) = 3.046 \left(\frac{0.0864}{0.027} \right) = 9.75 \text{ kips}$$

(1) SEE FIGURE 3-2.4-13 FOR FREQUENCY DETERMINATION.

(2) SEE FIGURE 3-2.4-14 FOR FREQUENCY DETERMINATION.

Table 3-2.2-15

MULTIPLE DOWNCOMER CHUGGING LOAD
MAGNITUDE DETERMINATION



CHUGGING LOADS FOR MULTIPLE DOWNCOMERS (kips) ⁽¹⁾		
NUMBER OF DOWNCOMERS	FSTF LOAD PER DOWNCOMER	QUAD CITIES UNITS 1 & 2 LOAD PER DOWNCOMER
5	3.05	9.75
10	2.10	6.75
20	1.42	4.54
40	1.00	3.20
60	0.72	2.30
80	0.58	1.86
120	0.54	1.73

(1) BASED ON PROBABILITY OF EXCEEDANCE OF 10^{-4} , IN ACCORDANCE WITH NUREG-0661.

Table 3-2.2-16

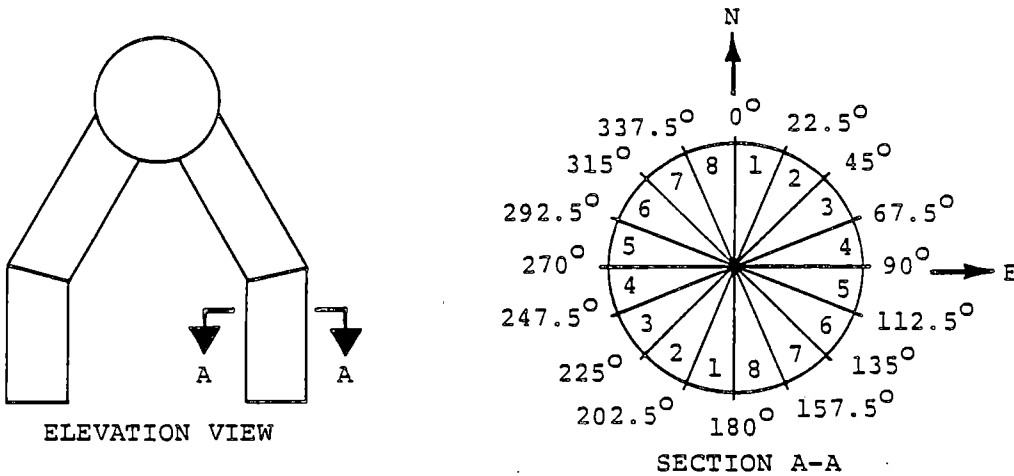
CHUGGING LATERAL LOADS FOR MULTIPLE DOWNCOMERS -
MAXIMUM OVERALL EFFECTS

LOAD CASE NUMBER	NUMBER OF DOWNCOMERS LOADED	LOAD DESCRIPTION	LOAD (1) MAGNITUDE (kips)
1	96	ALL DOWNCOMERS, PARALLEL TO N-S PLANE, SAME DIRECTION, MAXIMIZE OVERALL LATERAL LOAD	1.80
2	96	ALL DOWNCOMERS, PARALLEL TO ONE VL, SAME DIRECTION, MAXIMIZE OVERALL LATERAL LOAD	1.80
3	96	ALL DOWNCOMERS, PARALLEL TO VH, SAME DIRECTION, MAXIMIZE VL BENDING	1.80
4	96	ALL DOWNCOMERS PERPENDICULAR TO VH, SAME DIRECTION, MAXIMIZE VH TORQUE	1.80
5	12	DOWNCOMERS CENTERED ON ONE VL, PERPENDICULAR TO VH, OPPOSING DIRECTIONS, MAXIMIZE VL BENDING	4.16
6	12	DOWNCOMERS CENTERED ON ONE VL, PERPENDICULAR TO VH, SAME DIRECTIONS, MAXIMIZE VL AXIAL LOADS	4.16
7	12	ALL DOWNCOMERS BETWEEN TWO VL'S, PERPENDICULAR TO VH, SAME DIRECTION, MAXIMIZE VH BENDING	4.16
8-10	4	NVB DOWNCOMERS NEAR MITER, PARALLEL TO VH, PERMUTATE DIRECTIONS, MAXIMIZE DC BRACING LOADS	7.48

(1) MAGNITUDES OBTAINED FROM TABLE 3-2.2-16.

Table 3-2.2-17

LOAD REVERSAL HISTOGRAM FOR CHUGGING
DOWNCOMER LATERAL LOAD FATIGUE EVALUATION



KEY DIAGRAM

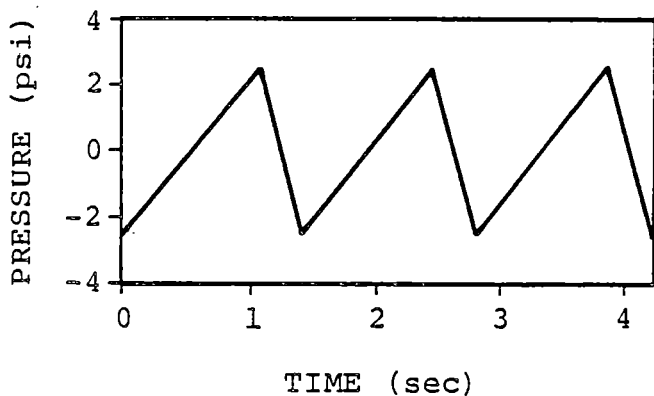
PERCENT OF MAXIMUM LOAD RANGE (2)	ANGULAR SECTOR LOAD REVERSALS (cycles) (1)							
	1	2	3	4	5	6	7	8
5 - 10	4706	2573	2839	3076	3168	2673	2563	4629
10 - 15	2696	1206	1100	1104	1096	1052	1163	2545
15 - 20	1399	727	653	572	709	708	679	1278
20 - 25	676	419	452	377	370	398	368	621
25 - 30	380	250	252	225	192	255	197	334
30 - 35	209	187	139	121	97	114	162	208
35 - 40	157	62	84	86	62	60	90	150
40 - 45	113	53	28	39	48	44	58	86
45 - 50	83	33	32	26	18	23	33	67
50 - 55	65	26	14	11	9	7	16	40
55 - 60	51	26	11	5	11	11	23	28
60 - 65	44	9	2	4	0	5	9	26
65 - 70	32	16	7	5	0	2	9	21
70 - 75	12	9	11	5	0	4	7	19
75 - 80	26	4	2	0	2	4	7	18
80 - 85	7	5	2	0	0	0	0	12
85 - 90	4	11	0	0	0	0	5	11
90 - 95	7	4	0	0	2	0	0	9
95 - 100	2	5	0	0	0	2	4	7

- (1) VALUES SHOWN ARE FOR CHUGGING DURATION OF 900 SECONDS.
- (2) THE MAXIMUM SINGLE DOWNCOMER LOAD MAGNITUDE RANGE USED FOR FATIGUE IS $3.936 \times 3.2 = 12.6$ KIPS (SEE TABLE 3-2.2-15).

Table 3-2.2-18

CHUGGING VENT SYSTEM INTERNAL PRESSURES

LOAD TYPE		LOAD DESCRIPTION	COMPONENT LOAD MAGNITUDE (psi)		
NUMBER	DESCRIPTION		VENT LINE	VENT HEADER	DOWN-COMER
1	GROSS VENT SYSTEM PRESSURE OSCILLATION	TRANSIENT PRESSURE UNIFORM DISTRIBUTION	±2.5	±2.5	±5.0
2	ACOUSTIC VENT SYSTEM PRESSURE OSCILLATION	SINGLE HARMONIC IN 6.9 TO 9.5 Hz RANGE UNIFORM DISTRIBUTION	±2.5	±3.0	±3.5
3	ACOUSTIC DOWNCOMER PRESSURE OSCILLATION	SINGLE HARMONIC IN 40.0 TO 50.0 Hz RANGE. UNIFORM DISTRIBUTION	N/A	N/A	±13.0

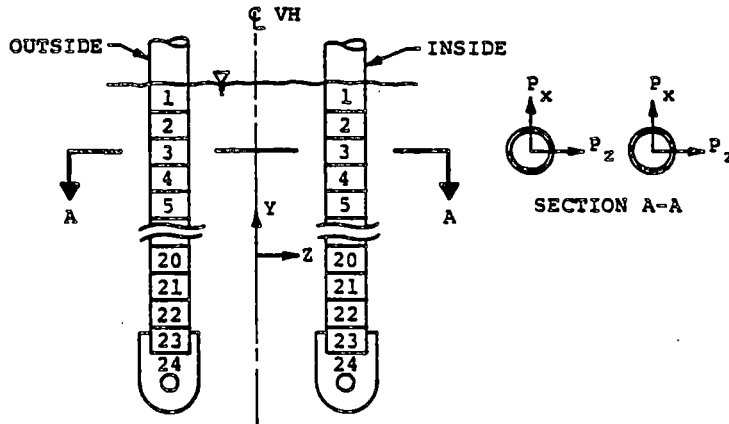


LOADING INFORMATION
1. DOWNCOMER LOADS SHOWN USED FOR HOOP STRESS CALCULATIONS ONLY.
2. LOADS ACT IN ADDITION TO INTERNAL PRESSURE LOADS SHOWN IN FIGURES 3-2.2-2 AND 3-2.2-3.

FORCING FUNCTION FOR LOAD TYPE 1

Table 3-2.2-19

SUPPORT COLUMN PRE-CHUG SUBMERGED STRUCTURE
LOAD DISTRIBUTION



ELEVATION VIEW - MITERED JOINT

SEGMENT NUMBER	AVERAGE PRESSURE (psi)			
	INSIDE COLUMN		OUTSIDE COLUMN	
	P_x	P_z	P_x	P_z
1	0.02	0.04	0.02	0.04
2	0.05	0.11	0.06	0.09
3	0.08	0.19	0.09	0.13
4	0.13	0.29	0.13	0.15
5	0.18	0.40	0.16	0.17
6	0.25	0.52	0.20	0.17
7	0.32	0.63	0.23	0.17
8	0.37	0.70	0.25	0.17
9	0.38	0.72	0.26	0.18
10	0.35	0.67	0.25	0.18
11	0.31	0.58	0.23	0.18
12	0.26	0.47	0.21	0.18
13	0.22	0.37	0.18	0.19
14	0.19	0.28	0.16	0.19
15	0.16	0.22	0.14	0.19
16	0.15	0.17	0.13	0.18
17	0.14	0.13	0.11	0.17
18	0.13	0.11	0.11	0.17
19	0.12	0.09	0.10	0.16
20	0.12	0.08	0.09	0.16
21	0.11	0.08	0.09	0.15
22	0.11	0.07	0.08	0.15
23	0.33	0.11	0.26	0.39
24	0.32	0.11	0.25	0.38

Table 3-2.2-20

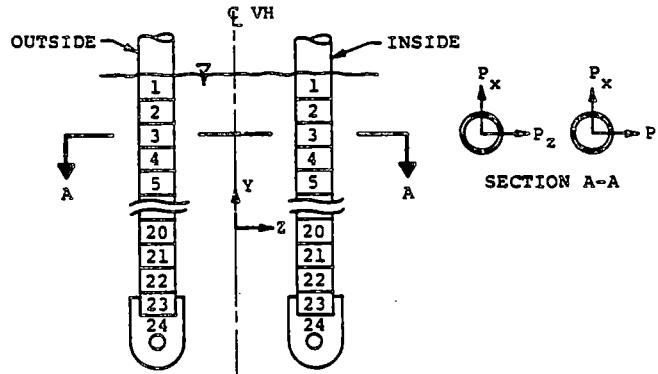
DOWNCOMER LONGITUDINAL BRACING AND LATERAL BRACING
PRE-CHUG SUBMERGED STRUCTURE LOAD DISTRIBUTION

ITEM ⁽¹⁾		AVERAGE PRESSURE (psi) ⁽²⁾		
		P _x	P _y	P _z
LONGITUDINAL BRACING MEMBER	① ⁽³⁾	0.00	0.11	0.05
	②	0.00	0.22	0.04
	③ ⁽³⁾	0.00	0.20	0.05
	④ ⁽³⁾	0.00	0.30	0.02
	⑤	1.25	1.84	0.08
	⑥	0.82	1.17	0.08
LATERAL BRACING MEMBER	⑦	0.20	0.16	0.00
STIFFENER RINGS	⑧	0.00	0.35	0.00

- (1) SEE FIGURE 3-2.2-9 FOR BRACINGS IDENTIFICATIONS.
- (2) LOADS SHOWN INCLUDE FSI AND DLF'S.
- (3) AVERAGE PRESSURE MAGNITUDES EXCLUDE THE PRESSURES OVER CONNECTIONS.

Table 3-2.2-21

SUPPORT COLUMN POST-CHUG SUBMERGED STRUCTURE
LOAD DISTRIBUTION



ELEVATION VIEW - MITERED JOINT

SEGMENT NUMBER	AVERAGE PRESSURE (psi)(1)			
	INSIDE COLUMN		OUTSIDE COLUMN	
	P _x	P _z	P _x	P _z
1	0.23	0.17	0.18	0.05
2	0.71	0.51	0.55	0.13
3	1.24	0.88	0.92	0.19
4	1.82	1.30	1.29	0.25
5	2.47	1.77	1.66	0.29
6	3.14	2.27	2.00	0.33
7	3.76	2.72	2.27	0.36
8	4.18	3.03	2.46	0.38
9	4.28	3.11	2.52	0.38
10	4.05	2.94	2.46	0.38
11	3.57	2.59	2.30	0.36
12	2.99	2.17	2.07	0.33
13	2.42	1.76	1.81	0.31
14	1.93	1.41	1.55	0.28
15	1.52	1.12	1.31	0.26
16	1.21	0.90	1.10	0.24
17	0.96	0.73	0.93	0.22
18	0.77	0.60	0.78	0.20
19	0.63	0.50	0.66	0.19
20	0.51	0.43	0.56	0.18
21	0.43	0.37	0.48	0.18
22	0.36	0.32	0.41	0.17
23	0.98	0.83	1.15	0.31
24	0.85	0.74	1.02	0.30

(1) LOADS SHOWN INCLUDE FSI EFFECTS AND DLF'S.

Table 3-2.2-22

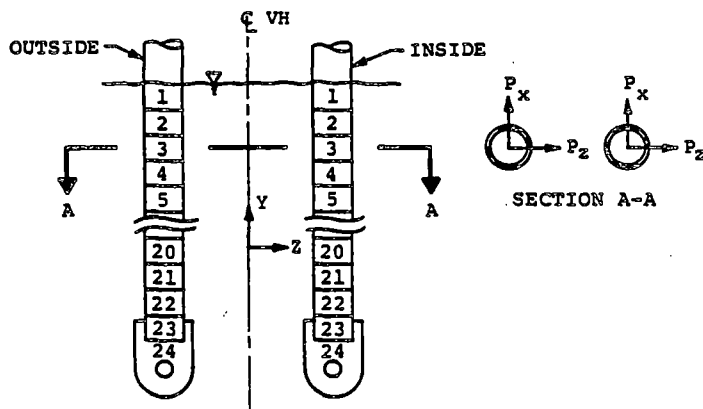
DOWNCOMER LONGITUDINAL BRACING AND LATERAL BRACING
POST-CHUG SUBMERGED STRUCTURE LOAD DISTRIBUTION

ITEM ⁽¹⁾		AVERAGE PRESSURE (psi) ⁽²⁾		
		P _x	P _y	P _z
LONGITUDINAL BRACING MEMBER	① ⁽³⁾	0.00	3.52	0.96
	② ⁽³⁾	0.00	1.09	0.39
	③ ⁽³⁾	0.00	5.96	1.01
	④ ⁽³⁾	0.00	1.81	1.10
	⑤	1.23	2.08	0.88
	⑥	1.47	2.09	0.86
LATERAL BRACING MEMBER	⑦ ⁽³⁾	4.48	2.61	0.00
STIFFENER RINGS	⑧	0.00	4.01	0.00

- (1) SEE FIGURE 3-2.2-9 FOR BRACINGS IDENTIFICATIONS.
- (2) LOADS SHOWN INCLUDE FSI AND DLF'S.
- (3) AVERAGE PRESSURE MAGNITUDES EXCLUDE THE PRESSURES OVER CONNECTIONS.

Table 3-2.2-23

SUPPORT COLUMN SRV DISCHARGE SUBMERGED STRUCTURE
LOAD DISTRIBUTION



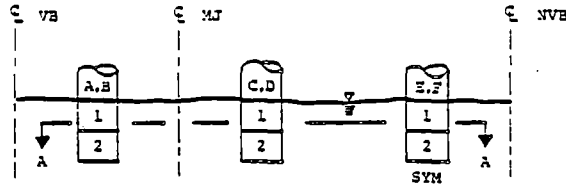
ELEVATION VIEW - MITERED JOINT

SEGMENT NUMBER	T-QUENCHER WATER JET (psi) ⁽¹⁾				T-QUENCHER BUBBLE DRAG (psi) ⁽¹⁾			
	INSIDE COLUMN		OUTSIDE COLUMN		INSIDE COLUMN		OUTSIDE COLUMN	
	P_x	P_z	P_x	P_z	P_x	P_z	P_x	P_z
1	0.00	0.00	0.00	0.00	0.29	0.10	0.29	0.10
2	0.00	0.00	0.00	0.00	0.86	0.28	0.86	0.28
3	0.00	0.00	0.00	0.00	1.01	0.34	1.01	0.34
4	0.00	0.00	0.00	0.00	1.13	0.39	1.13	0.39
5	0.00	0.00	0.00	0.00	1.23	0.43	1.23	0.43
6	0.00	0.00	0.00	0.00	1.37	0.49	1.37	0.49
7	0.00	0.00	0.00	0.00	1.56	0.56	1.56	0.56
8	0.00	0.00	0.00	0.00	1.67	0.60	1.67	0.60
9	0.00	0.00	0.00	0.00	1.58	0.57	1.58	0.57
10	0.00	0.00	0.00	0.00	1.67	0.61	1.67	0.61
11	0.00	0.00	0.00	0.00	2.01	0.73	2.01	0.73
12	0.00	0.00	0.00	0.00	2.27	0.82	2.27	0.82
13	0.00	0.00	0.00	0.00	2.42	0.87	2.42	0.87
14	0.00	0.00	0.00	0.00	2.76	1.00	2.76	1.00
15	0.00	0.00	0.00	0.00	3.26	1.18	3.26	1.18
16	0.00	0.00	0.00	0.00	3.70	1.33	3.70	1.33
17	0.00	0.00	0.00	0.00	4.03	1.45	4.03	1.45
18	-2.42	12.18	2.42	-12.18	4.52	1.64	4.52	1.64
19	-2.95	14.82	2.95	-14.82	5.62	2.03	5.62	2.03
20	-2.95	14.82	2.95	-14.82	6.66	2.40	6.66	2.40
21	-2.95	14.82	2.95	-14.82	6.56	2.38	6.56	2.38
22	-2.95	14.82	2.95	-14.82	5.03	1.88	5.03	1.88
23	-2.95	14.82	2.95	-14.82	6.41	2.64	6.41	2.64
24	-2.37	11.93	2.37	-11.93	9.85	4.35	9.85	4.35

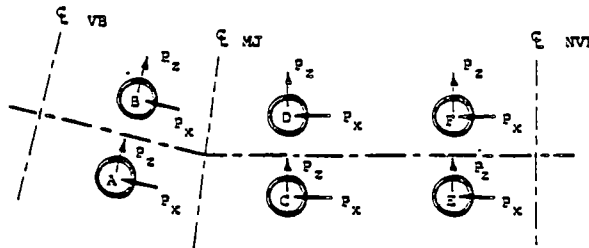
(1) LOADS SHOWN INCLUDE DLF OF 2.0 FOR WATER JET LOADS AND 2.5 FOR DRAG LOADS.

Table 3-2.2-24

DOWNCOMER T-QUENCHER BUBBLE DRAG SUBMERGED STRUCTURE
LOAD DISTRIBUTION



ELEVATION VIEW-DOWNCOMERS



SECTION A-A

ITEM	SEGMENT NUMBER	PRESSURE MAGNITUDE (psi) (1)		
		P_x	P_z	
DOWNCOMER	A	1	1.62	-0.82
		2	3.76	-2.13
	B	1	1.62	0.82
		2	3.76	2.13
	C	1	-0.43	-0.48
		2	-1.50	-1.68
	D	1	-1.15	0.19
		2	-3.21	0.63
	E	1	-0.47	-0.05
		2	-1.57	-0.14
	F	1	-0.47	0.05
		2	-1.57	0.14

(1) LOADS IN X AND Z DIRECTIONS INCLUDE DLF'S OF 2.5.

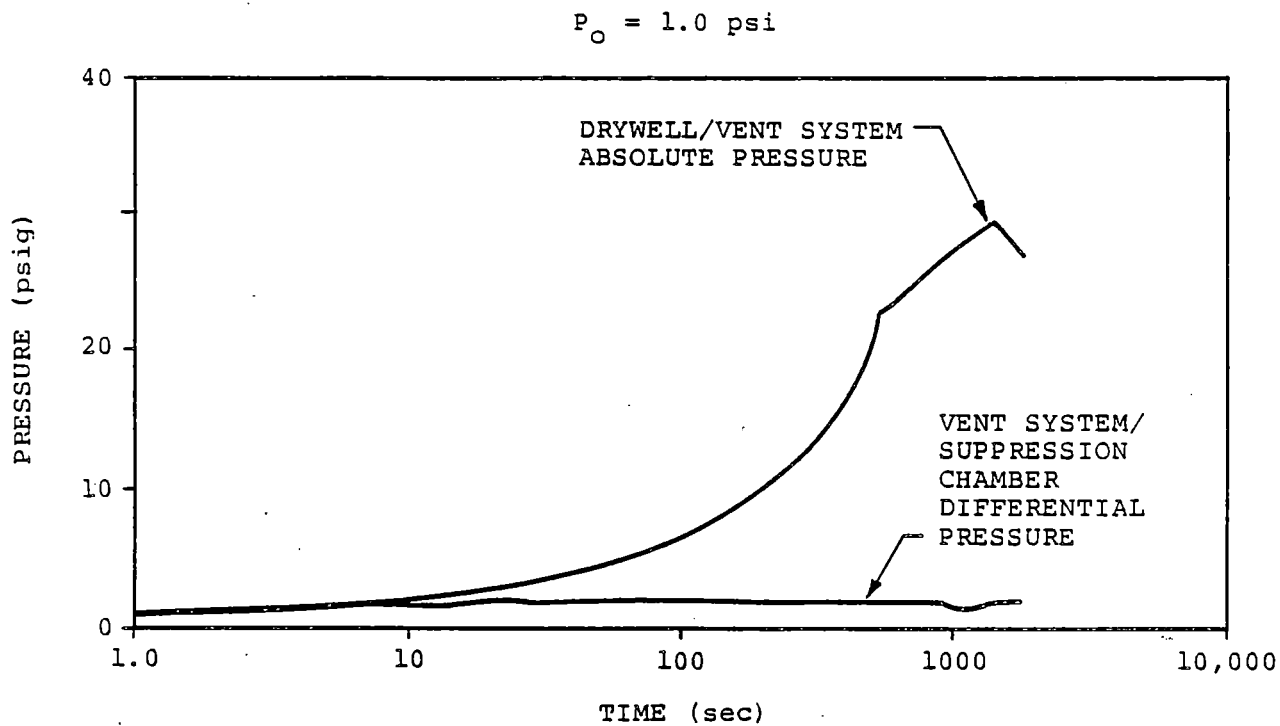
Table 3-2.2-25

DOWNCOMER LONGITUDINAL BRACING AND LATERAL BRACING
T-QUENCHER BUBBLE DRAG SUBMERGED STRUCTURE LOAD DISTRIBUTION

ITEM ⁽¹⁾		AVERAGE PRESSURE (psi) ⁽²⁾		
		P _x	P _y	P _z
LONGITUDINAL BRACING MEMBER	①	0.00	0.71	0.32
	②	0.00	0.49	0.00
	③	0.00	0.41	0.00
	④	0.00	0.50	0.00
	⑤	1.27	1.78	0.00
	⑥	1.24	1.77	0.00
LATERAL BRACING MEMBER	⑦	2.31	2.27	0.00
STIFFENER RINGS	⑧	0.00	1.54	0.00

(1) SEE FIGURE 3-2.2-9 FOR BRACINGS IDENTIFICATIONS.

(2) LOADS SHOWN INCLUDE A DLF OF 2.5.

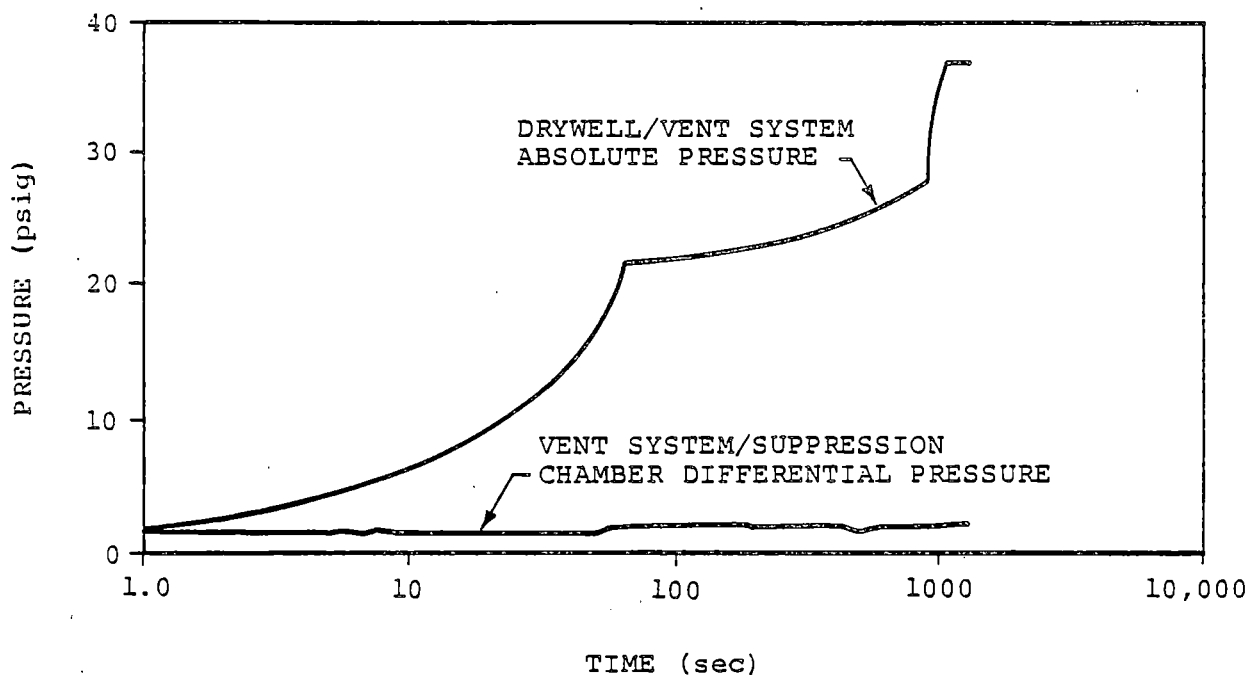


EVENT DESCRIPTION	PRESSURE DESIGNATION	TIME (sec)		PRESSURE (psig)			
		t_{min}	t_{max}	P_{min}	ΔP_{min}	P_{max}	ΔP_{max}
INSTANT OF BREAK TO ONSET OF CO AND CHUGGING	P_1	0.0	300.0	1.0	1.0	13.3	2.0
ONSET OF CO AND CHUGGING TO INITIATION OF ADS	P_2	300.0	600.0	13.0	2.0	23.3	2.0
INITIATION OF ADS TO RPV DEPRESSURIZATION	P_3	600.0	1200.0	23.3	2.0	28.0	1.6

Figure 3-2.2-1

VENT SYSTEM INTERNAL PRESSURES FOR SBA EVENT

$$P_o = 1.8 \text{ psi}$$

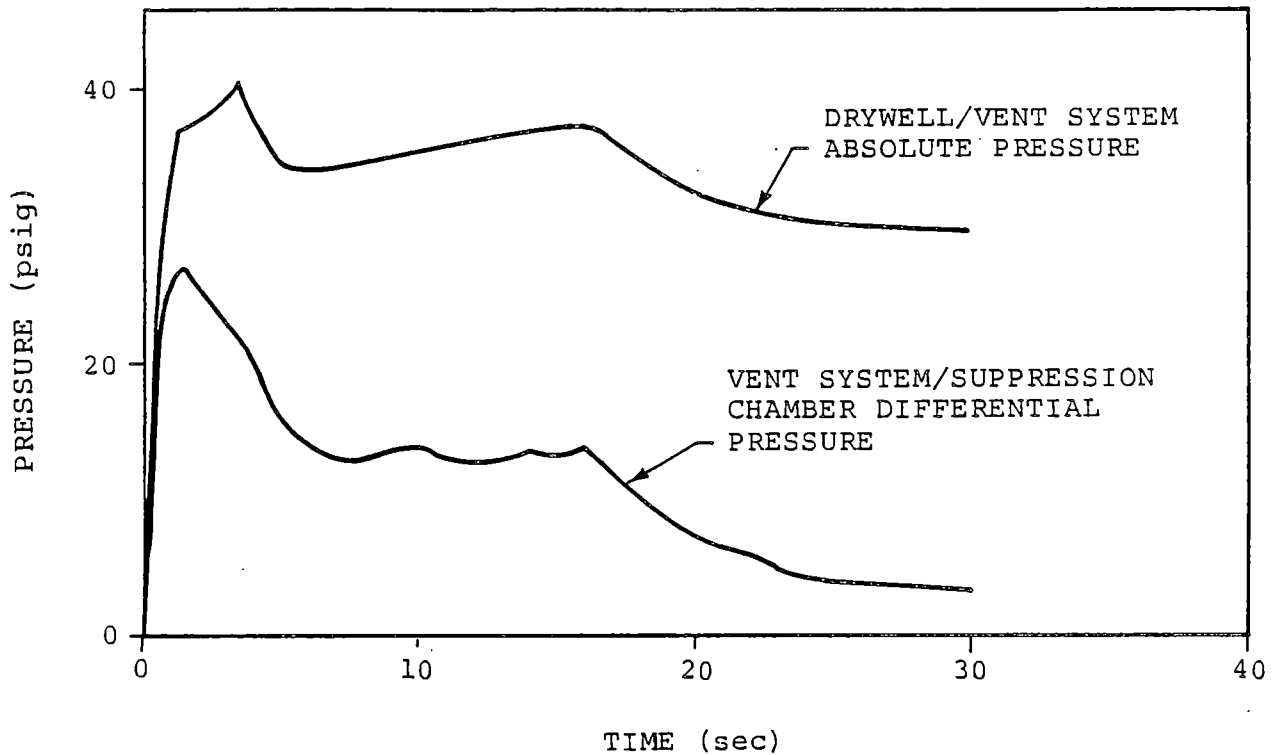


EVENT DESCRIPTION	PRESSURE DESIGNATION	TIME (sec)		PRESSURE (psig)			
		t_{min}	t_{max}	P_{min}	ΔP_{min}	P_{max}	ΔP_{max}
INSTANT OF BREAK TO ONSET OF CO AND CHUGGING	P_1	0.0	5.0	1.8	1.8	4.2	1.5
ONSET OF CO AND CHUGGING TO INITIATION OF ADS	P_2	5.0	900.0	4.2	1.5	28.0	2.0
INITIATION OF ADS TO RPV DEPRESSURIZATION	P_3	900.0	1100.0	28.0	2.0	36.0	2.2

Figure 3-2.2-2

VENT SYSTEM INTERNAL PRESSURES FOR IBA EVENT

$P_o = 0.0$ psi



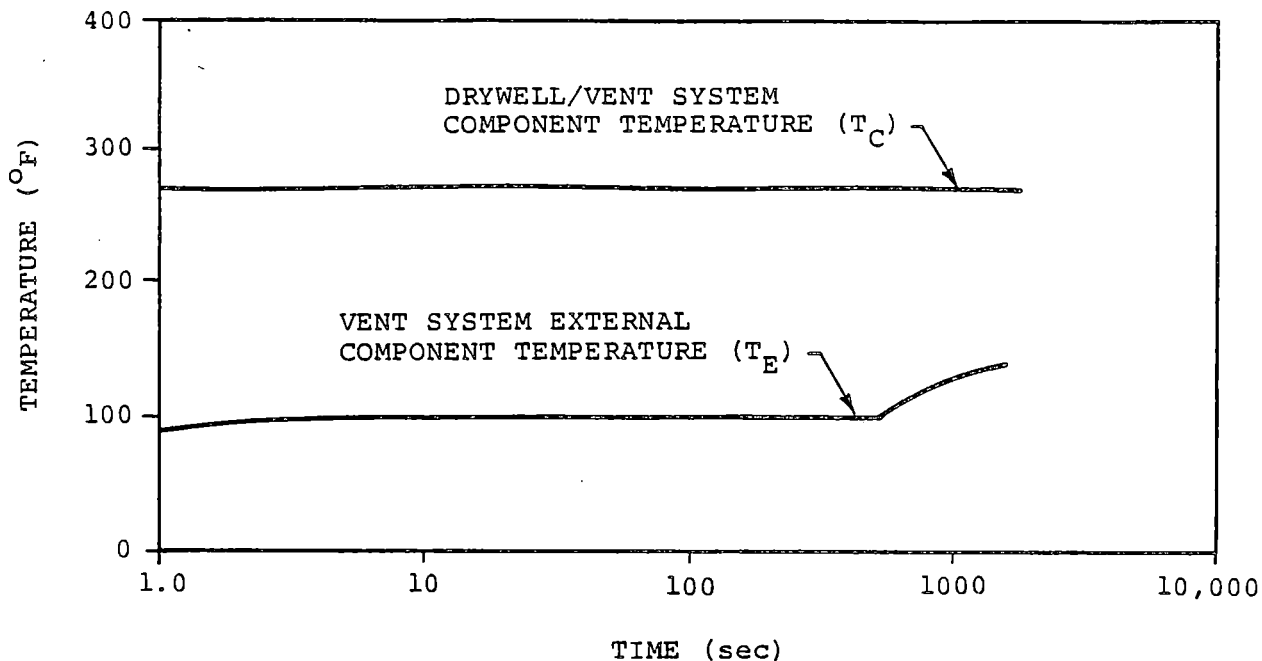
EVENT DESCRIPTION	PRESSURE DESIGNATION	TIME (sec)		PRESSURE (psig)			
		t_{min}	t_{max}	P_{min}	ΔP_{min}	P_{max}	ΔP_{max}
INSTANT OF BREAK TO TERMINATION OF POOL SWELL	P_1	0.0	1.5	0.0	0.0	37.0	27.0
TERMINATION OF POOL SWELL TO ONSET OF CO	P_2	1.5	5.0	37.0	27.0	35.0	16.0
ONSET OF CO TO ONSET OF CHUGGING	P_3	5.0	35.0	35.0	16.0	29.8	1.6
ONSET OF CHUGGING TO RPV DEPRESSURIZATION	P_4	35.0	65.0	29.8	1.6	29.8	1.6

1. DBA VENT SYSTEM INTERNAL PRESSURE LOADS ARE INCLUDED IN VENT SYSTEM PRESSURIZATION AND THRUST LOADS SHOWN IN TABLE 3-2.2-3.

Figure 3-2.2-3

VENT SYSTEM INTERNAL PRESSURES FOR DBA EVENT

$$T_o = 70^{\circ}\text{F}$$



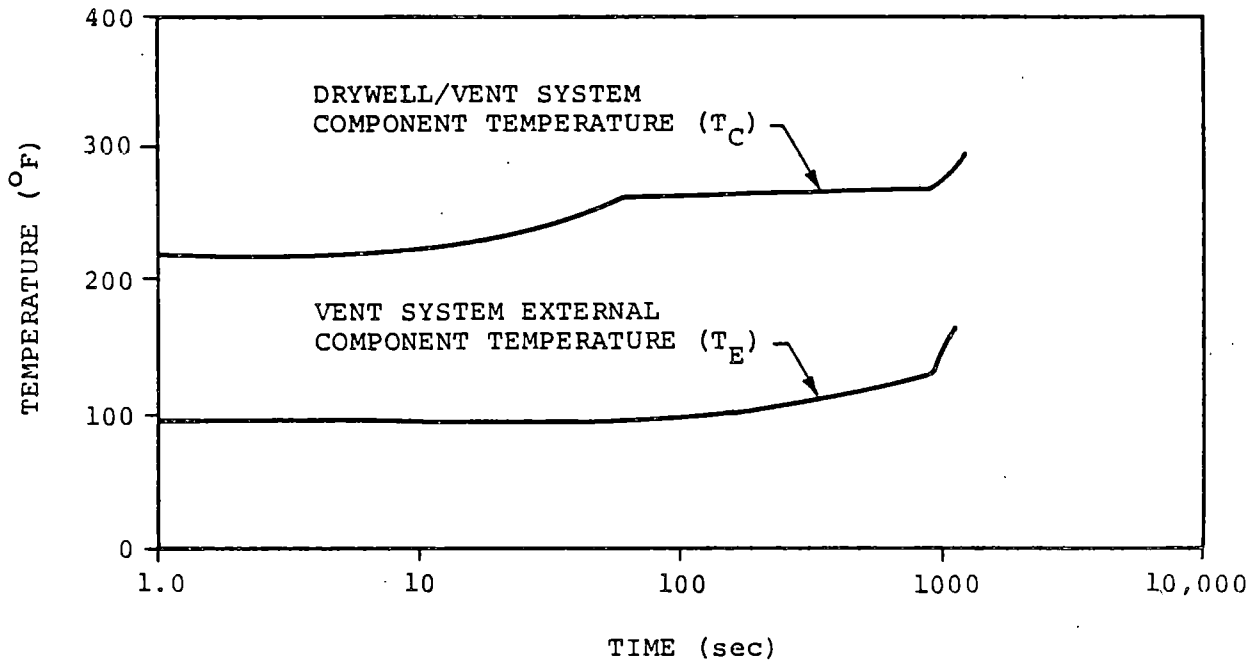
1. SEE FIGURE 3-2.2-1 FOR ADDITIONAL SBA EVENT TEMPERATURES.

EVENT DESCRIPTION	TEMPERATURE DESIGNATION	TIME (sec)		TEMPERATURE ($^{\circ}\text{F}$)			
		t_{\min}	t_{\max}	$T_{C_{\min}}$	$T_{E_{\min}}$	$T_{C_{\max}}$	$T_{E_{\max}}$
INSTANT OF BREAK TO ONSET OF CO AND CHUGGING	T_1	1.0	300.0	273.0	90.0	273.0	103.0
ONSET OF CO AND CHUGGUNG TO INITIATION OF ADS	T_2	300.0	600.0	273.0	100.0	273.0	108.0
INITIATION OF ADS TO RPV DEPRESSURIZATION	T_3	600.0	1200.0	273.0	108.0	273.0	134.0

Figure 3-2.2-4

VENT SYSTEM TEMPERATURES FOR SBA EVENT

$$T_o = 70^{\circ}\text{F}$$

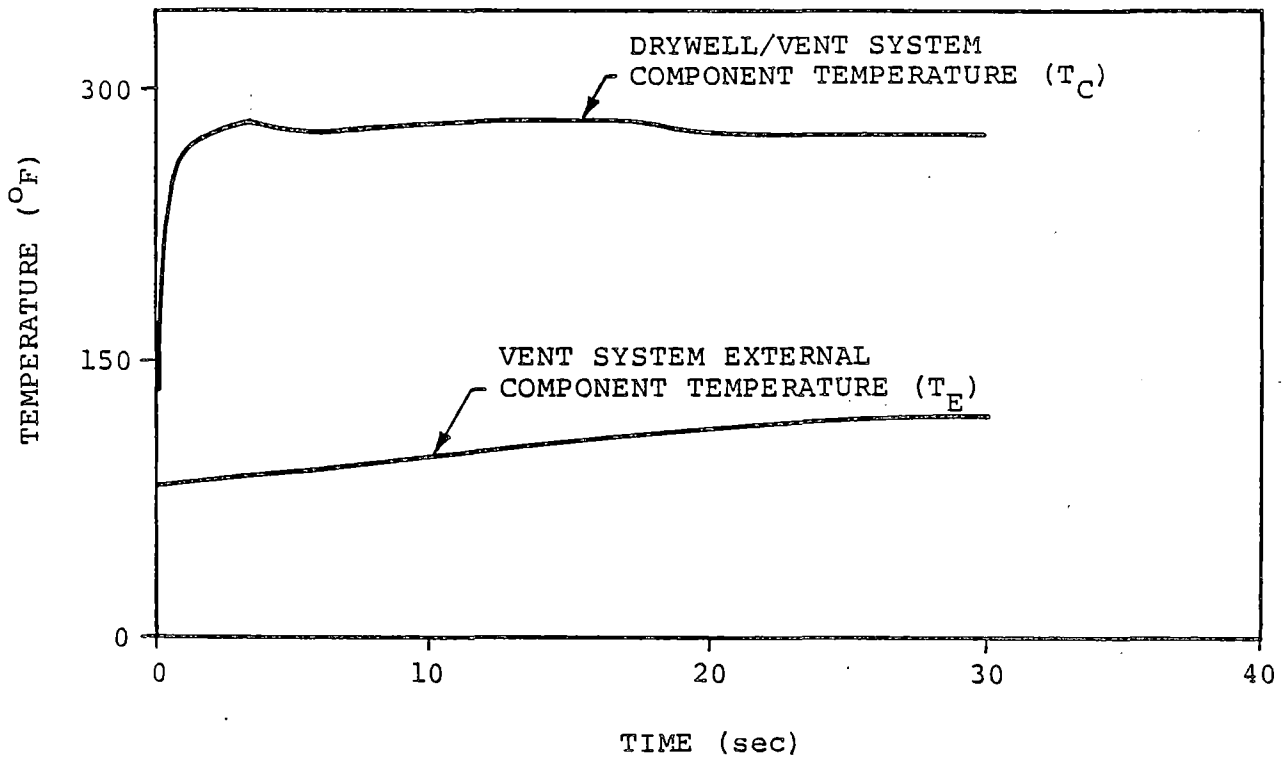


EVENT DESCRIPTION	TEMPERATURE DESIGNATION	TIME (sec)		TEMPERATURE ($^{\circ}\text{F}$)			
		t_{\min}	t_{\max}	$T_{C_{\min}}$	$T_{E_{\min}}$	$T_{C_{\max}}$	$T_{E_{\max}}$
INSTANT OF BREAK TO ONSET OF CO AND CHUGGING	T_1	1.0	5.0	210.0	95.0	220.0	95.0
ONSET OF CO AND CHUGGING TO INITIATION OF ADS	T_2	5.0	900.0	220.0	95.0	271.0	130.0
INITIATION OF ADS TO RPV DEPRESSURIZATION	T_3	900.0	1100.0	271.0	130.0	283.0	164.0

Figure 3-2.2-5

VENT SYSTEM TEMPERATURES FOR IBA EVENT

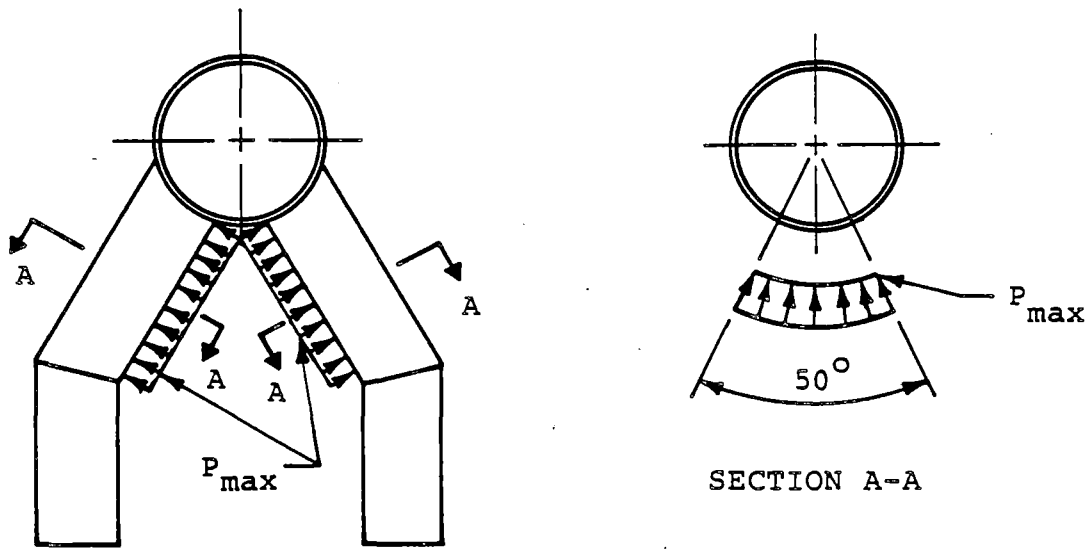
$$T_o = 70^{\circ}\text{F}$$



EVENT DESCRIPTION	TEMPERATURE DESIGNATION	TIME (sec)		TEMPERATURE (°F)			
		t_{\min}	t_{\max}	$T_{C_{\min}}$	$T_{E_{\min}}$	$T_{C_{\max}}$	$T_{E_{\max}}$
INSTANT OF BREAK TO TERMINATION OF POOL SWELL	T_1	0.0	1.5	135.0	83.0	270.0	85.5
TERMINATION OF POOL SWELL TO ONSET OF CO	T_2	1.5	5.0	270.0	85.5	277.0	90.0
ONSET OF CO TO ONSET OF CHUGGING	T_3	5.0	35.0	277.0	90.0	275.0	120.0
ONSET OF CHUGGING TO RPV DEPRESSURIZATION	T_4	35.0	65.0	275.0	120.0	275.0	120.0

Figure 3-2.2-6

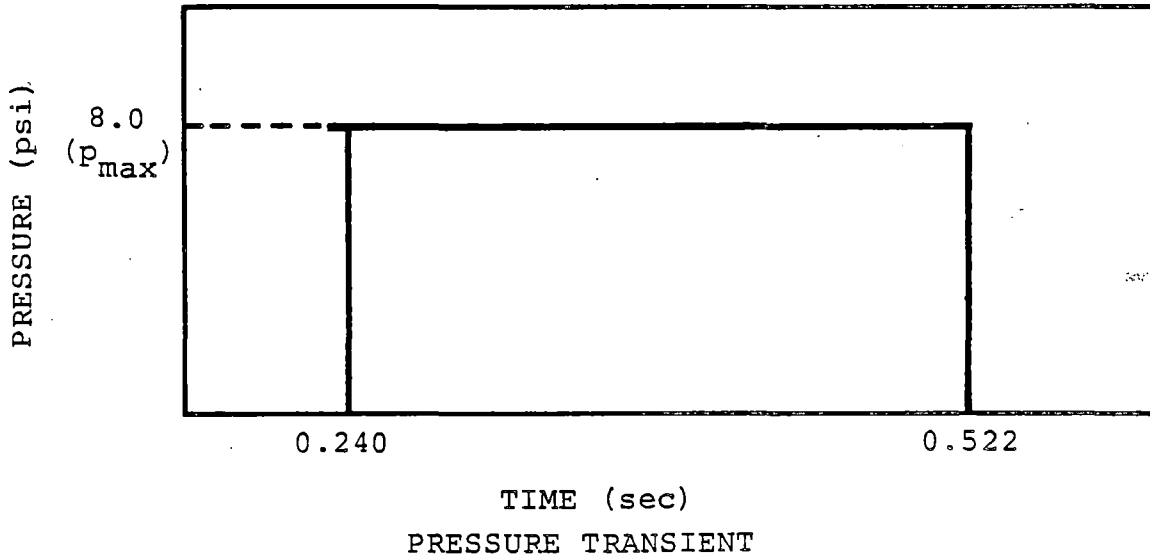
VENT SYSTEM TEMPERATURES FOR DBA EVENT



ELEVATION VIEW

SECTION A-A

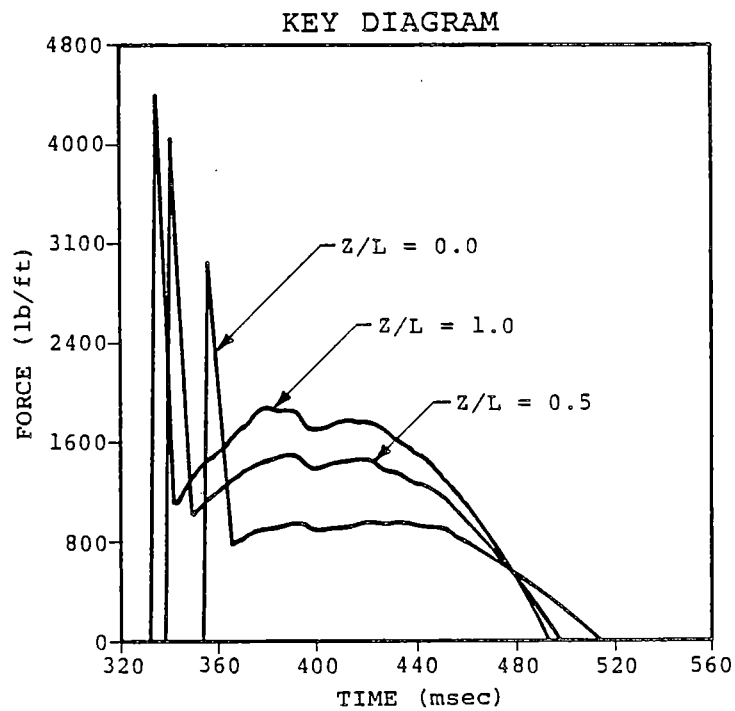
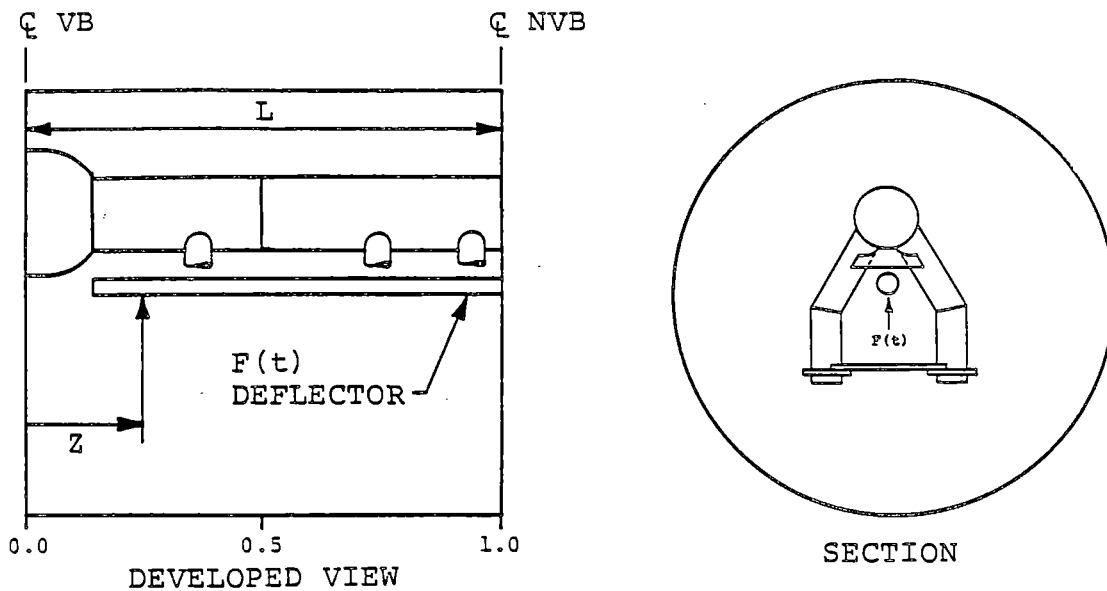
PRESSURE DISTRIBUTION



1. PRESSURES SHOWN ARE APPLIED IN A DIRECTION NORMAL TO DOWNCOMER'S SURFACE.

Figure 3-2.2-7

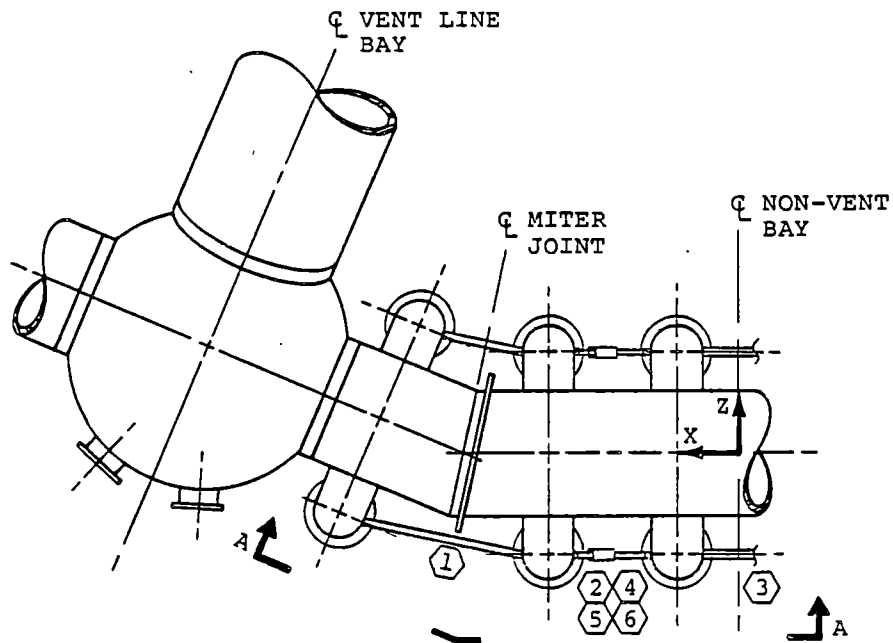
DOWNCOMER POOL SWELL IMPACT LOADS



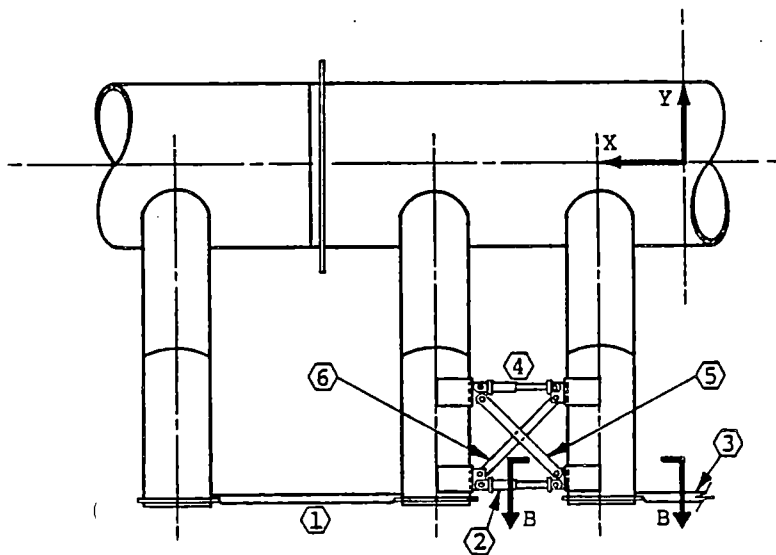
- LOADS AT DISCRETE LOCATIONS ALONG DEFLECTOR OBTAINED BY LINEAR INTERPOLATION.

Figure 3-2.2-8

POOL SWELL IMPACT LOADS FOR VENT HEADER
DEFLECTORS AT SELECTED LOCATIONS

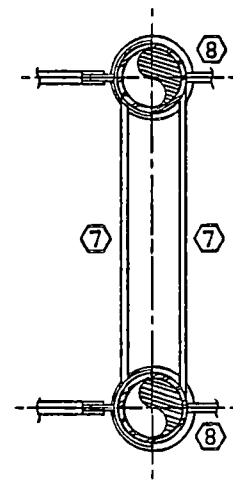


PLAN VIEW



⬡ DESIGNATES BRACING MEMBER NUMBER

VIEW A-A



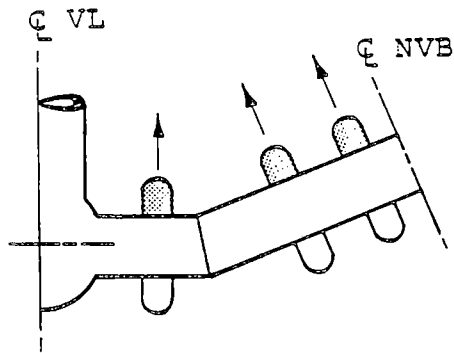
SECTION B-B
(TYPICAL AT ALL DOWNCOMERS)

Figure 3-2.2-9

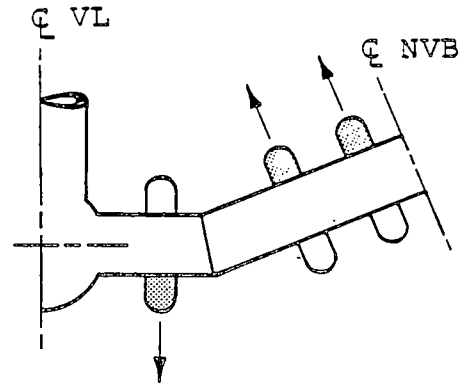
DOWNCOMER LONGITUDINAL BRACING AND LATERAL BRACING

COM-02-041-3
Revision 0

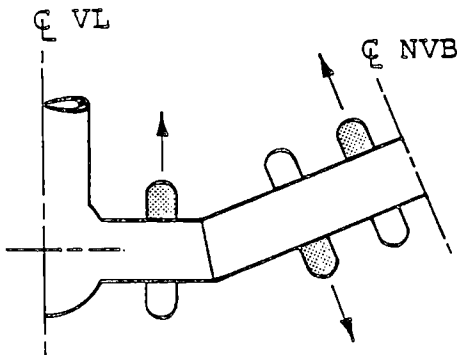
3-2.93



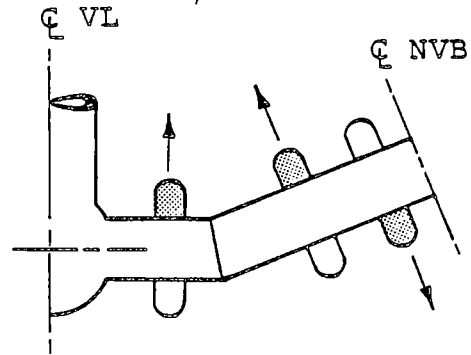
CASE 1



CASE 2



CASE 3

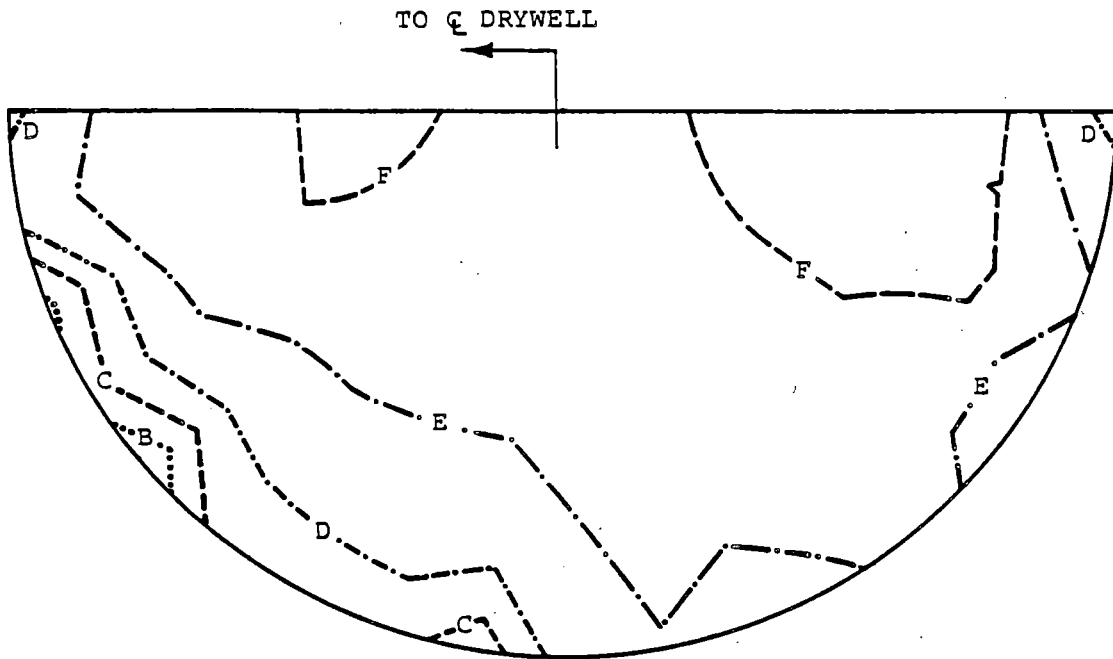


CASE 4

1. SEE TABLE 3-2.2-10 FOR IBA PRESSURE AMPLITUDES AND FREQUENCIES.
2. SEE TABLE 3-2.2-11 FOR DBA PRESSURE AMPLITUDES AND FREQUENCIES.
3. FOUR ADDITIONAL CASES WITH PRESSURES IN DOWNCOMERS OPPOSITE THOSE SHOWN ARE ALSO CONSIDERED.

Figure 3-2.2-10

IBA AND DBA CONDENSATION OSCILLATION DOWNCOMER
DIFFERENTIAL PRESSURE LOAD DISTRIBUTION



NORMALIZED POOL ACCELERATIONS	
PROFILE	POOL ACCELERATION (ft/sec ²)
B	155.0
C	115.0
D	75.0
E	35.0
F	15.0

1. POOL ACCELERATIONS DUE TO HARMONIC APPLICATION OF TORUS SHELL PRESSURES SHOWN IN FIGURE 2-2.2-12 AT A SUPPRESSION CHAMBER FREQUENCY OF 16.53 HERTZ.

Figure 3-2.2-11

POOL ACCELERATION PROFILE FOR DOMINANT SUPPRESSION CHAMBER FREQUENCY AT MIDBAY LOCATION

3-2.2.2 Load Combinations

The load categories and associated load cases for which the vent system is evaluated are presented in Section 3-2.2.1. The general NUREG-0661 criteria for grouping the respective loads and load categories into event combinations are discussed in Section 1-3.2 (Table 3-2.2-26).

The 27 general event combinations shown are expanded to form a total of 69 specific vent system load combinations for the Normal Operating, SBA, IBA, and DBA events. The specific load combinations reflect a greater level of detail than is contained in the general event combinations, including distinction between SBA and IBA, distinction between pre-chug and post-chug, and consideration of multiple cases of particular loadings. The total number of vent system load combinations consists of 3 for the Normal Operating event, 18 for the SBA event, 24 for the IBA event, and 24 for the DBA event. Several different service level limits and corresponding sets of allowable stresses are associated with these load combinations.

Not all of the possible vent system load combinations are evaluated since many are enveloped by others and do not lead to controlling vent system stresses. The enveloping load combinations are determined by examining the possible vent system load combinations and comparing the respective load cases and allowable stresses. Table 3-2.2-27 shows the results of this examination. Here each enveloping load combination is assigned a number for ease of identification.

The enveloping load combinations are further reduced by examining relative load magnitudes and individual load characteristics to determine which load combinations lead to controlling vent system stresses. The load combinations which have been found to produce controlling vent system stresses are the SBA II, IBA I, DBA I, DBA II, and DBA III combinations are used to evaluate stresses in all vent system components except those associated with the vent line-SRV piping penetrations. An explanation of the logic behind these controlling vent system load combinations is presented in the following paragraphs. Table 3-2.2-28 summarizes the controlling load combinations and identifies which load combinations are enveloped by each of the controlling combinations.

Many of the general event combinations (Table 3-2.2-26) have the same allowable stresses and are enveloped by others which contain the same or additional load cases. There is no distinction between Service Level A and B conditions for the vent system since the Service Level A and B allowable stress values are the same.

Except for seismic loads, many pairs of load combinations contain identical load cases. One of the load combinations in the pair contains OBE loads and has Service Level A or B allowables, while the other contains SSE loads with Service Level C allowables. Examining the load magnitudes presented in Section 3-2.2.1 shows that both the OBE and SSE vertical accelerations are small compared to gravity. As a result, vent system stresses and support column reactions due to vertical seismic loads are small compared to those caused by other loads in the load combination. The horizontal loads for OBE and SSE are less than 60% of gravity and result in small vent system stresses compared to those caused by other loads in the load combinations, except at the vent line-drywell penetrations which provide horizontal support for the vent system. The Service Level C primary stress allowables for the load combinations containing SSE loads are 40% to 80% higher than the Service Level B allowables for

the corresponding load combination containing OBE loads. Therefore, for evaluation of all vent system components except the vent line-drywell penetration, the controlling load combinations are those containing OBE loads and Service Level B allowables.

For the vent line-drywell penetration, evaluation of both OBE and SSE combinations is necessary since seismic loads are a large contributor to the total lateral load acting on the vent system for which the penetrations provide support.

Application of the above reasoning to the total number of vent system load combinations yields a reduced number of enveloping load combinations for each event. Table 3-2.2-27 shows the resulting vent system load combinations for the Normal Operating, SBA, IBA and DBA events, along with the associated service level assignments. For ease of identification, each load combination in each event is assigned a number. The reduced number of enveloping load combinations (Table 3-2.2-27) consists of one for the Normal Operating event, four for the SBA event, five for the the IBA event, and six for the DBA event. The load case designations for the loads which make up the combinations are the same as those presented in Section 3-2.2.1.

An examination of Table 3-2.2-27 shows that further reductions are possible in the number of vent system load combinations requiring evaluation. Any of the SBA or IBA combinations envelop the NOC I combination since they contain the same loadings as the NOC I combination and, in addition, contain CO or chugging loads. The NOC I combination does, however, result in local thermal effects in the vent line-SRV piping penetration when the penetration assembly is cold and the corresponding SRV piping is hot (during a SRV discharge). The SBA and IBA combinations, therefore, envelop the NOC I combination for all vent system components except the vent line-SRV piping penetration. The effects of the NOC I combination are also considered in the vent system fatigue evaluation.

The SBA II combination is the same as the IBA III combination, except for negligible differences in internal pressure loads. Thus, IBA III can be eliminated from consideration. The SBA II combination envelops the SBA I and IBA II combinations since the submerged structure loads due to post-chug are more severe than those due to pre-chug. According to the reasoning presented earlier for OBE and SSE loads, the SBA II combination envelops the SBA III, SBA IV,

IBA IV, and IBA V combinations, except when the effects of lateral loads on the vent line-drywell penetration are evaluated. Similarly, the SBA II combination envelops the DBA V and DBA VI combinations; these combinations, however, contain vent system discharge loads which are somewhat larger than the pressure loads for the SBA II combination. This effect is accounted for by substituting the vent system discharge loads which occur during the chugging phase of a DBA event for the SBA II pressure loads when evaluating this load combination.

Examination of Table 3-2.2-27 shows that the load combinations which result in maximum lateral loads on the vent line-drywell penetration are SBA IV, IBA V, and DBA VI. All of these contain SSE loads and chugging downcomer lateral loads which, when combined, result in the maximum possible lateral load on the vent system. As previously discussed, the SBA II combination envelops the above combinations, except for seismic loads. The effects of seismic loads are accounted for by substituting SSE loads for OBE loads when evaluating the SBA II combination.

The DBA I combination is evaluated based on normal operation, drywell-to-wetwell pressure differential conditions, with Service Level B limits assigned.

However, the effect of the loss of this differential pressure in the DBA I combination (with Service Level D limits), was also investigated and found not to be as critical as in the operating pressure differential condition.

The DBA II combination envelops the DBA IV combination since the SRV discharge loads which occur late in the DBA event have a negligible effect on the vent system. The DBA II combination also has more restrictive allowables than the DBA IV combination.

The controlling vent system load combinations evaluated in the remaining sections can now be summarized. The SBA II, IBA I, DBA I, DBA II, and DBA III combinations are evaluated for all vent system components except those associated with the vent line-SRV piping penetration, which are evaluated in Volume 5 of this report. As previously noted, SSE loads and the vent system discharge loads which occur during the chugging phase of the DBA event are conservatively substituted for OBE loads and the SBA pressure loads when evaluating the SBA II load combination.

To ensure that fatigue is not a concern for the vent system over the life of the plant, the combined effects

of fatigue due to Normal Operating plus SBA events and Normal Operating plus IBA events are evaluated. Figures 3-2.2-12, 3-2.2-13 and 3-2.2-14 show the relative sequencing and timing of each loading in the SBA, IBA, and DBA events used in this evaluation. The fatigue effects for Normal Operating plus DBA events are enveloped by the Normal Operating plus SBA or IBA events since the combined effects of SRV discharge loads and other loads for the SBA and IBA events are more severe than those for DBA. Table 3-2.2-27 summarizes additional information used in the vent system fatigue evaluation.

The load combinations and event sequencing described in the preceding paragraphs envelop those which could actually occur during a LOCA or SRV discharge event. An evaluation of these load combinations results in a conservative estimate of the vent system response and leads to bounding values of vent system stresses and fatigue effects.

Table 3-2.2-26

MARK I CONTAINMENT EVENT COMBINATIONS⁽¹⁾

EVENT COMBINATIONS		SRV			SBA IBA		SBA + EQ IBA + EQ				SBA+SRV IBA+SRV		SBA + SRV + EQ IBA + SRV + EQ				DBA		DBA + EQ				DBA + SRV + EQ							
		0	1	2	CO, CH	0	1	2	3	4	5	6	7	8	9	10	11	PS (2)	CO, CH	0	1	2	3	4	5	6	7	8	9	
TYPE OF EARTHQUAKE		0	1	2		0	1	2	3				0	1	2	3			0	1	2	3				0	1	2	3	
COMBINATION NUMBER		1	2	3		4	5	6	7	8	9	10	11	12	13	14	15	16	17	18	19	20	21	22	23	24	25	26	27	
LOADS	NORMAL	N	X	X	X	X	X	X	X	X	X	X	X	X	X	X	X	X	X	X	X	X	X	X	X	X	X	X	X	
	EARTHQUAKE	EQ		X	X			X	X	X	X			X	X	X	X		X	X	X	X				X	X	X	X	
	SRV DISCHARGE	SRV	X	X	X							X	X	X	X	X	X						X	X	X	X	X	X	X	
	LOCA THERMAL	T _A				X	X	X	X	X	X	X	X	X	X	X	X	X	X	X	X	X	X	X	X	X	X	X	X	X
	LOCA REACTIONS	R _A				X	X	X	X	X	X	X	X	X	X	X	X	X	X	X	X	X	X	X	X	X	X	X	X	X
	LOCA QUASI-STATIC PRESSURE	P _A				X	X	X	X	X	X	X	X	X	X	X	X	X	X	X	X	X	X	X	X	X	X	X	X	X
	LOCA POOL SWELL	P _{PS}																X		X	X			X		X	X			
	LOCA CONDENSATION OSCILLATION	P _{CO}					X			X	X		X			X	X		X				X	X		X			X	X
LOCA CHUGGING	P _{CH}					X			X	X		X			X	X		X				X	X		X			X	X	

- (1) SEE SECTION 1-3.2 FOR ADDITIONAL EVENT COMBINATION INFORMATION.
- (2) WITH THE LOSS OF NORMAL OPERATING DRYWELL/WETWELL PRESSURE DIFFERENTIAL, LEVEL D SERVICE LIMITS ARE ASSIGNED.

Table 3-2.2-27

CONTROLLING VENT SYSTEM LOAD COMBINATIONS

SECTION 3-2.2.1 LOAD DESIGNATION	CONDITION/EVENT	NOC	SBA				IBA					DBA					
	VOLUME 3 LOAD COMBINATION NUMBER	I	I	II	III	IV	I	II	III	IV	V	I	II	III	IV	V	VI
	TABLE 3-2.2-24 LOAD COMBINATION NUMBER	2	14	14	15	15	14	14	14	15	15	18	20	25	27	27	27
DEAD WEIGHT		1a															1a
SEISMIC	OBE	2a		2a			2a		2a			2a	2a				
	SSE				2b	2b				2b	2b			2b			2b
PRESSURE ⁽¹⁾		P ⁽²⁾	P ₂ , P ₃	P ₂ , P ₃	P ₂ , P ₃	P ₂ , P ₃	P ₂ , P ₃	P ₂ , P ₃	P ₂ , P ₃	P ₂ , P ₃	P ₂ , P ₃	P ₁	P ₃	P ₁	P ₃	P ₄	P ₄
TEMPERATURE ⁽³⁾		T ⁽⁴⁾	T ₂ , T ₃	T ₂ , T ₃	T ₂ , T ₃	T ₂ , T ₃	T ₂ , T ₃	T ₂ , T ₃	T ₂ , T ₃	T ₂ , T ₃	T ₂ , T ₃	T ₁	T ₃	T ₁	T ₃	T ₄	T ₄
VENT SYSTEM DISCHARGE												4a					4a
POOL SWELL												5a-5f		5a, 5f			
CONDENSATION OSCILLATION							6a, 6c 6c						6b, 6d 6f		6b, 6d 6f		
CHUGGING	PRE-CHUG		7a-7c		7a-7c			7a-7c		7a-7c						7a-7c	
	POST-CHUG			7a, 7b 7d		7a, 7b 7d			7a, 7b 7d		7a, 7b 7d						7a, 7b 7d
SRV DISCHARGE		8b									8b		8b	8b ⁽⁵⁾	8b	8b	
PIPING REACTIONS		9a															9a
CONTAINMENT INTERACTION		10a															10a
SERVICE LEVEL		0	B	0	C	C	0	B	B	C	C	0 ^(6, 7)	0 ⁽⁷⁾	C	C	C	C
NUMBER OF EVENT OCCURENCES ⁽⁸⁾		150	1														1
NUMBER OF SRV ACTUATIONS ⁽⁹⁾		550	50			50	25				25	0	0	1			1

NOTES TO TABLE 3-2.2-27

- (1) SEE FIGURES 3-2.2-1 THROUGH 3-2.2-3 FOR SBA, IBA, AND DBA INTERNAL PRESSURE VALUES.
- (2) THE RANGE OF NORMAL OPERATING INTERNAL PRESSURES IS -0.2 TO 1.0 PSI AS SPECIFIED BY THE SAR.
- (3) SEE FIGURES 3-2.2-4 THROUGH 3-2.2-6 FOR SBA, IBA, AND DBA TEMPERATURE VALUES.
- (4) THE RANGE OF NORMAL OPERATING TEMPERATURES IS 70.0° TO 131.0°F AS SPECIFIED BY THE SAR. SEE TABLE 3-2.2-2 FOR ADDITIONAL NORMAL OPERATING TEMPERATURES.
- (5) THE SRV DISCHARGE LOADS WHICH OCCUR DURING THIS PHASE OF THE DBA EVENT HAVE A NEGLIGIBLE EFFECT ON THE VENT SYSTEM.
- (6) EVALUATION OF PRIMARY-PLUS-SECONDARY STRESS RANGE OR FATIGUE IS NOT REQUIRED; SHELL STRESSES DUE TO THE LOCAL POOL SWELL IMPINGEMENT PRESSURES DO NOT EXCEED SERVICE LEVEL C LIMITS.
- (7) THE ALLOWABLE STRESS VALUE FOR LOCAL PRIMARY MEMBRANE STRESS AT PENETRATIONS IS INCREASED BY 1.3.
- (8) THE NUMBER OF SEISMIC LOAD CYCLES USED FOR FATIGUE IS 1,000.
- (9) THE VALUES SHOWN ARE CONSERVATIVE ESTIMATES OF THE NUMBER OF ACTUATIONS EXPECTED FOR A BWR 3 PLANT WITH A REACTOR SIZE OF 251.

COM-02-041-3
Revision 0

3-2.106

COM-02-041-3
Revision 0

Table 3-2.2-28

ENVELOPING LOGIC FOR CONTROLLING
VENT SYSTEM LOAD COMBINATIONS

CONDITION/EVENT		NOC	SBA				IBA					DBA							
TABLE 3-2.2.24 ENVELOPING LOAD COMBINATIONS		2	14	14	15	15	14	14	14	15	15	18	20	25	27	27	27		
TABLE 3-2.2-24 LOAD COMBINATIONS ENVELOPED		1	4-6, 8, 10-12	4-6, 8, 10-12	3,7, 9, 13	3,7, 9, 13	4-6, 8, 10-12	4-6, 8, 10-12	4-6, 8, 10-12	3,7, 9, 13	3,7, 9, 13	16	17	19, 22, 24	21, 23, 26	21, 23, 26	21, 23, 26		
VOLUME 3 LOAD COMBINATION DESIGNATION		I	I	II	III	IV	I	II	III	IV	V	I	II	III	IV	V	VI		
CONTROLLING LOAD COMBINATIONS EVALUATED	VENT SYSTEM COMPONENTS AND SUPPORTS	SBA II (1)	X	X		X	X		X	X	X					X	X		
		IBA I	X																
		DBA I																	
		DBA II														X			
		DBA III																	

1. SSE LOADS AND DBA PRESSURIZATION AND THRUST LOADS ARE SUBSTITUTED FOR OBE LOADS AND SBA II INTERNAL PRESSURE LOADS WHEN EVALUATING THE SBA II LOAD COMBINATION.

3-2.107

SECTION 3-2.2.1 LOAD DESIGNATION

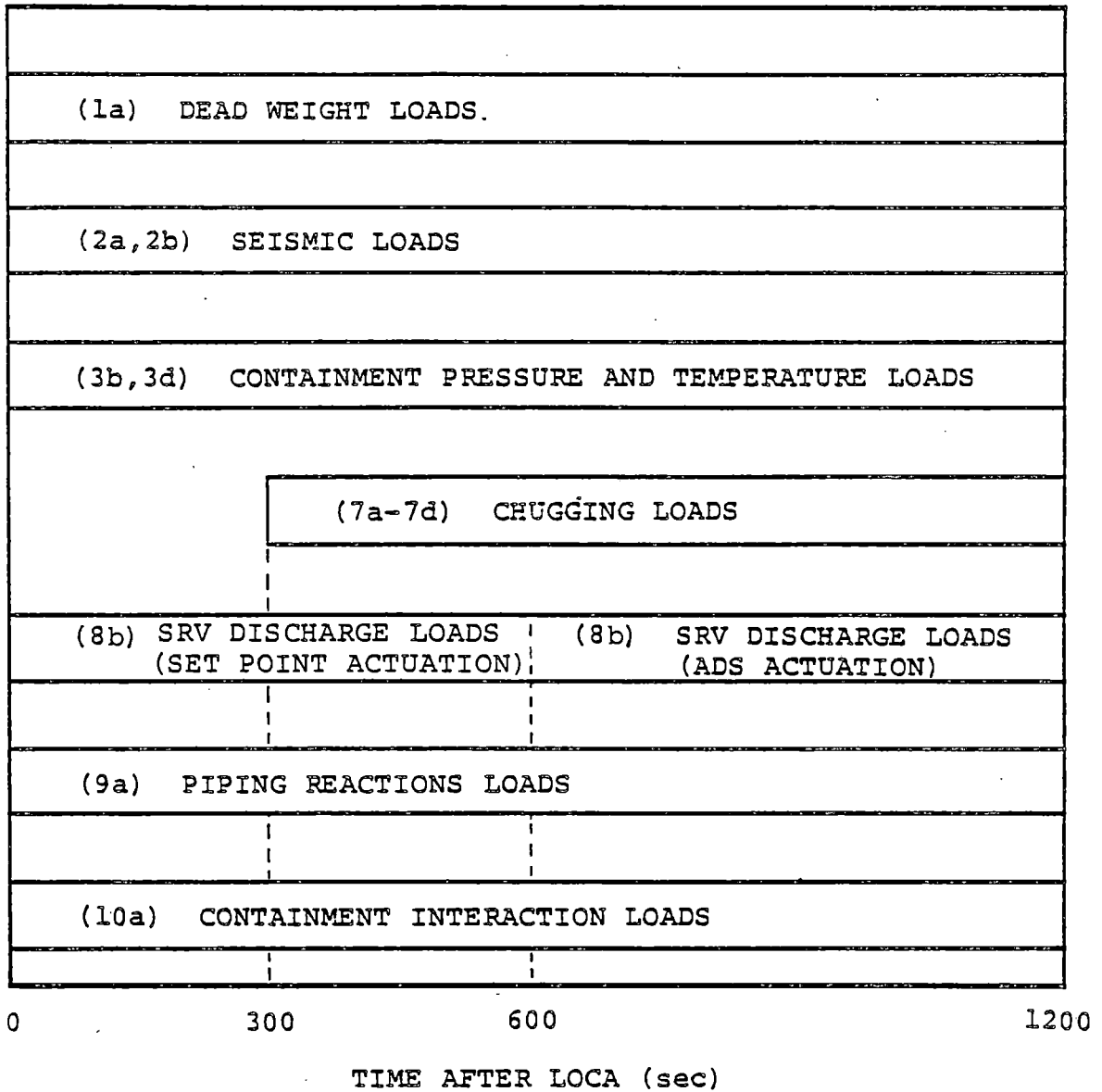


Figure 3-2.2-12

VENT SYSTEM SBA EVENT SEQUENCE

SECTION 3-2.2.1 LOAD DESIGNATION

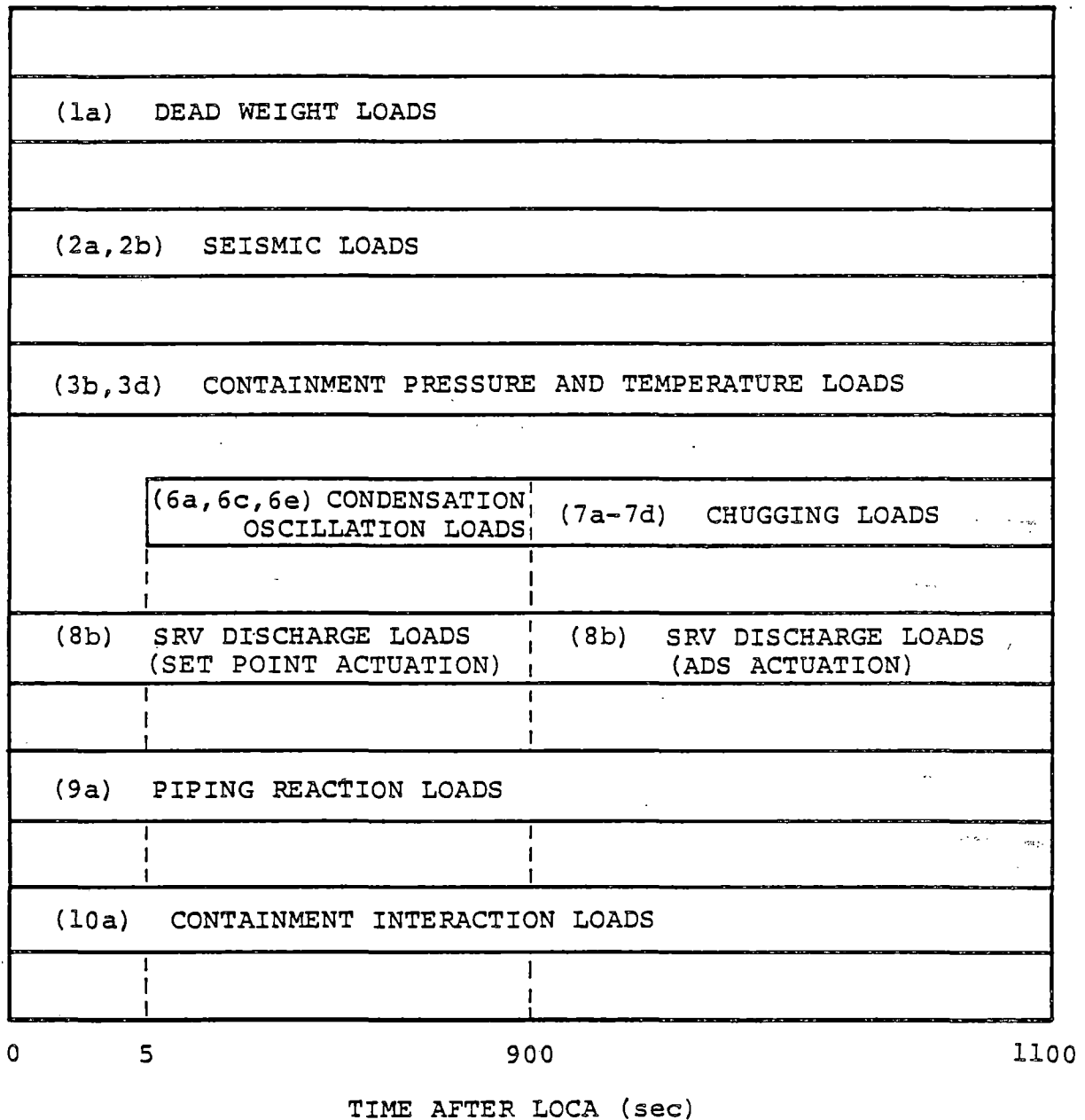
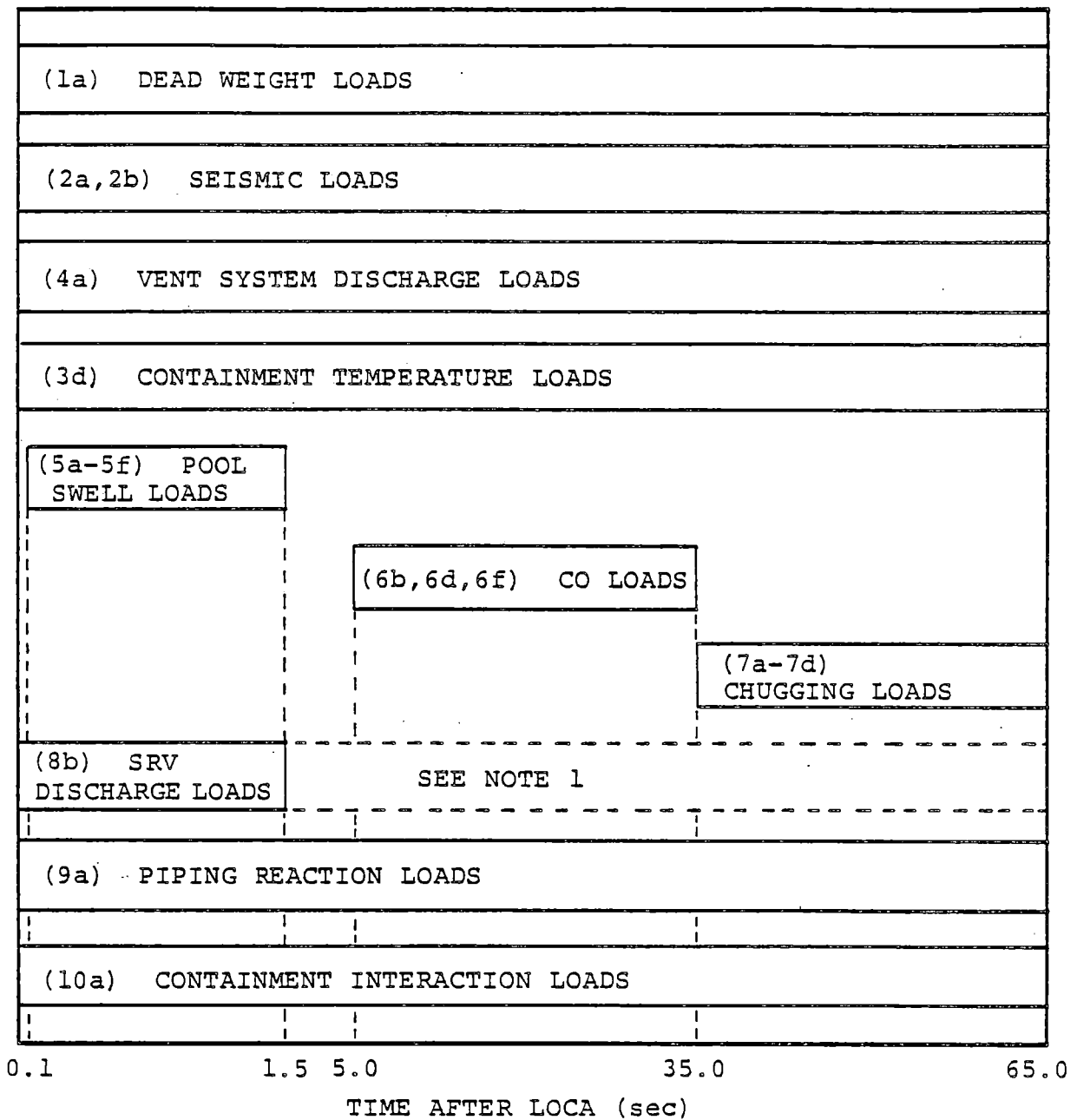


Figure 3-2.2-13
VENT SYSTEM IBA EVENT SEQUENCE

SECTION 3-2.2.1 LOAD DESIGNATION



1. THE SRV DISCHARGE LOADS WHICH OCCUR DURING THIS PHASE OF THE DBA EVENT ARE NEGLIGIBLE.

Figure 3-2.2-14

VENT SYSTEM DBA EVENT SEQUENCE

3-2.3 Acceptance Criteria

The NUREG-0661 acceptance criteria on which the Dresden Units 2 and 3 vent system analysis is based are discussed in Section 1-3.2. In general, the acceptance criteria follow the rules contained in the ASME Code, Section III, Division 1, including the Summer 1977 Addenda for Class MC components and component supports (Reference 6). The corresponding service limit assignments, jurisdictional boundaries, allowable stresses, and fatigue requirements are consistent with those contained in the applicable subsections of the ASME Code and the PUAAG. The following paragraphs summarize the acceptance criteria used in the analysis of the vent system.

The items evaluated in the analysis of the vent system are the vent lines, the spherical junction, the vent header, the downcomers, the downcomer ring plates, the support columns and associated support elements, the drywell shell near the vent line penetrations, the vent header deflectors, the downcomer-vent header intersection stiffener plates, the downcomer bracing systems, the vent header support collar, and the vent line bellows assemblies. Figures 3-2.1-1 through 3-2.1-16 identify the specific components associated with each of these items.

The vent lines, the vent line-vent header spherical junctions, the vent header, the downcomers, the drywell shell, the downcomer-vent header intersection stiffener plates, the downcomer ring plates, and the vent header support collars are evaluated in accordance with the requirements for Class MC components contained in Subsection NE of the ASME Code. Fillet welds and partial penetration welds joining these components or attaching other structures to them are also examined in accordance with the requirements for Class MC welds contained in Subsection NE of the ASME Code.

The support columns, the downcomer bracing members, and the associated connecting elements and welds are evaluated in accordance with the requirements contained in Subsection NF of the ASME Code for Class MC component supports. The vent header deflectors and associated components and welds are also evaluated in accordance with the requirements for Class MC component supports, with allowable stresses corresponding to Service Level D limits.

The NOC I, SBA II, IBA I, DBA I, and DBA II combinations all have Service Level B limits, while the DBA III combination has Service Level C limits (Table 3-2.2-27). Since these load combinations have somewhat

different maximum temperatures, the allowable stresses for the two load combination groups with Service Level B and C limits are conservatively determined at the highest temperature for each load combination group.

The allowable stresses for all the major components of the vent system, such as the vent line, the spherical junction, the vent header and the downcomers, are determined at the maximum DBA temperature of 284°F. Table 3-2.3-1 shows the allowable stresses for the load combinations with Service Level B and C limits.

Table 3-2.3-2 shows the allowable displacements and associated number of cycles for the vent line bellows. These values are taken from the design specification, as permitted by NUREG-0661, in cases where the analysis technique used in the evaluation is the same as that contained in the plant's design specification.

The acceptance criteria described in the preceding paragraphs result in conservative estimates of the existing margins of safety and assure that the original vent system design margins are restored.

Table 3-2.3-1

ALLOWABLE STRESSES FOR VENT SYSTEM
COMPONENTS AND COMPONENT SUPPORTS

ITEM	MATERIAL	MATERIAL PROPERTIES ⁽¹⁾ (ksi)	STRESS TYPE	ALLOWABLE STRESS (ksi)		
				SERVICE ⁽²⁾ LEVEL B	SERVICE ⁽³⁾ LEVEL C	
COMPONENTS	DRYWELL SHELL	SA-516 GRADE 70	$s_{mc} = 19.30$ $s_{ml} = 22.61$ $s_y = 33.87$	LOCAL PRIMARY MEMBRANE	28.95	50.81
				PRIMARY + ⁽⁴⁾ SECONDARY STRESS RANGE	67.83	N/A
	VENT LINE	SA-516 GRADE 70	$s_{mc} = 19.30$ $s_{ml} = 22.61$ $s_y = 33.87$	PRIMARY MEMBRANE	19.30	33.87
				LOCAL PRIMARY MEMBRANE	28.95	50.81
				PRIMARY + ⁽⁴⁾ SECONDARY - STRESS RANGE	67.83	N/A
	VENT LINE/ VENT HEADER SPHERICAL JUNCTION	SA-516 GRADE 70	$s_{mc} = 19.30$ $s_{ml} = 22.61$ $s_y = 33.87$	PRIMARY MEMBRANE	19.30	33.87
				LOCAL PRIMARY MEMBRANE	28.95	50.81
				PRIMARY + ⁽⁴⁾ SECONDARY STRESS RANGE	67.83	N/A
	VENT HEADER	SA-516 GRADE 70	$s_{mc} = 19.30$ $s_{ml} = 22.61$ $s_y = 33.87$	PRIMARY MEMBRANE	19.30	33.87
				LOCAL PRIMARY MEMBRANE	28.95	50.81
				PRIMARY + ⁽⁴⁾ SECONDARY STRESS RANGE	67.83	N/A
	DOWNCOMER	SA-516 GRADE 70	$s_{mc} = 19.30$ $s_{ml} = 22.61$ $s_y = 33.87$	PRIMARY MEMBRANE	19.30	33.87
				LOCAL PRIMARY MEMBRANE	28.95	50.81
				PRIMARY + ⁽⁴⁾ SECONDARY STRESS RANGE	67.83	N/A
	SUPPORT COLLAR PLATE	SA-516 GRADE 70	$s_{mc} = 19.30$ $s_{ml} = 22.61$ $s_y = 33.87$	PRIMARY MEMBRANE	19.30	33.87
				LOCAL PRIMARY MEMBRANE	28.95	50.81
				PRIMARY + ⁽⁴⁾ SECONDARY STRESS RANGE	67.83	N/A
	COMPONENT SUPPORTS	COLUMNS ⁽⁷⁾	SA-333 GRADE 1	$s_y = 28.27$	BENDING	18.66
TENSILE					16.96	22.61
COMBINED					1.00	1.00
COMPRESSIVE					11.84	15.79
INTERACTION					1.00	1.00
WELDS	SUPPORT COLLAR PLATE TO VENT HEADER	SA-516 GRADE 70	$s_{mc} = 19.30$ $s_y = 33.87$	PRIMARY	15.01	26.42
				SECONDARY	45.03	N/A

COM-02-041-3
Revision 0

3-2.114

NOTES TO TABLE 3-2.3-1

- (1) MATERIAL PROPERTIES TAKEN AT MAXIMUM EVENT TEMPERATURES.
- (2) SERVICE LEVEL B ALLOWABLES ARE USED WHEN EVALUATING NOC I, SBA II, IBA I, DBA I, AND DBA II LOAD COMBINATION RESULTS.
- (3) SERVICE LEVEL C ALLOWABLES ARE USED WHEN EVALUATING THE DBA III LOAD COMBINATION RESULTS.
- (4) THERMAL BENDING STRESSES ARE EXCLUDED WHEN EVALUATING PRIMARY-PLUS-SECONDARY STRESS RANGE.
- (5) EVALUATION OF PRIMARY-PLUS-SECONDARY STRESS INTENSITY RANGE AND FATIGUE ARE NOT REQUIRED FOR LOAD COMBINATION DBA I.
- (6) THE ALLOWABLE STRESSES FOR LOCAL PRIMARY MEMBRANE STRESSES AT PENETRATIONS ARE INCREASED BY 1.3 WHEN EVALUATING LOAD COMBINATIONS DBA I AND DBA II.
- (7) STRESSES DUE TO THERMAL LOADS MAY BE EXCLUDED WHEN EVALUATING COMPONENT SUPPORTS.

Table 3-2.3-2

ALLOWABLE DISPLACEMENTS AND CYCLES
FOR VENT LINE BELLOWS

TYPE		ALLOWABLE VALUE (INCH)
AXIAL	COMPRESSION	0.875
	EXTENSION	0.375
LATERAL	MERIDIONAL	±0.625
	LONGITUDINAL	±0.625
NUMBER OF CYCLES OF MAXIMUM DISPLACEMENTS		1000

3-2.4 Methods of Analysis

Section 3-2.2.1 presents the governing loads for which the Dresden Units 2 and 3 vent systems are evaluated. Section 3-2.4.1 discusses the methodology used to evaluate the vent system for the overall effects of all loads except for those loads which exhibit asymmetric characteristics. The effects of asymmetric loads on the vent system are evaluated using the methodology discussed in Section 3-2.4-2. The methodology used to examine the local effects at the penetrations and intersections of the vent system major components is discussed in Section 3-2.4.3.

Section 3-2.4.4 discusses the methodology used to formulate results for the controlling load combinations, examines fatigue effects, and evaluates the analysis results for comparison with the applicable acceptance limits.

3-2.4.1 Analysis for Major Loads

With the exception of a few minor differences, the Dresden Units 2 and 3 vent system geometry is identical to that of Quad Cities Units 1 and 2. These differences are:

- o The vent line angle of inclination at Dresden is approximately one degree higher than at Quad Cities.
- o The Dresden units drywell-vent line penetrations include a 1/2" thick conical transition segment connected to a 3-5/8" thick cylindrical nozzle at the drywell ends. The Quad Cities penetrations include a 1/2" thick spherical transition segment connected to a 3" thick nozzle at the drywell ends.
- o The inclined portion of the downcomer is 1/2" thick in the Dresden units, whereas in Quad Cities it is 3/8" thick.
- o The vacuum breakers in the Dresden units are located outside of the suppression chambers, and their headers penetrate the vent lines near the

drywell ends; in the Quad Cities units they are attached to the vent line-vent header spherical junctions.

The effect of these differences in the overall vent system analysis were investigated and found to be insignificant. Therefore, the analyses were performed on analytical models which are based on Quad Cities Units 1 and 2 plant unique geometry. Various models used in the analysis are described in the following paragraphs.

With the exception of the non-repetitive pattern of the downcomer longitudinal bracing system in Dresden Unit 2, the repetitive nature of the vent system geometry is such that the vent system can be divided into 16 identical segments which extend from midbay (MB) of the vent line bay to midbay of the non-vent line bay (Figure 3-2.1-1). To account for the non-repetitive pattern of the longitudinal bracing system in Dresden Unit 2, two conditions may be idealized. First, it is assumed the bracing system is included in the 1/16 segment. In this assumption, all 96 downcomers are assumed to be braced longitudinally (100% bracing condition). Second, it is assumed that the 1/16 segments do not include any bracing system. With this

assumption, a no bracing condition is developed. These two idealized conditions will bound any particular bracing condition which might exist in any particular 1/16 segment of the two Dresden vent systems. The governing loads which act on the vent system, except for seismic loads and a few chugging load cases, exhibit symmetric or anti-symmetric characteristics (or both) with respect to a 1/16 segment of the vent system. The analysis of the vent system for the majority of the governing loads is therefore performed for the two 1/16 segments described above.

Two beam models of the 1/16 segment reflecting the above conditions are used to obtain the response of the vent system to all loads except those resulting in asymmetric effects on the vent system. The resulting responses from the two models are compared and the more severe of the two is selected for Code evaluation (Figures 3-2.4-1 and 3-2.4-2). The models include the vent line, the vent header, the downcomers, the support columns, and the downcomer lateral bracings. The longitudinal bracing is also included in one model.

The local stiffness effects at the penetrations and intersections of the major vent system components (Figures 3-2.1-7, 3-2.1-8, and Figures 3-2.1-10 through 3-2.1-12) are included by using stiffness matrix

elements of these penetrations and intersections. A matrix element for the vent line-drywell penetration, which connects the upper end of the vent line to the transition segment, is developed using the finite difference model of the penetration (Figure 3-2.4-3). A matrix element which connects the lower end of the vent line to the beams on the centerline of the vent header and to the beams on the centerline of the Quad Cities vacuum breaker nozzles, is developed using the finite element model of the vent line-vent header spherical junction (Figure 3-2.4-4).

Finite element models of each downcomer-vent header intersection, similar to the one shown in Figure 3-2.4-5, are used to develop matrix elements which connect the beams on the centerline of the vent header to the upper ends of the downcomers at the downcomer miters. The length of the vent header segment in the analytical models used for downcomer-vent header intersection stiffness determination is increased to ensure that vent header ovaling effects are properly accounted for. Use of this modeling approach has been verified using results from FSTF tests. Additional information on the analytical models used to evaluate the penetrations and intersections of major vent system components is contained in Section 3-2.4.3.

The 1/16 beam model with longitudinal bracing contains 217 nodes, 214 beam elements, and 5 matrix elements. The model without the bracing contains 205 nodes, 192 beam elements, and 5 matrix elements. The node spacings used in the two analytical models are identical and are refined to ensure adequate distribution of mass and determination of component frequencies and mode shapes and to facilitate accurate application of loadings. The stiffness and mass properties used in the two models are identical and are based on the nominal dimensions and densities of the materials used to construct the vent system. Small displacement linear-elastic behavior is assumed throughout.

The boundary conditions used in the two 1/16 beam models are both physical and mathematical in nature. The physical boundary conditions consist of pins provided at the attachments of the support columns to the suppression chamber ring girder. The vent system columns are also assumed to be pinned in all directions at their upper ends. Additional physical boundary conditions include the elastic restraints provided at the attachment of the vent line to the drywell. The associated vent line-drywell penetration stiffnesses are included as a stiffness matrix element; its

development is discussed in the preceding paragraphs. The mathematical boundary conditions consist of either symmetry, anti-symmetry, or a combination of both at the midbay planes, depending on the characteristics of the load being evaluated.

Additional mass is lumped along the length of the submerged portions of the downcomers, support columns, and bracings to account for the effective mass of water which acts with these components during dynamic loadings. The total mass of water added is equal to the mass of water displaced by each of these components. For all but the pool swell and CO dynamic loadings, the mass of water inside the submerged portion of the downcomers is included. The downcomers are assumed to contain air or steam (or both) during pool swell and condensation oscillation. The mass of this mixture is considered negligible.

A modal extraction analysis is performed using the two 1/16 beam models of the vent system for the case with water inside the downcomers and for the case with no water inside the downcomers. All structural modes in the range of 0 to 60 hertz and 0 to 200 hertz, respectively, are extracted for these cases. Tables 3-2.4-1 through 3-2.4-4 show the resulting frequencies and mass

participation factors. A comparison of the two 1/16 beam models' frequency analyses indicates that the two models have very similar dynamic behavior. As a result, in the remaining portion of this section, the results presented are based on the model which yields the higher magnitude of loads and stresses, where applicable.

Dynamic analyses using the two 1/16 beam models of the vent system are performed for the pool swell loads and CO loads specified in Section 3-2.2-1. The analyses consist of a transient analysis for pool swell loads and a harmonic analysis for CO loads. The modal superposition technique with 2% damping is utilized in both the transient and harmonic analyses. The pool swell and CO load frequencies are enveloped by including vent system frequencies to 100 hertz and 50 hertz, respectively.

The remaining vent system load cases specified in Section 3-2.2.1 involve either static loads or dynamic loads, which are evaluated using an equivalent static approach. For the latter, conservative dynamic amplification factors are developed and applied to the maximum spatial distributions of the individual dynamic loadings.

The effects of asymmetric loads are evaluated using the two 180° beam models (discussed in Section 3-2.4.2). Inertia forces due to horizontal seismic loads and concentrated forces due to chugging downcomer lateral loads are also applied to the 180° beam model. Additional information related to the vent system analysis for asymmetric loads is provided in Section 3-2.4.2.

The two 1/16 beam models are also used to generate loads for the evaluation of stresses in the major vent system component penetrations and intersections. Beam end loads, distributed loads, reaction loads, and inertia loads are developed from the two models and the critical cases are applied to the detailed analytical models of the vent system penetrations and intersections (Figures 3-2.4-3 through 3-2.4-5). Additional information related to the vent system penetrations and intersection stress evaluation is provided in Section 3-2.4.3.

The specific treatment of each load in the load categories identified in Section 3-2.2.1 is discussed in the following paragraphs.

1. Dead Weight Loads

- a. Dead Weight of Steel: A static analysis is performed for a unit vertical acceleration applied to the weight of vent system steel.

2. Seismic Loads

- a. OBE Loads: A static analysis is performed for a 0.067g vertical seismic acceleration applied to the weight of steel included in the 180° symmetric beam model. An additional static analysis is performed for the associated inertia loads generated for a 0.25g seismic acceleration applied in each horizontal direction using the 180° symmetric and anti-symmetric beam model, respectively. The results of the three earthquake directions are combined using the square root of the sum of the squares (SRSS).
- b. SSE Loads: The procedure used to evaluate the 0.134g vertical and 0.50g horizontal SSE accelerations is the same as that discussed for OBE loads in Load Case 2a.

3. Pressure and Temperature Loads

a. Normal Operating Internal Pressure Loads: A static analysis is performed for a 1.2 psi internal pressure applied as concentrated forces to the unreacted areas of the vent system.

b. LOCA Internal Pressure Loads: A static analysis is performed for the SBA and IBA net internal pressures applied as concentrated forces to the unreacted areas of the major components of the vent system. Figures 3-2.2-1 through 3-2.2-3 show these pressures. The effects of DBA internal pressure loads are included in the pressurization and thrust loads discussed in Load Case 4a.

The movement of the suppression chamber due to internal pressure, although small in magnitude, is also applied.

c. Normal Operating Temperature Loads: A static analysis is performed for the maximum normal operating temperature (Table 3-2.2-2). This temperature is uniformly applied to the portion of the vent system inside the suppres-

sion chamber. Corresponding temperatures of 70°F for the drywell and vent system components outside the suppression chamber and 131°F for the suppression chamber are also applied in this analysis.

- d. LOCA Temperature Loads: A static analysis is performed for the SBA, IBA, and DBA temperatures, which are uniformly applied to the major components and external components of the vent system. Figures 3-2.2-4 through 3-2.2-6 show these temperatures. Initial displacements are induced at the support column attachment points to the suppression chamber to consider the thermal expansion of the torus.

Concentrated forces are applied at the vent line-drywell penetration to account for the thermal expansion of the drywell during the SBA, IBA, and DBA events. The greater of the temperatures specified in Figure 3-2.2-4 and Table 3-2.2-2 is used in the analysis for SBA temperatures.

4. Vent System Discharge Loads

- a. DBA Pressurization and Thrust Loads: An equivalent static analysis is performed for the DBA pressurization and thrust loads. Table 3-2.2-3 shows these loads. The values of the loads include dynamic amplification factors, which are computed on the basis of methods described in Reference 11 and through use of the dominant frequencies of affected components. The dominant frequencies are derived from harmonic analyses of these components. Figures 3-2.4-6 through 3-2.4-8 show the results of these harmonic analyses.

5. Pool Swell Loads

- a. Vent System Impact and Drag Loads: A dynamic analysis is performed for the vent line, the vent header, the spherical junction, downcomers, and the vent header deflector pool swell impact loads (Table 3-2.2-4, Figures 3-2.2-7 and 3-2.2-8).
- b. Drag Loads on Submerged Structures: A dynamic analysis is performed for pool swell drag loads on the downcomer longitudinal bracing. Table 3-2.2-5 shows these loads.

- c. Froth Impingement and Fallback Loads: A dynamic analysis is performed for froth impingement and fallback loads on the vent line and spherical junction.

- d. Pool Fallback Loads: Dynamic loads associated with pool fallback loads are calculated for the downcomer lateral bracings, the downcomer ring plates, and the downcomer longitudinal bracing. For these dynamic loads, equivalent static loads are obtained which are applied to these components. Table 3-2.2-5 shows these loads.

- e. LOCA Water Jet Loads: An equivalent static analysis is performed for LOCA water clearing submerged structure loads on the vent system support columns. Table 3-2.2-6 shows these loads. The values of the loads include dynamic amplification factors which are computed on the basis of methods described in Reference 11 and through use of the dominant frequency of the support columns. The dominant frequencies are derived from harmonic

analyses of these components. Figure 3-2.4-6 shows the results of these harmonic analyses.

f. LOCA Bubble-Induced Loads: An equivalent static analysis is performed for LOCA air clearing submerged structure loads on the downcomers, the downcomer lateral bracings, the downcomer ring plates, the downcomer longitudinal bracing, and the support columns. Tables 3-2.2-6, 3-2.2-7, and 3-2.2-8 show these loads. The values of the loads include dynamic amplification factors computed using the dominant frequencies of the affected structures. The dominant frequencies are derived from harmonic analyses of these components (Figures 3-2.4-6 through 3-2.4-11).

6. Condensation Oscillation Loads

a. IBA CO Downcomer Loads: A dynamic analysis is performed for the IBA CO downcomer loads (Table 3-2.2-9). The dominant downcomer frequency is determined from the harmonic results. Figure 3-2.4-12 indicates that the dominant downcomer frequency occurs in the frequency range of the second CO downcomer

load harmonic. The first and third CO downcomer load harmonics are therefore applied at frequencies equal to 0.5 and 1.5 times the value of the dominant downcomer frequency.

- b. DBA CO Loads: The procedure used to evaluate the DBA CO downcomer loads (Table 3-2.2-10) is the same as that discussed for IBA CO downcomer loads in Load Case 6a.

- c. IBA CO Vent System Pressures: A dynamic analysis is performed for IBA CO vent system pressures on the vent line and vent header. Table 3-2.2-11 shows these loads. The dominant vent line and vent header frequencies are determined from the harmonic analysis results (Figure 3-2.4-13). An additional static analysis is performed for a 1.7 psi internal pressure applied as concentrated forces to the unreacted areas of the vent system.

- d. DBA CO Vent System Pressure Loads: The procedure used to evaluate the DBA CO vent system pressure loads (Table 3-2.2-11) is the

same as that discussed for IBA CO vent system pressure loads in Load Case 6c.

e. IBA CO Submerged Structure Loads: As previously discussed, pre-chug loads described in Load Case 7c are specified in lieu of IBA CO loads.

f. DBA CO Submerged Structure Loads: An equivalent static analysis is performed for the DBA CO submerged structure loads on the downcomer lateral bracings, the downcomer ring plates, the downcomer longitudinal bracing, and the support columns. Tables 3-2.2-12 and 3-2.2-13 show these loads, which include dynamic amplification factors computed using the methodology described for LOCA water jet and air bubble-induced drag loads in Load Cases 5e and 5f.

7. Chugging Loads

a. Chugging Downcomer Lateral Loads: A harmonic analysis of the downcomers is performed to determine the dominant downcomer frequency for use in calculating the maximum chugging

load magnitude. Figures 3-2.4-14 and 3-2.4-15 show the harmonic analysis results. Table 3-2.2-14 shows the resulting chugging load magnitudes. A static analysis using the 180° beam model is performed for chugging downcomer lateral Load Cases 1 through 10. Tables 3-2.2-15 and 3-2.2-16 show these load cases.

A static analysis is also performed for the maximum chugging load (Table 3-2.2-17) applied to a single downcomer in the in-plane and out-of-plane directions. The results of this analysis are used in evaluating fatigue.

- b. Chugging Vent System Pressures: A dynamic analysis is performed for the acoustic vent system pressure oscillation applied to the unreacted areas of the vent system. Table 3-2.2-19 shows these loads. The dominant vent line and vent header frequencies are determined from the harmonic analysis results (Figure 3-2.4-16). Gross vent system pressure oscillation with a frequency of 0.7 hertz is bounded by acoustic vent system

pressure oscillation with a frequency range of 6.9 to 9.5 hertz. Therefore, no separate analysis was performed for this case.

c. Pre-Chug Submerged Structure Loads: An equivalent static analysis is performed for the pre-chug submerged structure loads on the downcomer lateral bracing, the downcomer ring plates, the downcomer longitudinal bracing, and the support columns. Tables 3-2.2-19 and 3-2.2-20 show these loads. The loads include dynamic amplification factors which are computed using the methodology described for LOCA air bubble-induced drag loads on submerged structures in Load Case 5f.

d. Post-Chug Submerged Structure Loads: The procedure used to evaluate the post-chug submerged structure loads on the downcomer lateral bracings and the downcomer ring plates, the downcomer longitudinal bracing members, and the support columns is the same as that discussed for pre-chug submerged structure loads in Load Case 6c. Tables 3-2.2-21 and 3-2.2-22 show these loads.

8. Safety Relief Valve Discharge Loads

a. T-quencher Water Jet Loads: An equivalent static analysis is performed for SRV discharge water clearing submerged structure loads on the vent system support columns. Table 3-2.2-23 shows these loads. The values of the loads include dynamic amplification factors which are calculated on the basis of methods described in Reference 11 and use of the dominant frequency of the support columns.

b. SRV Bubble-Induced Drag Loads: An equivalent static analysis is performed for SRV discharge drag loads on the downcomers, the downcomer lateral bracing, the downcomer rings, the downcomer longitudinal bracing members, and the support columns. Tables 3-2.2-23, 3-2.2-24, and 3-2.2-25 show these loads. The loads include a DLF of 2.5, as discussed in Section 1-4.2.4.

9. Piping Reaction Loads

a. At the vent line-SRV piping penetration, the reaction loads are developed using the procedures described in Volume 5. These loads are

applied to the vent system model to evaluate the overall vent system response.

10. Containment Interaction Loads

- a. Containment Structure Motions: The motions of the drywell and the suppression chamber due to internal pressure and thermal expansion are applied to the 1/16 beam model. The motions caused by loads in other load categories acting on the drywell and suppression chamber have been evaluated and found to have a negligible effect on the vent system.

The methodology described in the preceding paragraphs results in a conservative evaluation of the vent system response and associated stresses for the governing loads.

Table 3-2.4-1

VENT SYSTEM FREQUENCY ANALYSIS RESULTS WITH WATER
INSIDE DOWNCOMERS, BASED ON DOWNCOMERS BRACED LONGITUDINALLY

MODE NUMBER	FREQUENCY (Hz)	MASS PARTICIPATION FACTOR (lb)		
		x (1)	y (1)	z (1)
1	9.277	14.91	0.32	16701.92
2	12.319	57.89	0.45	1014.07
3	12.336	0.86	0.00	7.63
4	12.336	1243.89	0.01	25.93
5	12.340	0.00	0.00	0.00
6	13.928	263.21	13.37	2204.80
7	23.065	170.21	263.75	2804.29
8	24.905	0.07	877.91	3260.09
9	26.778	7.19	8558.96	192.09
10	29.490	57.09	2826.57	148.13
11	30.484	63.54	86.51	211.65
12	31.153	101.72	89.42	2118.27
13	31.333	0.64	0.03	20.14
14	33.251	9.16	3248.48	466.12
15	42.011	20.92	3882.26	35.86
16	45.379	17.18	0.17	2.11
17	45.428	52.94	19.41	13.46
18	45.450	0.00	0.09	0.00
19	45.591	20.52	9.89	8.82
20	46.140	1974.73	347.75	186.46
21	49.788	51.46	12.76	12.50
22	50.384	138.71	63.57	9.30
23	50.763	5.22	4.88	19.92
24	51.855	6.68	0.52	4.39
25	51.910	0.27	0.00	0.02
26	51.915	34.42	1.48	2.18
27	51.969	0.23	0.06	123.16
28	54.878	190.32	67.57	906.60
29	60.750	5969.17	0.20	53.36

Table 3-2.4-2

VENT SYSTEM FREQUENCY ANALYSIS RESULTS WITHOUT WATER
INSIDE DOWNCOMERS, BASED ON DOWNCOMERS BRACED LONGITUDINALLY

MODE NUMBER	FREQUENCY (Hz)	MASS PARTICIPATION FACTORY (lb)		
		X (1)	Y (1)	Z (1)
1	11.251	3.57	0.17	13949.57
2	12.335	164.26	0.06	51.08
3	12.336	1127.06	0.02	14.63
4	12.340	0.00	0.00	0.00
5	12.369	1.80	0.35	122.94
6	17.326	209.78	43.66	2137.90
7	24.396	58.24	944.14	4900.36
8	26.767	1.71	8719.36	136.36
9	29.276	126.63	889.58	124.81
10	29.693	5.66	2206.97	0.01
11	30.571	8.64	1.73	13.20
12	31.331	0.25	0.86	2.60
13	31.791	88.29	19.47	2245.28
14	33.374	0.04	3188.73	838.22
15	42.107	0.29	3896.08	22.69
16	45.378	3.55	0.26	0.36
17	45.447	18.08	8.03	5.73
18	45.450	1.08	1.03	0.43
19	45.710	0.93	0.49	1.49
20	46.661	1693.78	297.06	108.40
21	49.914	0.20	19.63	12.18
22	50.522	12.67	69.14	18.07
23	51.005	5.26	5.90	43.99

Table 3-2.4-2

VENT SYSTEM FREQUENCY ANALYSIS RESULTS WITHOUT WATER
INSIDE DOWNCOMERS, BASED ON DOWNCOMERS BRACED LONGITUDINALLY

(Continued)

MODE NUMBER	FREQUENCY (Hz)	MASS PARTICIPATION FACTOR (lb)		
		X (1)	Y (1)	Z (1)
24	51.866	1.79	0.31	2.02
25	51.910	0.06	0.00	0.00
26	51.921	20.18	2.15	5.08
27	51.976	0.70	0.07	130.22
28	57.026	11.64	87.73	1037.09
29	72.082	1696.91	52.28	133.79
30	75.320	2592.92	11.49	23.99
31	81.639	3676.24	1.87	1.21
32	86.984	147.08	10.37	0.03
33	98.983	77.87	62.28	20.44
34	104.056	33.16	87.25	0.33
35	106.916	331.12	13.88	0.18
36	117.093	468.25	7.21	1.71
37	119.289	117.48	0.02	3.38
38	122.180	2399.03	0.76	44.96
39	123.984	84.18	1.86	0.02
40	124.575	7.25	0.03	22.95
41	124.605	0.00	0.00	5.79
42	124.621	0.00	0.00	0.00
43	124.939	86.47	0.18	0.35
44	128.170	196.78	38.45	16.42
45	131.974	371.66	77.83	5.03
46	135.544	409.87	16.26	0.27

Table 3-2.4-2

VENT SYSTEM FREQUENCY ANALYSIS RESULTS WITHOUT WATER
INSIDE DOWNCOMERS, BASED ON DOWNCOMERS BRACED LONGITUDINALLY

(Concluded)

MODE NUMBER	FREQUENCY (Hz)	MASS PARTICIPATION FACTOR (lb)		
		x (1)	y (1)	z (1)
47	138.842	141.08	65.09	4.66
48	142.816	48.30	0.03	9.73
49	144.294	14.10	4.57	1.38
50	148.277	34.36	0.08	0.06
51	151.016	626.81	12.51	11.86
52	155.896	108.64	0.17	5.43
53	156.475	406.52	2.81	7.48
54	156.850	626.25	2.79	11.57
55	157.193	99.69	0.58	1.98
56	158.028	23.70	0.00	0.81
57	158.456	52.55	0.22	6.45
58	163.809	368.44	17.50	2.31
59	166.077	58.27	0.05	0.03
60	170.558	38.68	1.93	10.84
61	171.660	2.39	31.03	0.98
62	181.975	62.99	0.16	1.25
63	188.423	0.00	7.41	8.92
64	191.721	109.35	11.93	8.50
65	194.756	0.00	0.48	0.07
66	197.158	10.61	1.47	2.49

(1) SEE FIGURE 3-2.4-1 FOR COORDINATE DIRECTIONS.

Table 3-2.4-3

VENT SYSTEM FREQUENCY ANALYSIS RESULTS WITH WATER
INSIDE DOWNCOMERS, BASED ON DOWNCOMERS NOT
BRACED LONGITUDINALLY

MODE NUMBER	FREQUENCY (Hz)	MASS PARTICIPATION FACTOR (lb)		
		X	Y	Z
1	9.170	6.28	0.25	13100.91
2	12.272	140.88	0.75	2416.99
3	12.334	1279.56	0.13	10.87
4	12.335	241.29	0.00	24.73
5	12.340	0.00	0.00	0.00
6	12.519	63.14	0.34	804.25
7	13.576	7195.09	29.14	366.76
8	13.824	271.25	0.99	63.70
9	14.195	2170.71	0.89	930.28
10	14.579	615.18	2.51	118.02
11	15.228	1315.30	1.13	1.67
12	15.781	223.59	58.44	217.42
13	16.138	1.07	0.44	3.08
14	25.228	7.01	686.17	3958.61
15	27.125	0.66	5617.46	79.05
16	29.828	0.04	2836.92	88.31
17	30.362	51.78	0.08	44.15
18	31.171	0.87	5.60	1.40

Table 3-2.4-3

VENT SYSTEM FREQUENCY ANALYSIS RESULTS WITH WATER
INSIDE DOWNCOMERS, BASED ON DOWNCOMERS NOT
BRACED LONGITUDINALLY

(Concluded)

MODE NUMBER	FREQUENCY (Hz)	MASS PARTICIPATION FACTOR (lb)		
		X	Y	Z
19	32.214	42.56	229.04	2158.29
20	34.126	175.26	2810.08	1169.38
21	43.495	353.89	3077.73	127.05
22	45.993	757.12	1357.12	235.52
23	50.737	264.49	83.29	60.38
24	51.844	4.90	0.70	3.18
25	51.910	0.01	0.00	0.00
26	51.928	3.96	4.99	5.86
27	51.975	0.00	0.06	106.17
28	54.649	0.07	68.04	1121.59

Table 3-2.4-4

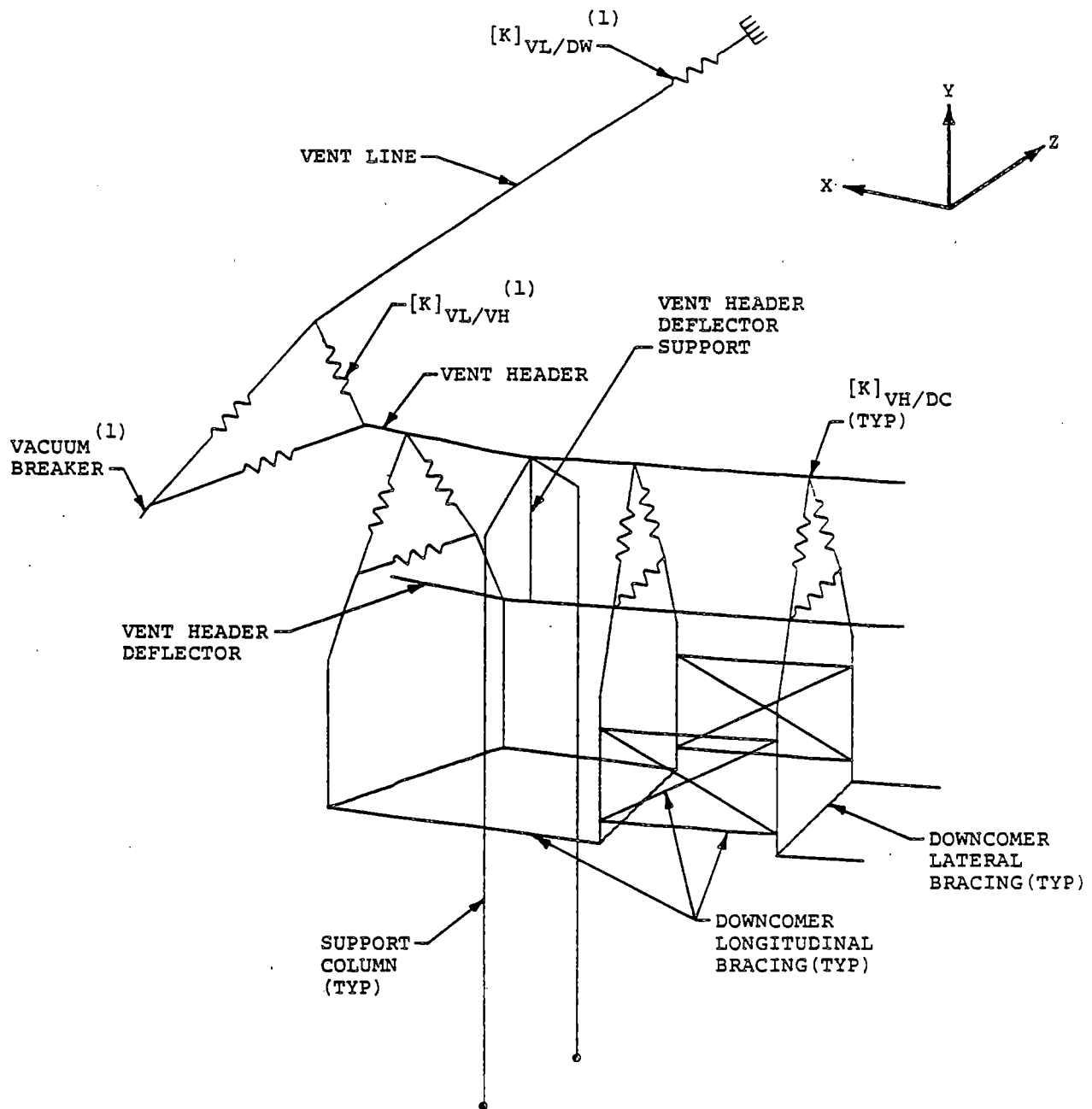
VENT SYSTEM FREQUENCY ANALYSIS RESULTS WITHOUT
WATER INSIDE DOWNCOMERS, BASED ON
DOWNCOMERS NOT BRACED LONGITUDINALLY

MODE NUMBER	FREQUENCY (Hz)	MASS PARTICIPATION FACTOR (lb)		
		X	Y	Z
1	11.330	9.25	0.16	10659.42
2	12.335	652.53	0.10	27.88
3	12.336	694.98	0.01	53.33
4	12.340	0.00	0.00	0.00
5	12.358	1.02	0.25	234.09
6	15.563	131.70	3.55	1853.38
7	16.973	4843.07	81.76	277.84
8	17.740	488.26	1.64	318.58
9	18.004	1141.53	0.01	613.86
10	18.547	131.06	6.45	0.24
11	19.267	837.61	3.00	0.99
12	19.926	87.64	153.07	147.35
13	20.777	0.00	1.56	16.39
14	25.733	19.89	781.12	2911.46
15	27.152	1.31	5372.76	90.24
16	29.873	0.11	2809.01	67.07
17	30.470	84.46	16.55	44.42
18	31.177	1.70	5.39	1.07

Table 3-2.4-4

VENT SYSTEM FREQUENCY ANALYSIS RESULTS WITHOUT
WATER INSIDE DOWNCOMERS, BASED ON
DOWNCOMERS NOT BRACED LONGITUDINALLY
 (Concluded)

MODE NUMBER	FREQUENCY (Hz)	MASS PARTICIPATION FACTOR (lb)		
		X	Y	Z
19	32.567	14.57	578.17	2009.90
20	34.494	248.99	2614.05	1605.61
21	43.654	315.11	3292.51	73.98
22	46.503	764.21	1036.62	149.28
23	50.960	288.89	84.47	71.92
24	51.853	3.07	0.54	1.92
25	51.910	0.01	0.00	0.00
26	51.935	1.67	6.56	12.47
27	51.989	0.00	0.28	111.18
28	55.554	5.46	86.55	1135.12
29	73.252	45.99	101.36	152.91
30	85.032	0.47	0.02	0.79
21	94.307	35.00	1.01	8.99
32	100.893	29.66	177.38	8.13



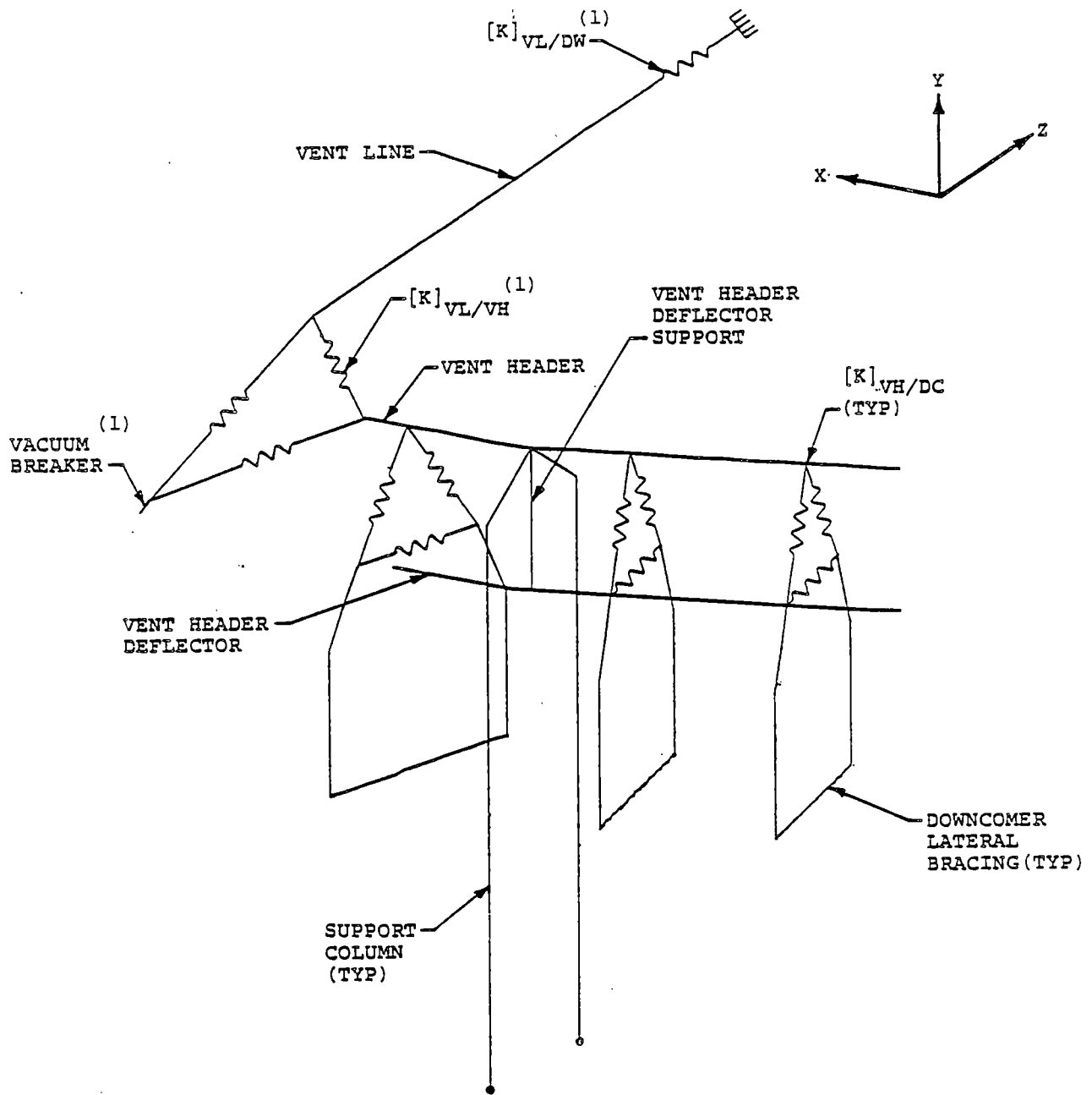
(1) BASED ON QUAD CITIES UNITS 1 AND 2 CONFIGURATION.

Figure 3-2.4-1

VENT SYSTEM 1/16 SEGMENT BEAM MODEL - ISOMETRIC VIEW
WITH DOWNCOMER LONGITUDINAL BRACING

COM-02-041-3
 Revision 0

3-2.146



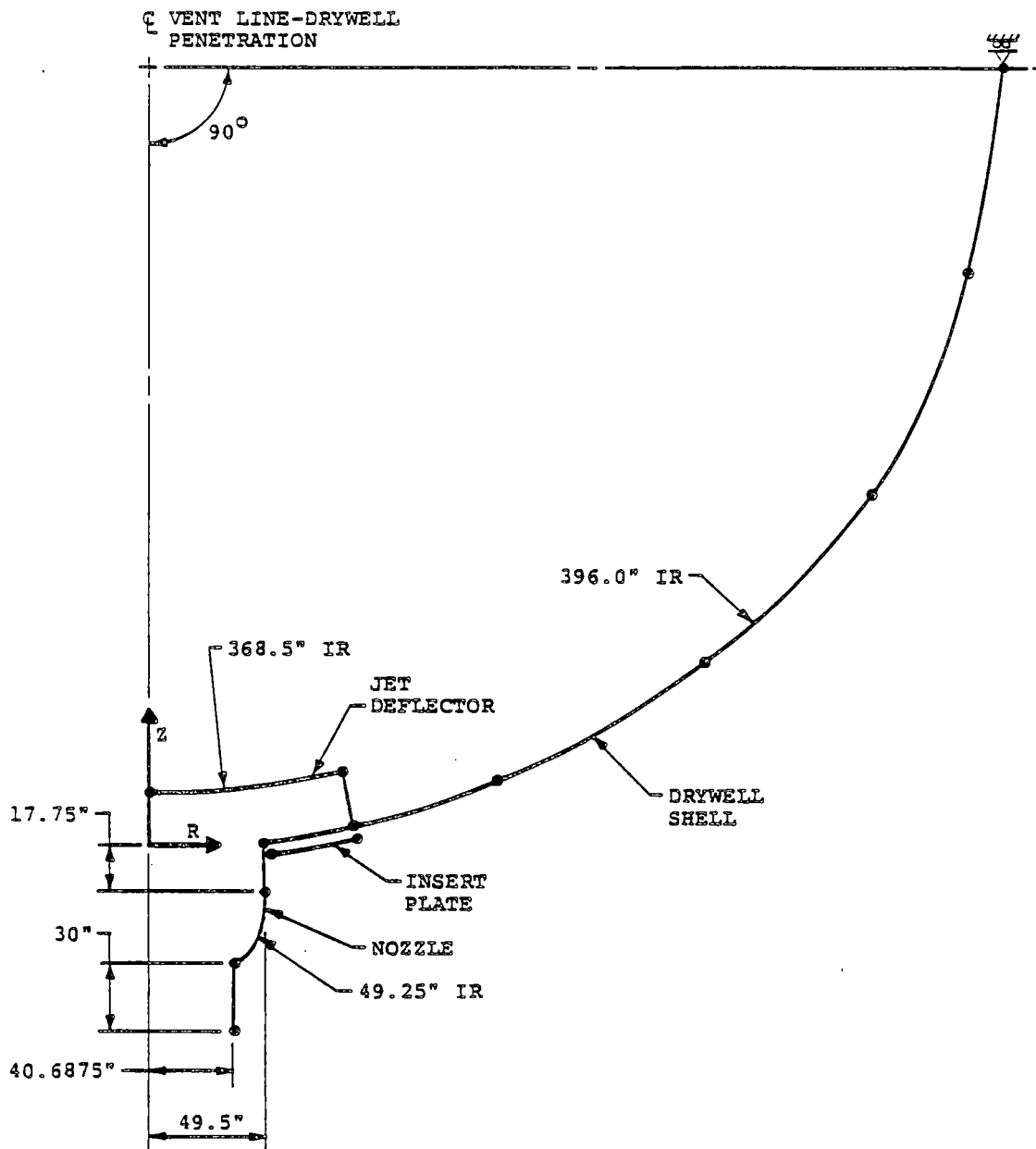
(1) BASED ON QUAD CITIES UNITS 1 AND 2 CONFIGURATION.

Figure 3-2.4-2

VENT SYSTEM 1/16 SEGMENT BEAM MODEL - ISOMETRIC VIEW
WITHOUT DOWNCOMER LONGITUDINAL BRACING

COM-02-041-3
 Revision 0

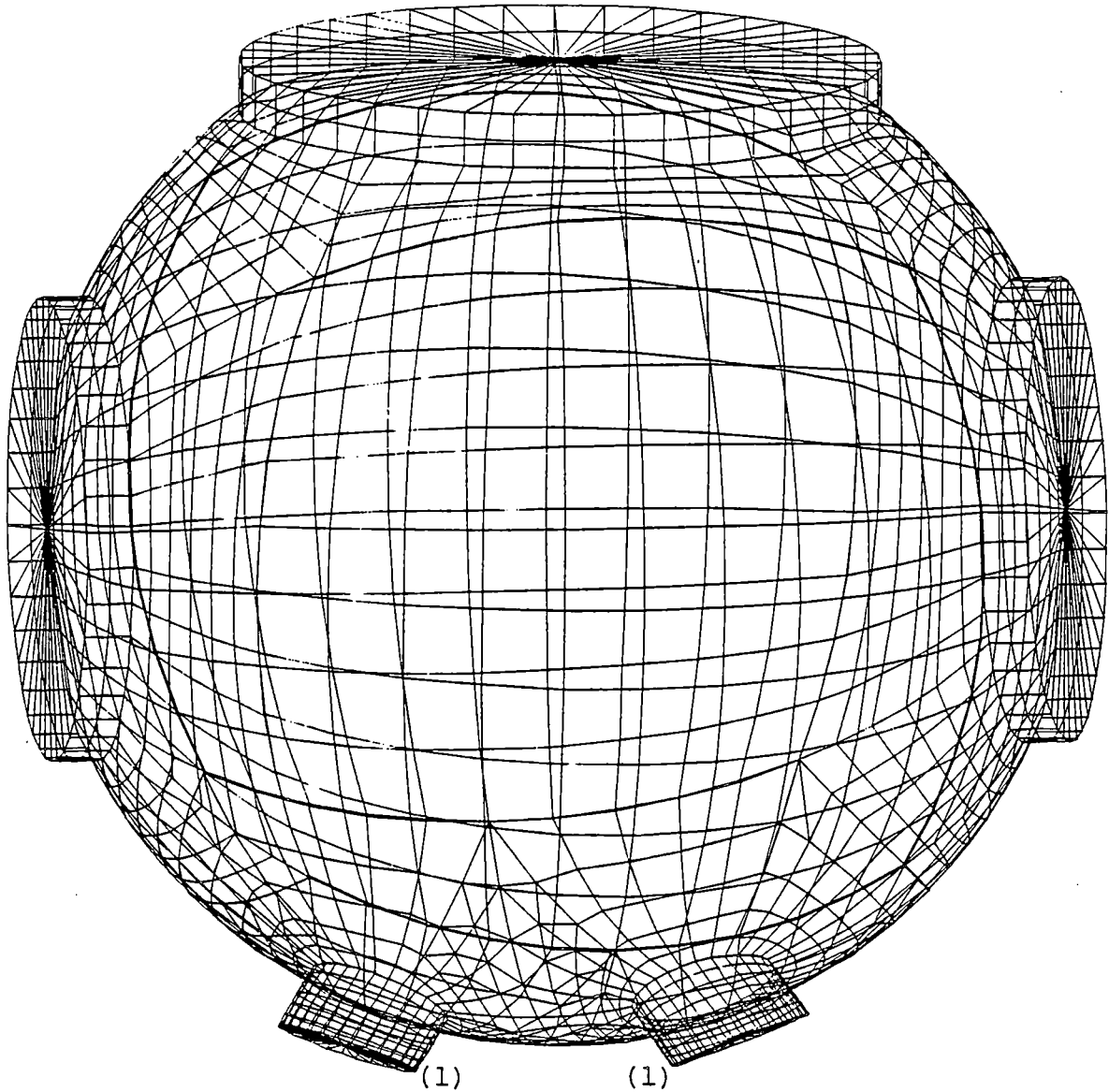
3-2.147



(1) BASED ON QUAD CITIES UNITS 1 AND 2 CONFIGURATION.

Figure 3-2.4-3

VENT LINE-DRYWELL PENETRATION AXISYMMETRIC
FINITE DIFFERENCE MODEL - VIEW OF TYPICAL MERIDIAN



(1) BASED ON QUAD CITIES UNITS 1 AND 2 CONFIGURATION.

Figure 3-2.4-4

VENT LINE-VENT HEADER SPHERICAL
JUNCTION FINITE ELEMENT MODEL

COM-02-041-3
Revision 0

3-2.149

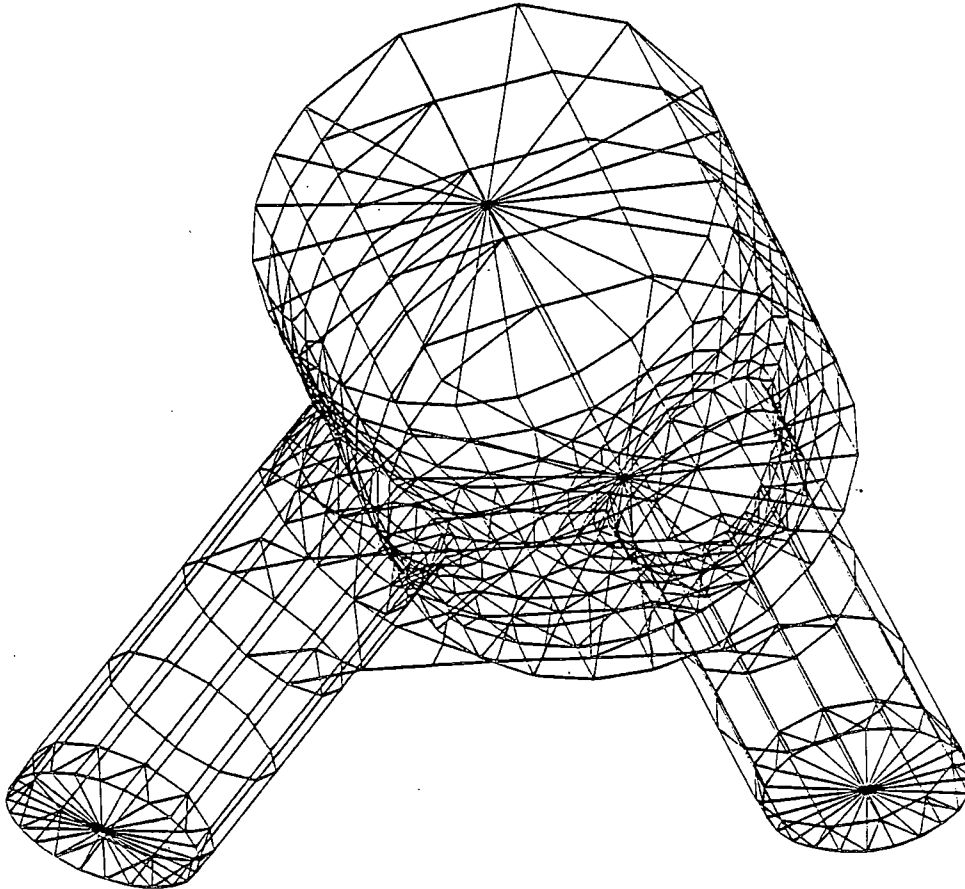


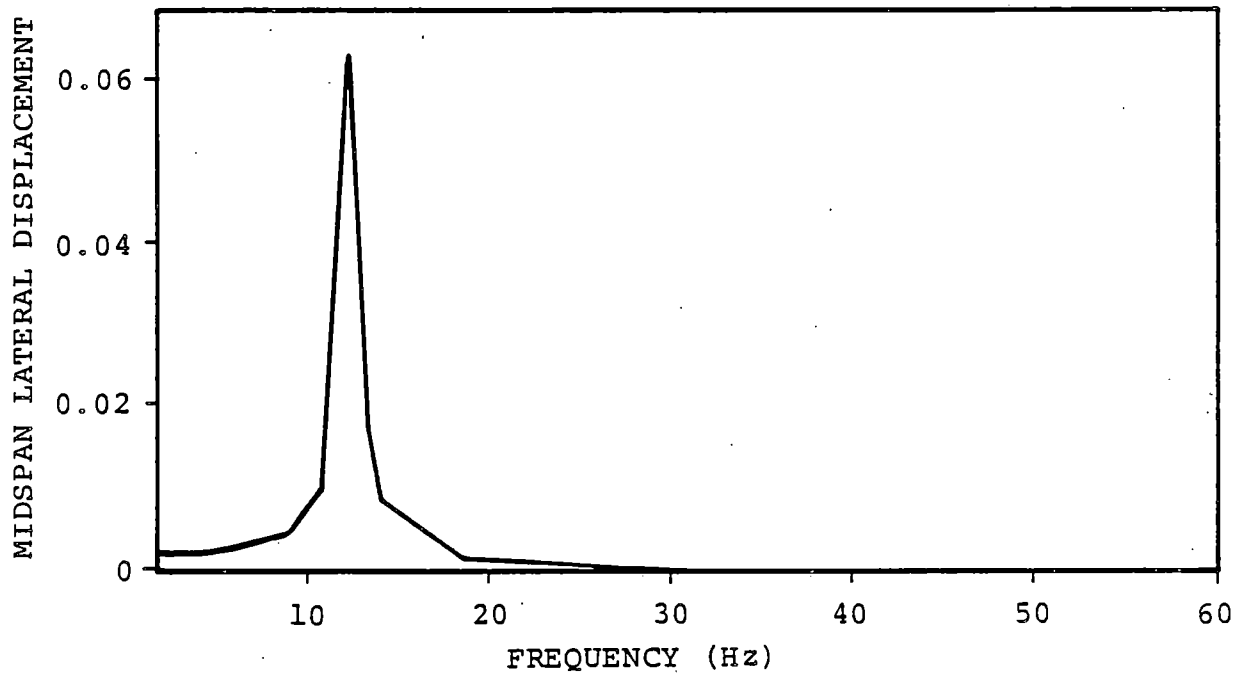
Figure 3-2.4-5

DOWNCOMER-VENT HEADER INTERSECTION
FINITE ELEMENT MODEL - ISOMETRIC VIEW

COM-02-041-3
Revision 0

3-2.150

SUPPORT COLUMN, $f_{cr} = 12.33$ Hz



1. RESULTS SHOWN ARE OBTAINED BY APPLYING UNIT DRAG PRESSURES TO SUBMERGED PORTION OF THE COLUMNS IN IN-PLANE AND OUT-OF-PLANE DIRECTIONS RELATIVE TO MITERED JOINT.
2. RESULTS SHOWN ARE TYPICAL FOR INSIDE AND OUTSIDE COLUMNS IN EITHER DIRECTION.

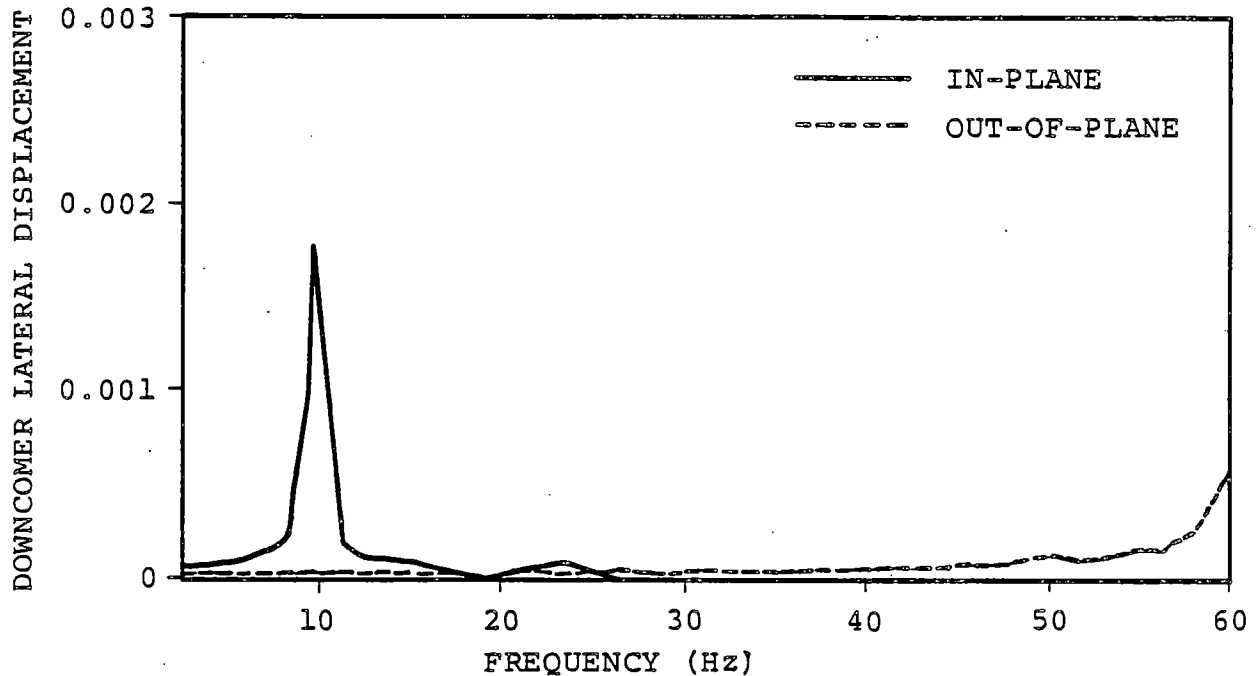
Figure 3-2.4-6

HARMONIC ANALYSIS RESULTS FOR SUPPORT COLUMN
SUBMERGED STRUCTURE LOAD FREQUENCY DETERMINATION

COM-02-041-3
Revision 0

3-2.151

IN-PLANE, $f_{cr} = 9.277$ Hz
OUT-OF-PLANE, $f_{cr} > 60.000$ Hz

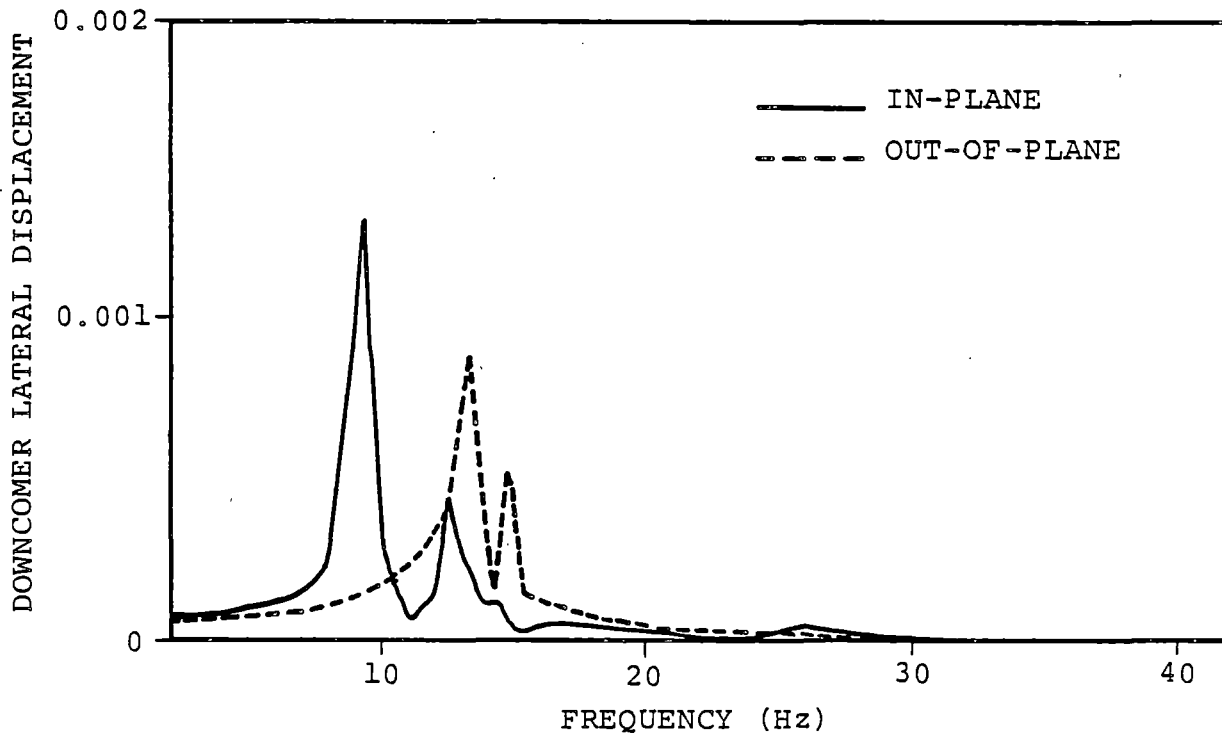


1. RESULTS SHOWN ARE OBTAINED BY APPLYING UNIT PRESSURES TO DOWNCOMER SUBMERGED PORTION IN IN-PLANE AND OUT-OF-PLANE DIRECTIONS.
2. FREQUENCIES ARE DETERMINED WITH WATER INSIDE SUBMERGED PORTION OF THE DOWNCOMERS.
3. RESULTS SHOWN ARE TYPICAL FOR ALL LONGITUDINALLY BRACED DOWNCOMERS.

Figure 3-2.4-7

HARMONIC ANALYSIS RESULTS FOR DOWNCOMER
SUBMERGED STRUCTURE LOAD FREQUENCY DETERMINATION,
BASED ON DOWNCOMERS BRACED LONGITUDINALLY

IN-PLANE, $f_{cr} = 9.170$ Hz
OUT-OF-PLANE, $f_{cr} = 13.576$ Hz

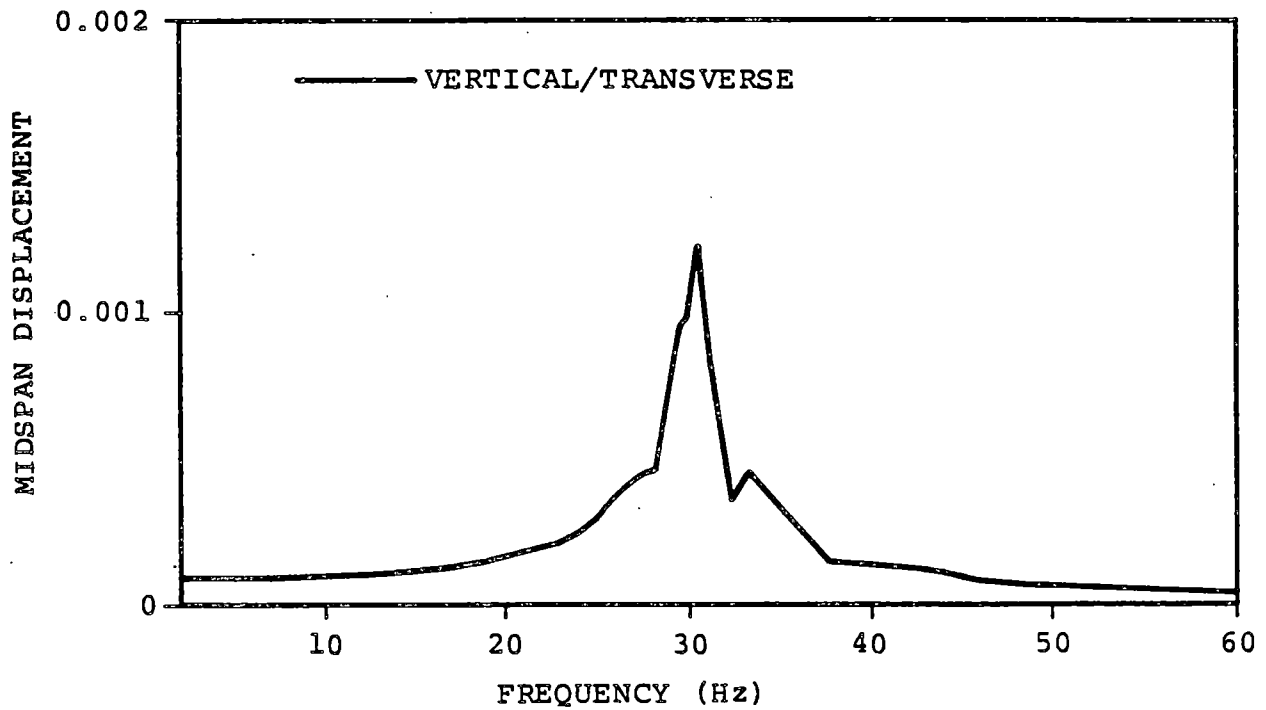


1. RESULTS SHOWN ARE OBTAINED BY APPLYING UNIT PRESSURES TO DOWNCOMER SUBMERGED PORTION IN IN-PLANE AND OUT-OF-PLANE DIRECTIONS.
2. FREQUENCIES ARE DETERMINED WITH WATER INSIDE SUBMERGED PORTION OF THE DOWNCOMERS.
3. RESULTS SHOWN ARE TYPICAL FOR ALL LONGITUDINALLY UNBRACED DOWNCOMERS.

Figure 3-2.4-8

HARMONIC ANALYSIS RESULTS FOR DOWNCOMER
SUBMERGED STRUCTURE LOAD FREQUENCY DETERMINATION,
BASED ON DOWNCOMERS NOT BRACED LONGITUDINALLY

VERTICAL $f_{cr} = 31.15$ Hz
TRANSVERSE $f_{cr} = 31.15$ Hz

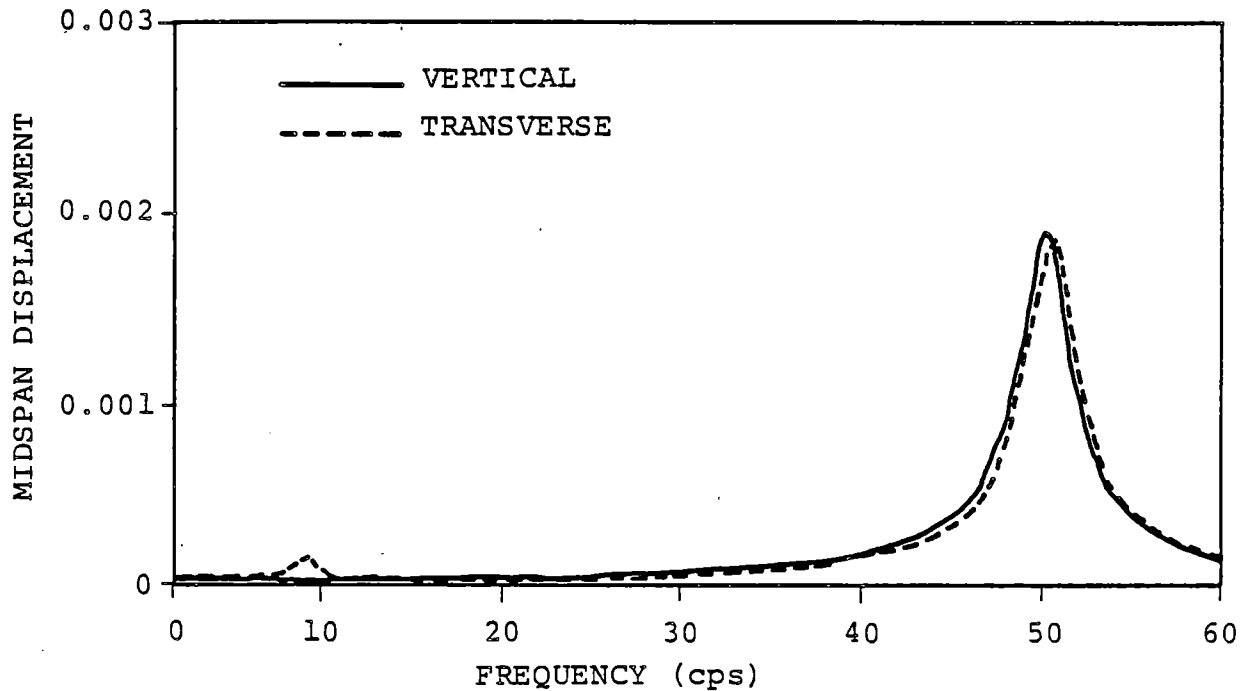


1. RESULTS SHOWN ARE OBTAINED BY APPLYING UNIT FORCES TO LATERAL BRACINGS MIDSPAN IN THE VERTICAL AND TRANSVERSE DIRECTIONS.
2. RESULTS SHOWN ARE TYPICAL FOR ALL LATERAL BRACINGS.

Figure 3-2.4-9

HARMONIC ANALYSIS RESULTS FOR LATERAL BRACING
SUBMERGED STRUCTURE LOAD FREQUENCY DETERMINATION

VERTICAL $f_{cr} = 50.09$ Hz
TRANSVERSE $f_{cr} = 50.76$ Hz



1. RESULTS SHOWN ARE OBTAINED BY APPLYING UNIT FORCES TO MIDSPAN OF THE LONGITUDINAL BRACINGS IN THE VERTICAL AND HORIZONTAL DIRECTIONS.
2. RESULTS SHOWN ARE TYPICAL FOR ALL BRACING COMPONENTS EXCEPT DIAGONAL BRACINGS.

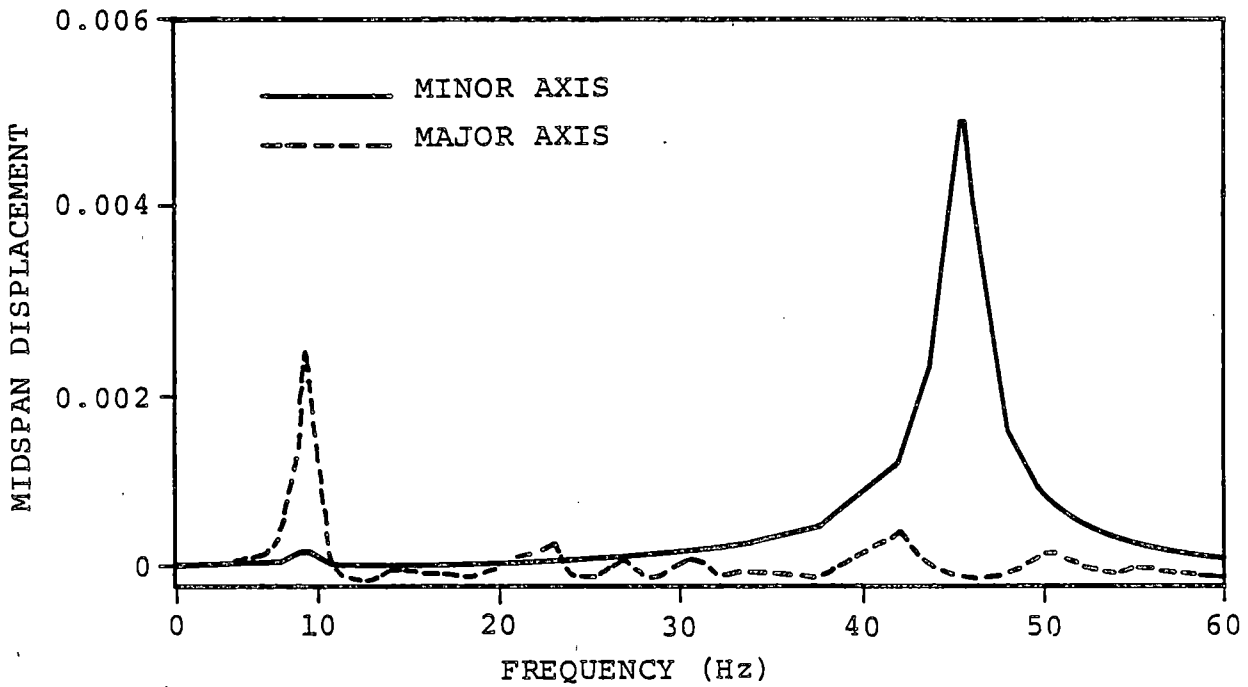
Figure 3-2.4-10

HARMONIC ANALYSIS RESULTS FOR LONGITUDINAL
BRACING HORIZONTAL MEMBER SUBMERGED STRUCTURE
LOAD FREQUENCY DETERMINATION

COM-02-041-3
Revision 0

3-2.155

MINOR AXIS $f_{cr} = 45.45$ Hz
MAJOR AXIS $f_{cr} > 60.00$ Hz



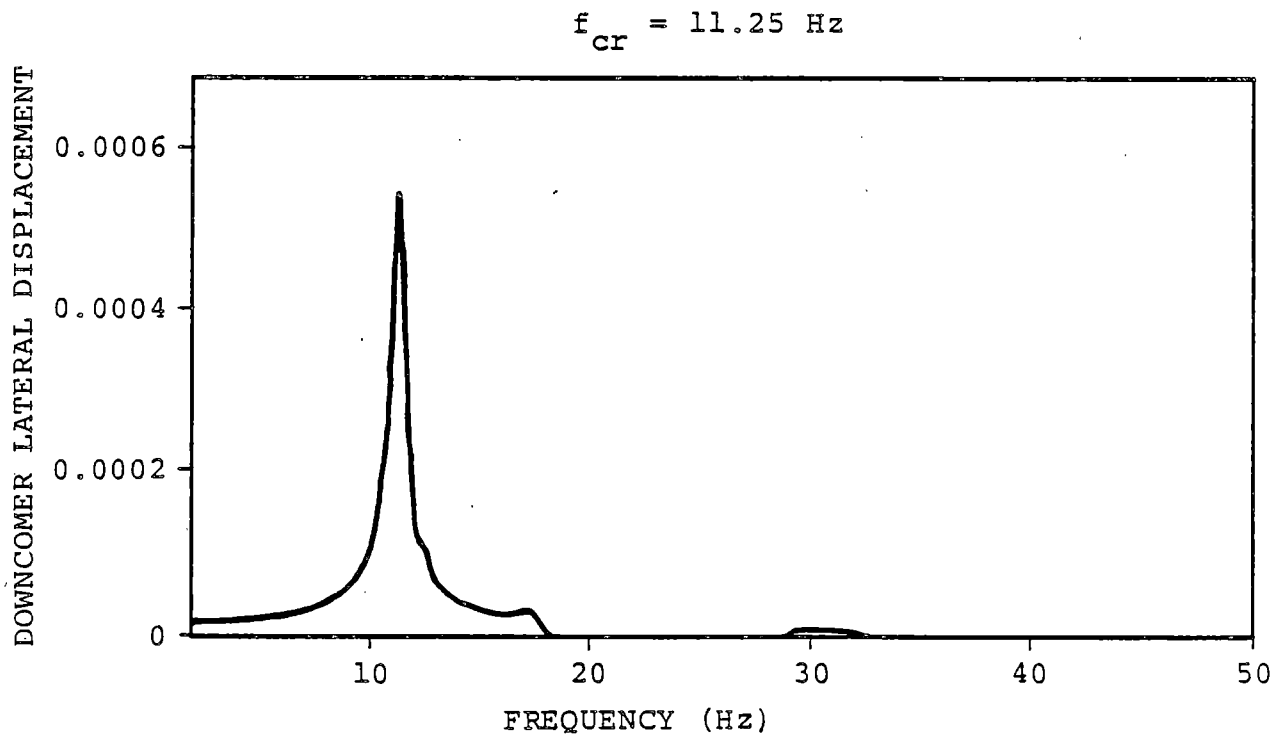
1. RESULTS SHOWN ARE OBTAINED BY APPLYING UNIT FORCES TO MIDSPAN OF THE DIAGONAL BRACING IN THE MAJOR AND MINOR AXES DIRECTIONS.
2. RESULTS SHOWN FOR MAJOR AXIS ARE MAGNIFIED 100 TIMES.
3. RESULTS SHOWN ARE TYPICAL FOR ALL DIAGONAL BRACINGS.

Figure 3-2.4-11

HARMONIC ANALYSIS RESULTS FOR LONGITUDINAL
BRACING DIAGONAL MEMBER SUBMERGED STRUCTURE
LOAD FREQUENCY DETERMINATION

COM-02-041-3
Revision 0

3-2.156



1. RESULTS SHOWN ARE OBTAINED BY APPLYING UNIT INTERNAL PRESSURES TO ONE DOWNCOMER IN A DOWNCOMER PAIR.
2. FREQUENCIES ARE DETERMINED WITHOUT WATER INSIDE SUBMERGED PORTION OF DOWNCOMERS.
3. RESULTS SHOWN ARE TYPICAL FOR ALL DOWNCOMERS.

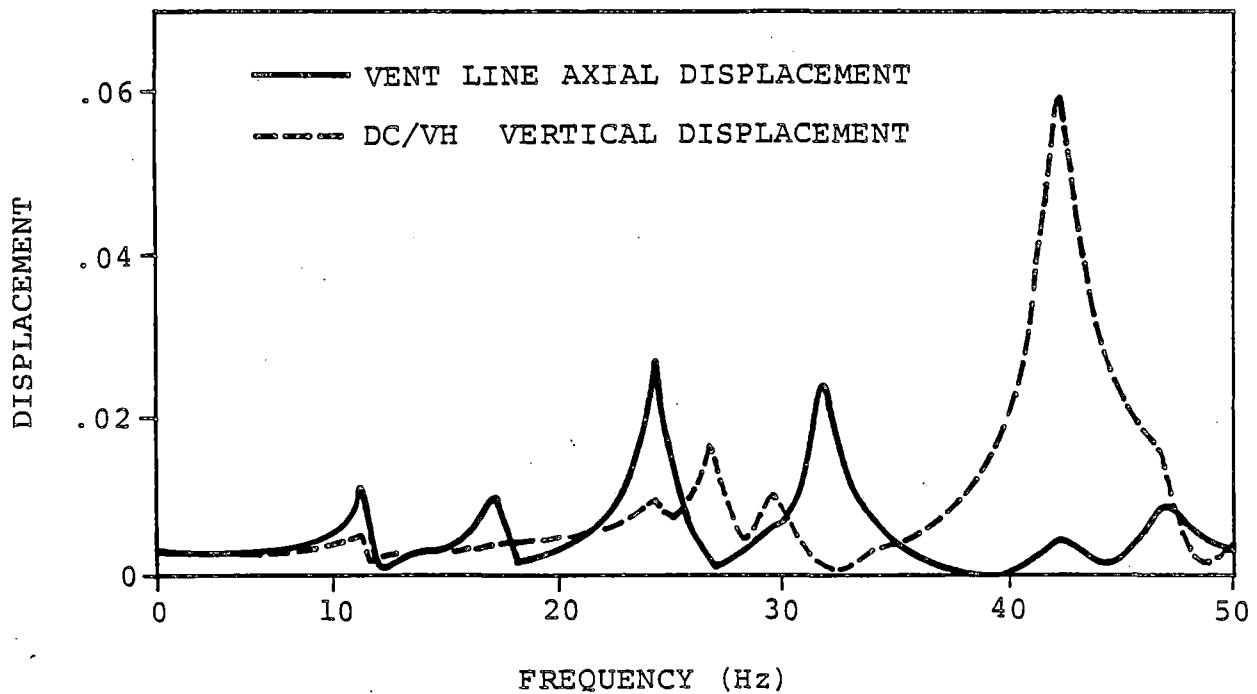
Figure 3-2.4-12

HARMONIC ANALYSIS RESULTS FOR CONDENSATION
OSCILLATION DOWNCOMER LOAD FREQUENCY DETERMINATION

COM-02-041-3
Revision 0

3-2.157

VENT LINE $f_{cr} = 42.10$ Hz
VENT HEADER $f_{cr} = 24.40$ Hz

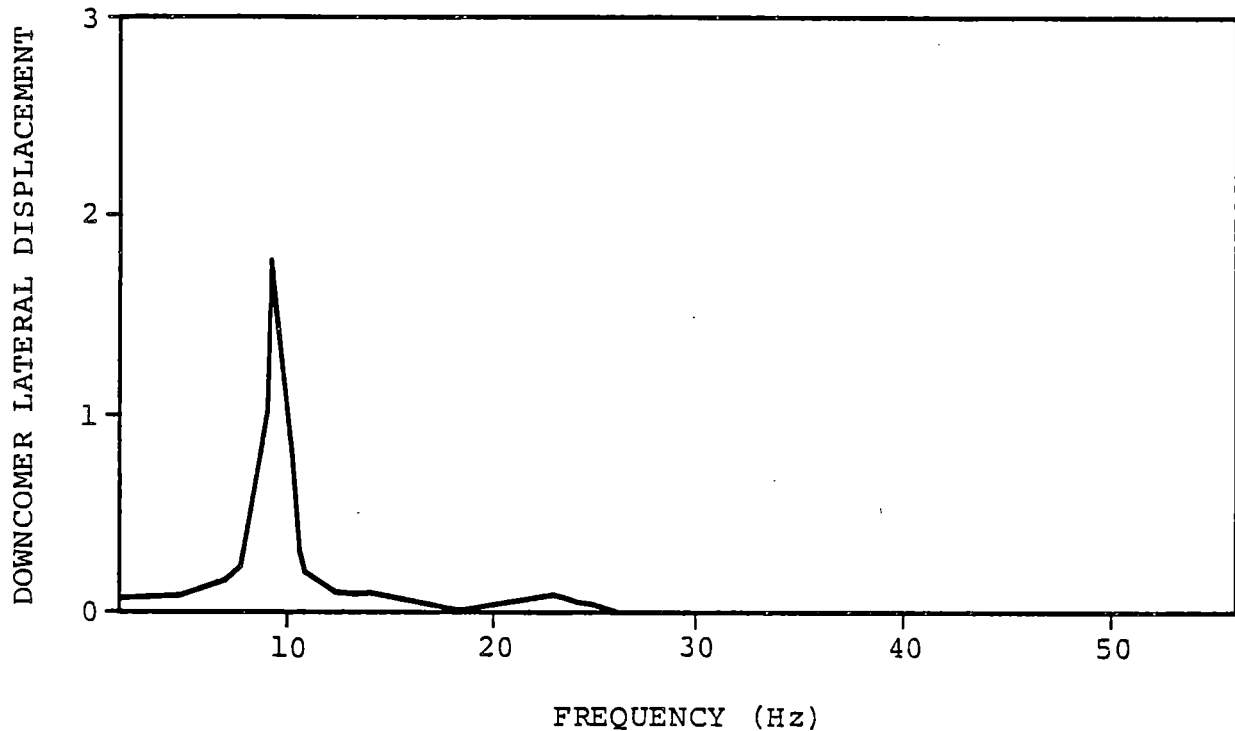


1. RESULTS SHOWN ARE OBTAINED BY APPLYING A 2.5 PSI INTERNAL PRESSURE TO UNREACTED AREAS OF THE VENT SYSTEM.

Figure 3-2.4-13

HARMONIC ANALYSIS RESULTS FOR CONDENSATION
OSCILLATION VENT SYSTEM PRESSURE LOAD
FREQUENCY DETERMINATION

$$f_{cr} = 9.277 \text{ Hz}$$



1. RESULTS SHOWN ARE OBTAINED BY APPLYING UNIT FORCES TO DOWNCOMER ENDS IN THE IN-PLANE DIRECTION.
2. FREQUENCIES ARE DETERMINED WITH WATER INSIDE SUBMERGED PORTION OF THE DOWNCOMERS.
3. RESULTS SHOWN ARE TYPICAL FOR ALL LONGITUDINALLY BRACED DOWNCOMERS.

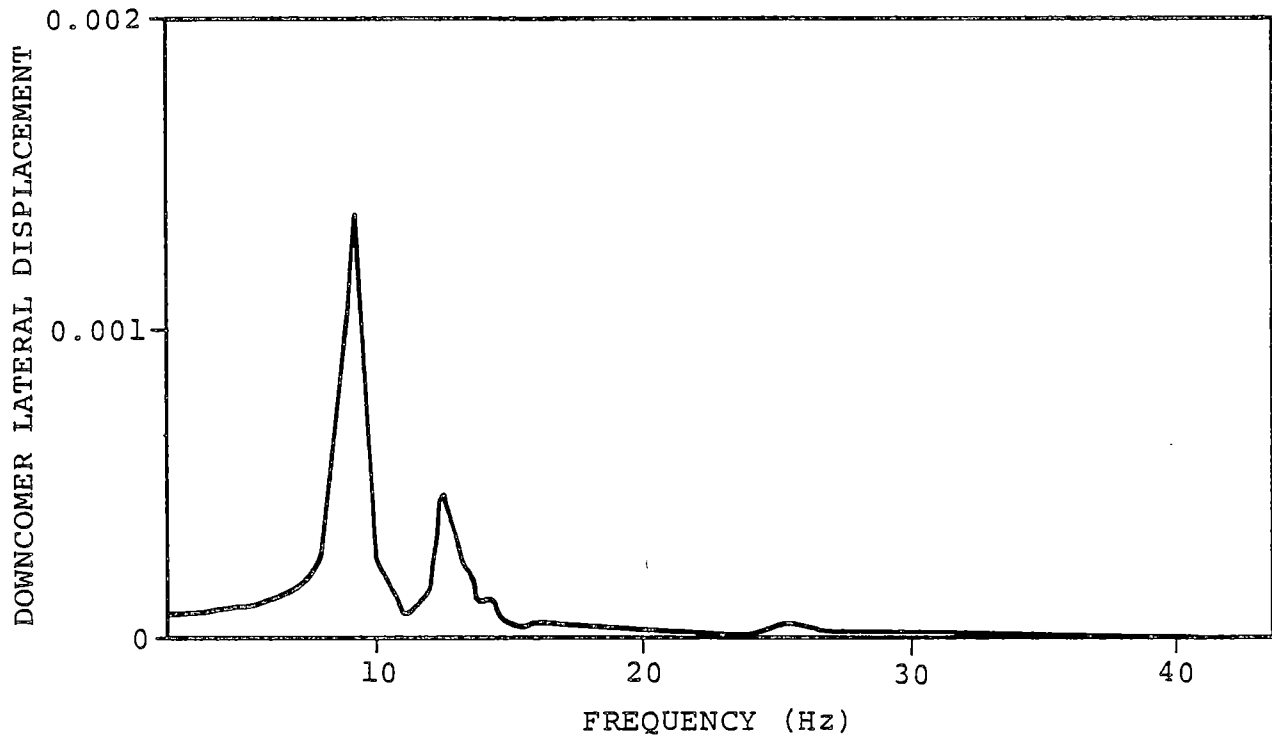
Figure 3-2.4-14

HARMONIC ANALYSIS RESULTS FOR CHUGGING DOWNCOMER
LATERAL LOADS FREQUENCY DETERMINATION, BASED ON
DOWNCOMERS BRACED LONGITUDINALLY

COM-02-041-3
Revision 0

3-2.159

$$f_{cr} = 9.170 \text{ Hz}$$



1. RESULTS SHOWN ARE OBTAINED BY APPLYING UNIT FORCES TO DOWNCOMER ENDS IN THE IN-PLANE DIRECTION.
2. FREQUENCIES ARE DETERMINED WITH WATER INSIDE SUBMERGED PORTION OF THE DOWNCOMERS.
3. RESULTS SHOWN ARE TYPICAL FOR ALL LONGITUDINALLY UNBRACED DOWNCOMERS.

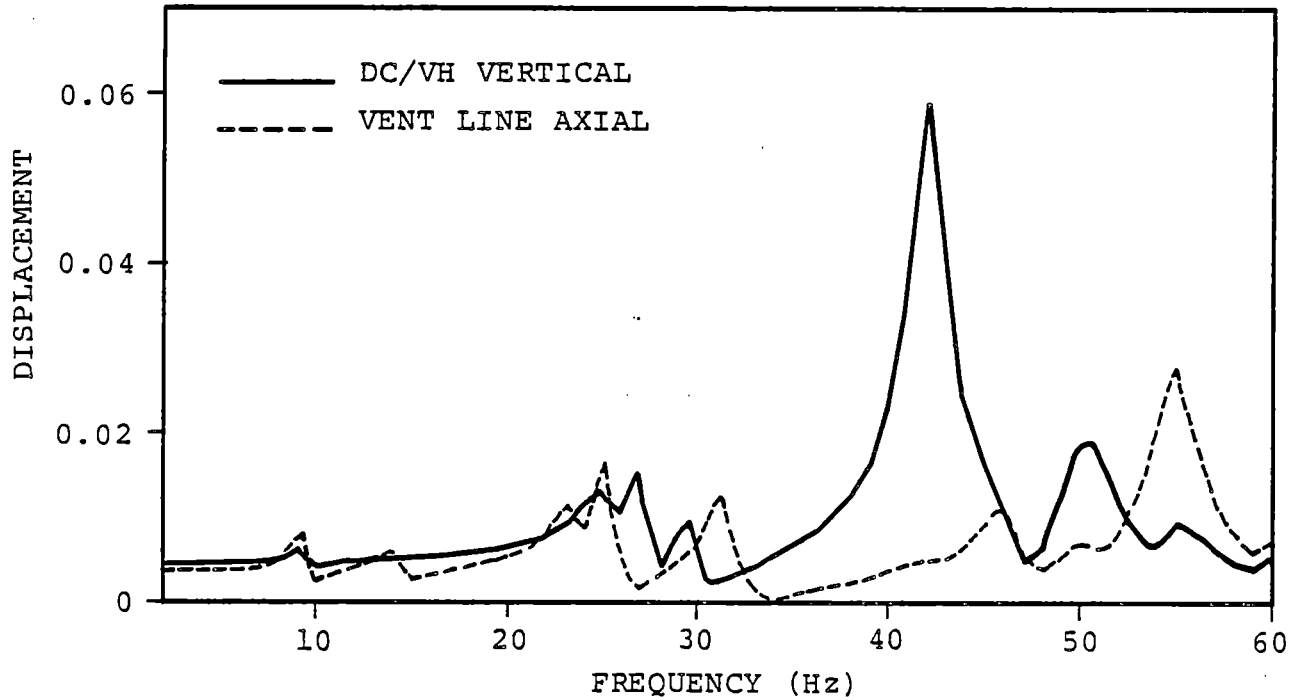
Figure 3-2.4-15

HARMONIC ANALYSIS RESULTS FOR CHUGGING DOWNCOMER
LATERAL LOADS FREQUENCY DETERMINATION, BASED ON
DOWNCOMERS NOT BRACED LONGITUDINALLY

COM-02-041-3
Revision 0

3-2.160

VENT HEADER $f_{cr} = 42.01$ Hz
VENT LINE $f_{cr} = 54.878$ Hz



1. RESULTS SHOWN ARE OBTAINED BY APPLYING 2.5 AND 3.0 PSI INTERNAL PRESSURES TO UNREACTED AREAS OF THE VENT LINE AND VENT HEADER, RESPECTIVELY.

Figure 3-2.4-16

HARMONIC ANALYSIS RESULTS FOR CHUGGING VENT SYSTEM
PRESSURE LOAD FREQUENCY DETERMINATION

COM-02-041-3
Revision 0

3-2.161

3-2.4.2 Analysis for Asymmetric Loads

The asymmetric loads acting on the vent system are evaluated by decomposing each of the asymmetric loadings into symmetric or anti-symmetric components (or both) with respect to a 180° segment of the vent system. The analysis of the vent system for asymmetric loads is performed for a 180° segment of the vent system.

A beam model of a 180° segment of the vent system (Figure 3-2.4-17), based on the Dresden Unit 2 downcomer longitudinal bracings configuration (Figure 3-2.1-13), is used to obtain the response of the vent system to asymmetric loads. The plane of symmetry due to the uniqueness of the bracing pattern is at a 45° clockwise rotation from true north (Figure 3-2.1-13). Another 180° beam model (Figure 3-2.4-18) based on the Dresden Unit 3 downcomer longitudinal bracing configurations (Figure 3-2.1-14) is also used to obtain the response of the vent system to asymmetric loads. The resulting responses from the two beam models are compared and the more severe of the two is selected for Code evaluation. The two models include the vent lines, the spherical junctions, the vent header, downcomers, downcomer lateral bracings, the downcomer longitudinal bracings, and the vent header deflector.

Many of the modeling techniques used in the two 180° beam models, such as those used for local mass and stiffness determination, are the same as those utilized in the 1/16 beam model of the vent system discussed in Section 3-2.4.1. The local stiffness effects at the vent line-drywell penetrations, vent line-vent header spherical junctions, and the downcomer-vent header intersections are included using stiffness matrix elements for these penetrations and intersections. The pin conditions are assumed at the attachments of the support columns to the suppression chamber.

The 180° beam model, based on Dresden Unit 2 downcomer longitudinal bracing configuration, contains 747 nodes, 749 elastic beams, and 34 matrix elements, whereas the 180° beam model, based on Dresden Unit 3 downcomer longitudinal bracing configuration, contains 701 nodes, 738 elastic beams, and 32 matrix elements. These models are as refined as the 1/16 beam model of the vent system and they are used directly to characterize the response of the vent system to asymmetric loadings. They include those components and local stiffnesses which have an effect on the overall response of the vent system. The stiffness and mass properties used in the model are based on the nominal

dimensions and densities of the materials used to construct the vent system. Small displacement linear-elastic behavior is assumed throughout.

The boundary conditions used in the two 180° beam models are both physical and mathematical in nature. The physical boundary conditions used in the models are similar to those used in the 1/16 beam model of the vent system. The mathematical boundary conditions used in the model consist of either symmetry, anti-symmetry, or a combination of both at the 0° and 180° planes. The specific boundary condition used depends on the characteristics of the load being evaluated.

Additional water mass is lumped along the length of the submerged portion of the downcomers and support columns in a manner similar to that used in the 1/16 beam model. The mass of water inside the submerged portion of the downcomers is also included.

The asymmetric loads which act on the vent system are horizontal seismic loads and asymmetric chugging loads, as specified in Section 3-2.2.1. An equivalent static analysis is performed for each of the loads using the 180° beam model.

The magnitudes and characteristics of governing asymmetric loads on the vent system are presented and discussed in Section 3-2.2.1. The overall effects of asymmetric loads on the vent system are evaluated using the two 180° beam models and the general analysis techniques discussed in the preceding paragraphs. The specific treatment of each load which results in asymmetric loads on the vent system is discussed in the following paragraphs.

2. Seismic Loads

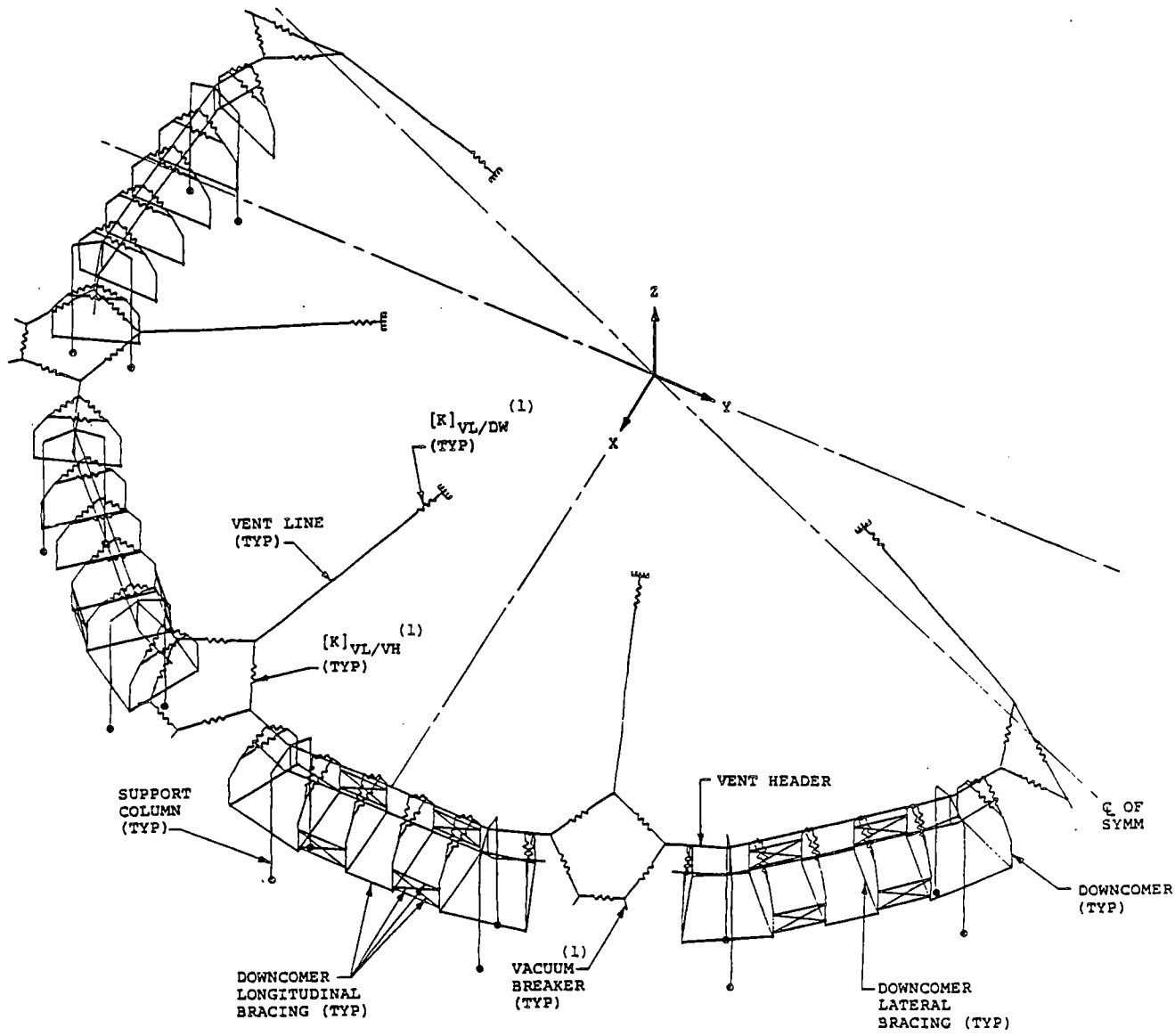
- a. OBE Loads: A static analysis is performed for a 0.25g horizontal and 0.067g vertical seismic acceleration applied to the weight of steel and water included in the 180° beam model. Horizontal seismic loads are applied in the direction of both principal azimuths.

- b. SSE Loads: The procedure used to evaluate 0.50g horizontal and 0.134g vertical SSE accelerations is the same as that discussed for OBE loads in Load Case 2a.

7. Chugging Loads

- a. Chugging Downcomer Lateral Loads: A static analysis is performed for chugging downcomer lateral Load Cases 1 through 10 (Table 3-2.2-16).

Use of the methodology described in the preceding paragraphs results in a conservative evaluation of vent system response to the asymmetric loads defined in NUREG-0661.



(1) BASED ON QUAD CITIES UNITS 1 AND 2 CONFIGURATION.

Figure 3-2.4-17

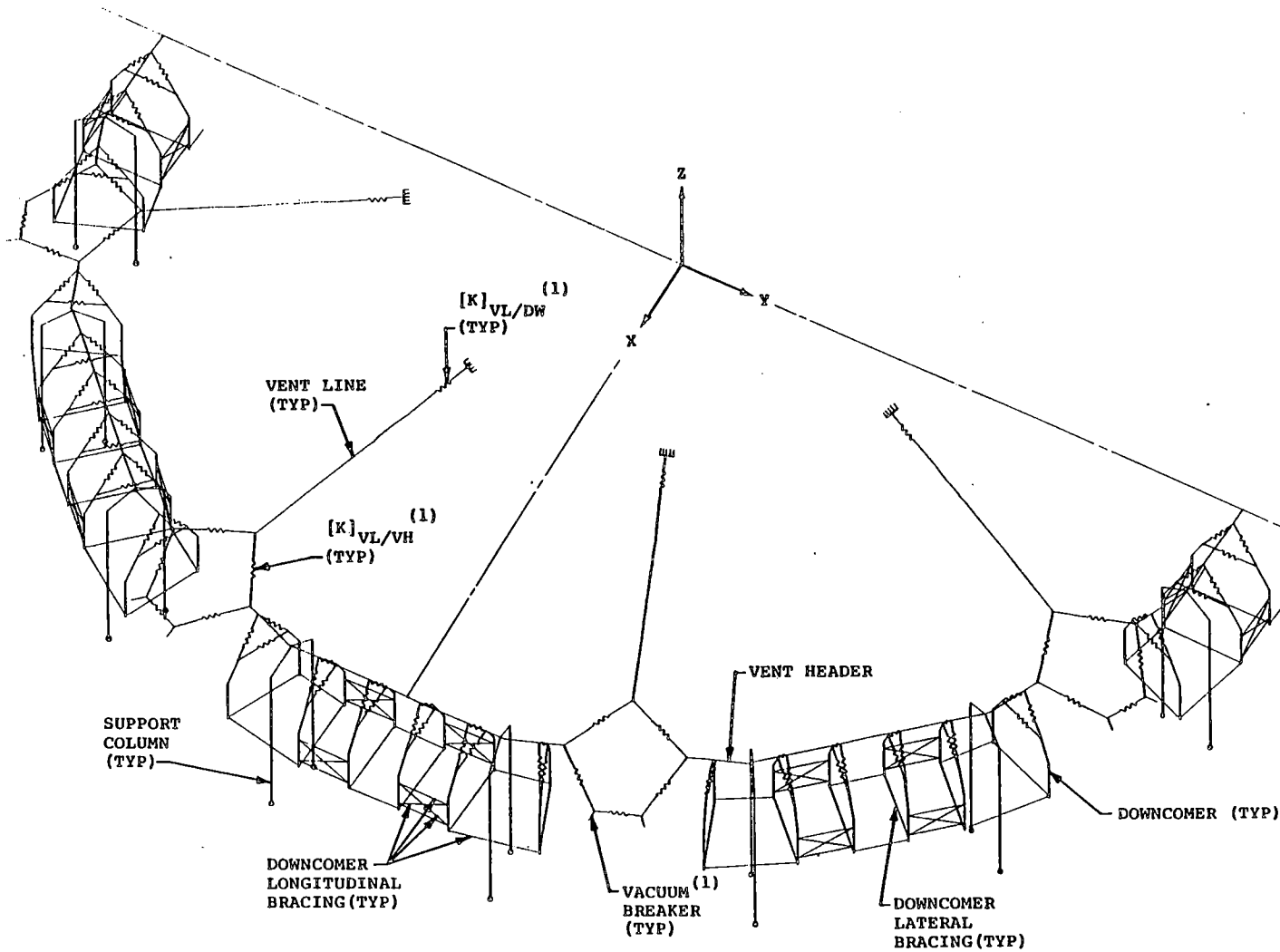
VENT SYSTEM 180° BEAM MODEL - ISOMETRIC VIEW
(DRESDEN UNIT 2)

COM-02-041-3
 Revision 0

3-2.167

COM-02-041-3
Revision 0

3-2.168



(1) BASED ON QUAD CITIES UNITS 1 AND 2 CONFIGURATION.

Figure 3-2.4-18

VENT SYSTEM 180° BEAM MODEL - ISOMETRIC VIEW
(DRESDEN UNIT 3)

3-2.4.3 Analysis for Local Effects

The penetrations and intersections of the major components of the vent system are evaluated using refined analytical models of each penetration and intersection. These include the vent line-drywell penetration, the vent line-vent header spherical junction, and the downcomer-vent header intersections. Figures 3-2.4-3 through 3-2.4-5 show analytical models used to evaluate these penetrations and intersections.

Each of the penetration and intersection analytical models includes mesh refinement near discontinuities to facilitate evaluation of local stresses. The stiffness properties used in the model are based on the nominal dimensions of the materials used to construct the penetrations and intersections. Small displacement linear-elastic theory is assumed throughout.

The analytical models are used to generate local stiffnesses of the penetrations and intersections for use in the 1/16 beam models and the 180° beam model, as discussed in Sections 3-2.4.1 and 3-2.4.2. Local stiffnesses are developed which represent the stiffness of the entire penetration or intersection in terms of a few local degrees of freedom on the penetration or

intersection. This is accomplished either by applying unit forces or displacements to the selected local degrees of freedom or by performing a matrix condensation to reduce the total stiffness of the penetration or intersection to those of the selected local degrees of freedom. The results are used to formulate stiffness matrix elements which are added to the 1/16 beam models and the 180° beam models at the corresponding penetration or intersection locations.

In order to account for the ovaling behavior of the shell segment of the vent header, the shell segment of the vent header at the downcomer intersection is extended at least to the location of the first circumferential collar for the intersection stiffness calculation.

The analytical models are also used to evaluate stresses in the penetrations and intersections. Stresses are computed by idealizing the penetrations and intersections as free bodies in equilibrium under a set of statically applied loads. The applied loads, which are extracted from either of the two 1/16 beam model results or from either of the two 180° beam models results, consist of loads acting on the penetration and intersection model boundaries and of loads

acting on the interior of penetration and intersection models. The loads acting on the penetration and intersection model boundaries are the beam end loads taken from the vent system at nodes coincident with the penetration or intersection model boundary locations.

The loads which act on the interior of the penetration or intersection models consist of reaction loads and distributed loads taken from the 1/16 beam model results. The reaction loads include the forces and moments applied to the appropriate penetration or intersection at the attachment points of the downcomer, the vent header, and the vent line. The distributed loads include the pressures and acceleration loads applied to penetration and intersection models to account for internal pressure loads, thrust loads, pool swell loads, and inertia loads. By the application of boundary loads, reaction loads, and distributed loads to the penetration and intersection models, equilibrium of the penetrations and intersections is achieved for each of the governing vent system loadings. The inertia loads are found to be insignificant for most of the load cases.

Loads which act on the shell segment boundaries are applied to the penetration and intersection models

through a system of radial beams. The radial beams extend from the middle surface of each of the shell segments to a node located on the centerline of the corresponding shell segment. The beams have large bending stiffnesses, zero axial stiffness, and are pinned in all directions at the shell segment middle surface. Boundary loads applied to the centerline nodes cause only shear loads to be transferred to the shell segment middle surface with no local bending effects. Use of this boundary condition minimizes end effects on penetration and intersection stresses in the local areas of interest. The system of radial beams constrains the boundary planes to remain plane during loading, which is consistent with the assumption made in small deflection beam theory.

Section 3-2.4.1 discusses the methodology used to evaluate the overall effects of the governing loads acting on the vent system using the governing 1/16 beam model. The general methodology used to evaluate local vent system penetration and intersection stresses is discussed in the preceding paragraphs. Descriptions of each vent system penetration and intersection analytical model and its use are provided in the following paragraphs.

- o Vent Line-Drywell Penetration Axisymmetric Finite Difference Model: The vent line-drywell penetration model which is based on the Quad Cities Units 1 and 2 configuration (Figure 3-2.4-3) includes a segment of the drywell shell, the jet deflector, the cylindrical penetration nozzle, the annular pad plate, and the spherical transition piece. The analytical model contains eight segments with 105 mesh points. The reaction loads applied to the model include those computed at the upper end of the vent line. The distributed loads applied to the model are internal pressure loads.

- o Vent Line-Vent Header Spherical Junction Finite Element Model: The vent line-vent header spherical junction finite element model which is based on the Quad Cities Units 1 and 2 configuration (Figure 3-2.4-4) includes a segment of the vent line, two segments of the vent header. The model contains 1,956 nodes, 312 beams, and 1,816 plate bending and stretching elements. The only difference between the Quad Cities Units 1 and 2 spherical junctions and those of Dresden Units 2 and 3 is the existence of two segments of the vacuum breaker nozzles in the Quad Cities plants. Boundary displacement and rotation loads

are applied at the end of the vent line shell segment and at each end of the vent header shell segment. The distributed loads applied to the analytical model are internal pressure thrust, pool swell, froth impingement, CO vent system pressure, and chugging vent system pressure loads.

- o Downcomer-Vent Header Intersection Finite Element Model: The downcomer-vent header intersection finite element model (Figure 3-2.4-5) includes a segment of the vent header, a segment of each downcomer, and the stiffener plate. The analytical model contains 453 nodes, 26 beam elements, and 712 plate bending and stretching elements. Boundary loads are applied at the ends of the vent header segment and at the ends of the downcomer segment. The distributed loads applied to the model are internal pressure loads, pool swell loads on the downcomers, and pool swell inertia loads.

Use of the methodology described in the preceding paragraphs results in a conservative evaluation of vent system local stresses due to the loads defined in NUREG-0661.

3-2.4.4 Methods for Evaluating Analysis Results

The methodology discussed in Sections 3-2.4.1 and 3-2.4.2 is used to determine element forces and component stresses in the vent system components. The following paragraphs discuss the methodology used to evaluate the analysis results, determine the controlling stresses in the vent system components, and examine fatigue effects.

To evaluate analysis results for the vent system Class MC components, membrane and extreme fiber stress intensities are computed. The values of the membrane stress intensities away from discontinuities are computed using the governing 1/16 beam model and the governing 180° beam model results. These stresses are compared with the primary membrane stress allowables (Table 3-2.3-1). The values of membrane stress intensities near discontinuities are computed using results from the penetration and intersection analytical models. These stresses are compared with local primary membrane stress allowables (Table 3-2.3-1). Primary stresses in vent system Class MC component welds are computed using maximum principal stresses or the resultant forces acting on the weld throat. The results are compared to primary weld stress allowables (Table 3-2.3-1).

Many of the loads contained in each of the controlling load combinations are dynamic loads which result in stresses which cycle with time and are partially or fully reversible. The maximum stress intensity ranges for all vent system Class MC components are calculated using the maximum values of the extreme fiber stress differences which occur near discontinuities in the penetration and intersection analytical models. These stresses are compared to the secondary stress range allowables (Table 3-2.3-1). A similar procedure is used to compute the stress range for the vent system Class MC component welds. The results are compared to the secondary weld stress allowables (Table 3-2.3-1).

To evaluate the vent system Class MC component supports, beam end loads obtained from the governing 1/16 beam model or the governing 180° beam model (or both) results are used to compute stresses. The results are compared with the corresponding allowable stresses (Table 3-2.3-1). Stresses in vent system Class MC component support welds are obtained using the governing 1/16 beam model or the governing 180° beam model (or both) results to compute the maximum resultant force acting on the associated weld throat. The results are compared to weld stress limits discussed in Section 3-2.3.

Section 3-2.2.2 defines the controlling vent system load combinations. During load combination formulation, the maximum stress intensities in a particular vent system class MC component at a given location are conservatively combined by the absolute sum method for the individual loads contained in each combination. For the vent system class MC component supports, stress components at a given location are conservatively combined by the absolute sum method for the individual loads contained in each combination. However, in a few combinations where the absolute sum method does not satisfy the structural acceptance criteria, the stress components of the individual dynamic loads are combined by the SRSS method as an alternative.

The maximum differential displacements of the vent line bellows are determined using results from the 1/16 beam model or the governing 180° beam model (or both) of the vent system and the analytical model of the suppression chamber discussed in Volume 2 of this report. The displacements of the attachment points of the bellows to the suppression chamber and to the vent line are determined for each load case. The differential displacement is computed from these values. The results

for each load are combined to determine the total differential displacements for the controlling load combinations. These results are compared to the allowable bellows displacements (Table 3-2.3-2).

To evaluate fatigue effects in the vent system Class MC components and associated welds, extreme fiber alternating stress intensity histograms are determined for each load in each event or combination of events. Fatigue effects for chugging downcomer lateral loads are evaluated using the stress reversal histograms (Table 3-2.2-17). Stress intensity histograms are developed for the most highly stressed area in the vent system, which is the downcomer-vent header intersection. For each combination of events, a load combination stress intensity histogram is formulated and the corresponding fatigue usage factors are determined using the curve shown in Figure 3-2.4-19. The usage factors for each event are then summed to obtain the total fatigue usage.

Use of the methodology described above results in a conservative evaluation of the vent system design margins.

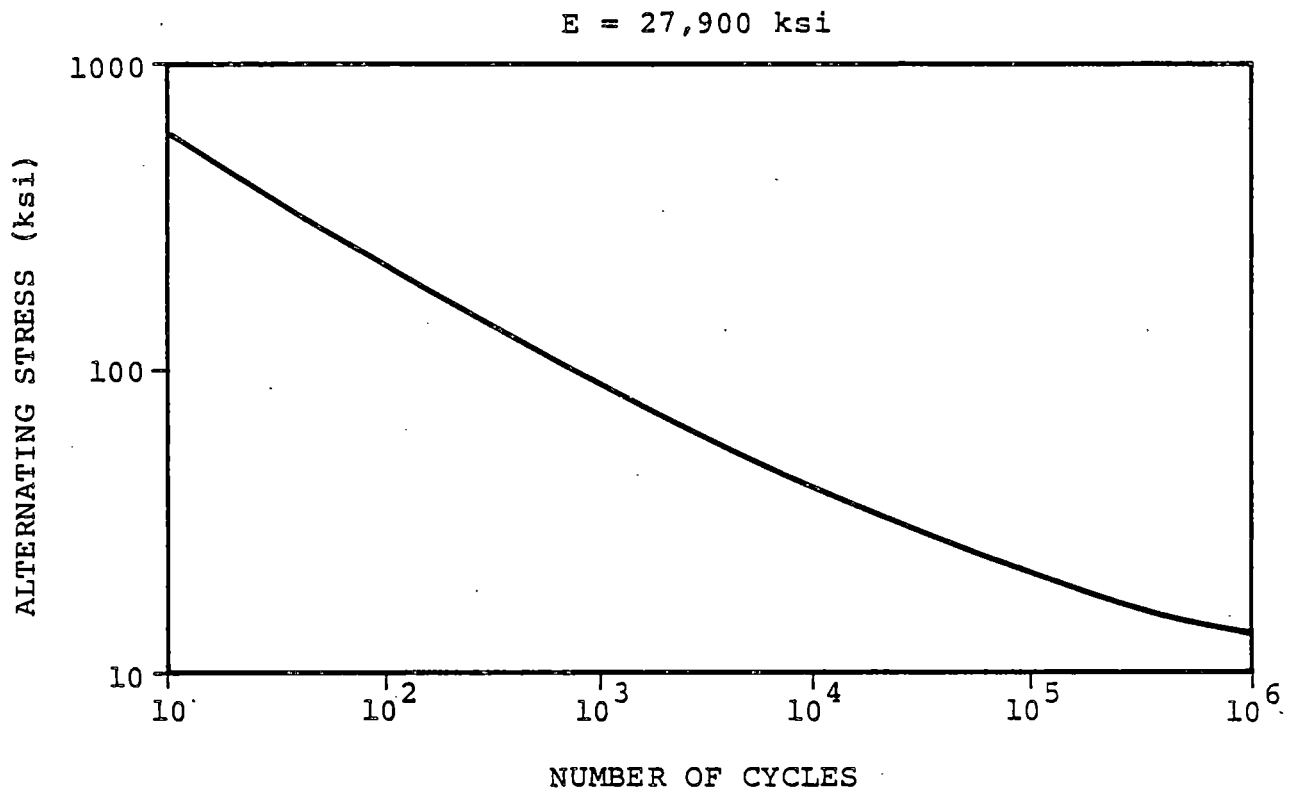


Figure 3-2.4-19

ALLOWABLE NUMBER OF STRESS CYCLES
FOR VENT SYSTEM FATIGUE EVALUATION

COM-02-041-3
Revision 0

3-2.179

3-2.5 Analysis Results

The geometry, loads and load combinations, acceptance criteria, and analysis methods used in the evaluation of the Dresden Units 2 and 3 vent systems are presented and discussed in the preceding sections. The results and conclusions derived from the evaluation of the vent systems are presented in the following paragraphs and sections. As discussed previously, the results of the two 1/16 and the 180° beam models analyses are compared and only the governing results are reported, when applicable.

Table 3-2.5-1 shows the maximum primary membrane stresses for the major vent system components for each of the governing loads. Tables 3-2.5-2 and 3-2.5-3 show the corresponding reaction loads for the vent system support columns and vent line-drywell penetration. Table 3-2.5-4 shows the maximum differential displacements of the vent line bellows for the governing load cases. Figures 3-2.5-1 and 3-2.5-2 show the transient response of the vent system support columns for pool swell loads.

Table 3-2.5-5 shows the maximum stresses and associated design margins for the major vent system components,

component supports, and welds for the SBA II, IBA I, DBA I, DBA II, and DBA III load combinations. Table 3-2.5-6 shows the maximum differential displacements and design margins for the vent line bellows for the SBA II, IBA I, DBA II, and DBA III load combinations. Table 3-2.5-7 shows the fatigue usage factors for the controlling vent system component and weld for the Normal Operating plus SBA events, and the Normal Operating plus IBA events.

Section 3-2.5.1 discusses the vent system evaluation results presented in the preceding paragraphs.

Table 3-2.5-1

MAJOR VENT SYSTEM COMPONENT MAXIMUM
MEMBRANE STRESSES FOR GOVERNING LOADS

SECTION 3-2.2.1 LOAD DESIGNATION		PRIMARY MEMBRANE STRESS (ksi)		
LOAD TYPE	LOAD CASE NUMBER	VENT LINE	VENT HEADER	DOWNCOMER
DEAD WEIGHT	1a	0.241	0.802	0.162
SEISMIC	2a	0.788	1.260	0.271
	2b	1.576	2.520	0.542
PRESSURE AND TEMPERATURE	3b	7.952	8.288	4.461
	3d	N/A	N/A	N/A
VENT SYSTEM DISCHARGE	4a	5.430	6.960	2.420
POOL SWELL	5a-5d	0.737	6.483	3.077
	5f	0.473	3.756	3.034
CONDENSATION OSCILLATION	6a+6c	1.192	1.657	0.498
	6b+6d	5.325	7.633	2.591
	6f	0.418	1.633	1.151
CHUGGING	7a	4.220	4.340	2.360
	7b	1.340	4.340	1.570
	7c	N/A	N/A	N/A
	7d	0.350	1.241	0.919
SRV DISCHARGE	8b	0.339	1.025	1.515
PIPING REACTIONS	9a	12.530	8.250	0.980

- VALUES SHOWN ARE MAXIMUMS IRRESPECTIVE OF TIME AND LOCATION FOR INDIVIDUAL LOAD TYPES AND MAY NOT BE ADDED TO OBTAIN LOAD COMBINATION RESULTS.

Table 3-2.5-2

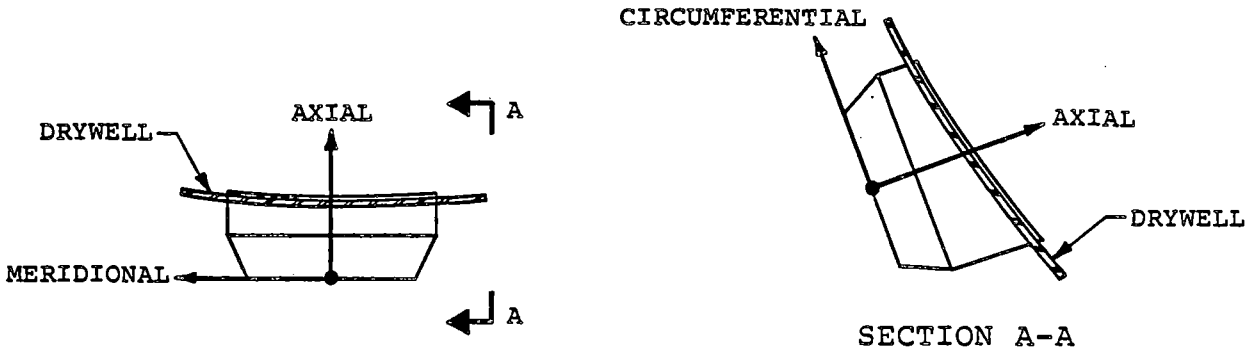
MAXIMUM COLUMN REACTIONS FOR GOVERNING VENT SYSTEM LOADS

SECTION 3-2.2.1 LOAD DESIGNATION			COLUMN REACTION LOAD (kips)			
LOAD TYPE	LOAD CASE NUMBER	DIRECTION	INSIDE	OUTSIDE	TOTAL ⁽¹⁾	
DEAD WEIGHT	1a	COMPRESSION	10.100	9.170	19.270	
SEISMIC	OBE	2a	TENSION	0.724	3.810	4.534
		2a	COMPRESSION	0.724	3.810	4.534
	SSE	2b	TENSION	1.448	7.620	9.068
		2b	COMPRESSION	1.448	7.620	9.068
INTERNAL PRESSURE	3b	TENSION	30.520	29.960	60.480	
TEMPERATURE	3d	COMPRESSION	26.150	5.385	31.535	
VENT SYSTEM DISCHARGE	4a	TENSION	34.500	33.900	68.400	
POOL SWELL	5a-5d	TENSION	66.830	61.710	128.540	
		COMPRESSION	22.860	24.200	47.060	
CONDENSATION OSCILLATION	IBA	6a+6c	TENSION	2.694	8.185	10.879
		6a+6c	COMPRESSION	2.694	8.185	10.879
	DBA	6b+6d	TENSION	16.957	27.116	44.073
		6b+6d	COMPRESSION	16.957	27.116	44.073
CHUGGING	7a+7b	TENSION	21.700	37.500	59.200	
		COMPRESSION	21.700	37.500	59.200	
PIPING REACTIONS	9a	TENSION	35.470	9.410	44.880	
		COMPRESSION	35.470	9.410	44.880	

(1) REACTIONS ARE ADDED IN THE TIME DOMAIN FOR DYNAMIC LOADS.

Table 3-2.5-3

MAXIMUM VENT LINE-DRYWELL PENETRATION
REACTIONS FOR GOVERNING VENT SYSTEM LOADS

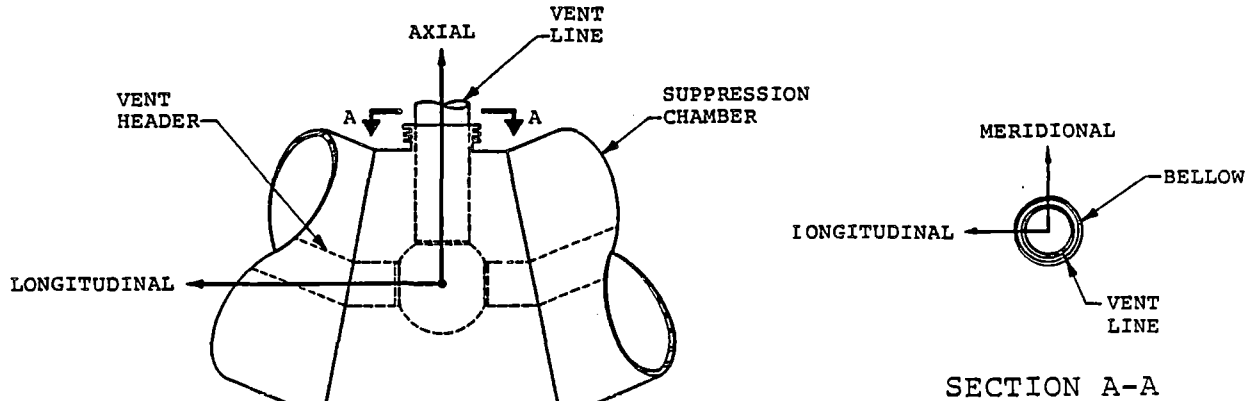


SECTION 3-2.2-1 LOAD DESIGNATION		PENETRATION REACTION LOAD					
LOAD TYPE	LOAD CASE NUMBER	FORCE (kips)			MOMENTS (in-kip)		
		RADIAL	MERIDIONAL	CIRCUMFERENTIAL	RADIAL	MERIDIONAL	CIRCUMFERENTIAL
DEAD WEIGHT	1a	0.9	0.0	1.6	0.0	59.1	0.0
SEISMIC	OBE 2a	23.0	4.3	0.9	201.0	423.0	449.0
	SSE 2b	46.0	8.6	1.8	402.0	846.0	898.0
INTERNAL PRESSURE	3b	89.6	0.0	0.0	0.0	394.8	0.0
TEMPERATURE	3d	65.8	0.0	17.9	0.0	5558.3	0.0
VENT SYSTEM DISCHARGE	4a	75.3	0.0	0.6	0.0	344.0	0.0
POOL SWELL	5a-5d	13.6	0.0	9.4	0.0	549.5	0.0
CONDENSATION OSCILLATION	IBA 6a+6c	8.3	0.0	0.6	0.0	45.5	0.0
	DBA 6b+6d	22.5	0.0	5.1	0.0	188.5	0.0
CHUGGING	7a+7b	51.7	27.0	11.2	4928.0	262.9	2937.0
PIPING REACTIONS	9a	42.7	20.9	48.6	1195.5	821.7	1877.6

1. VALUES SHOWN ARE IN ABSOLUTE TERMS.

Table 3-2.5-4

MAXIMUM VENT LINE BELLOWS DISPLACEMENTS FOR
GOVERNING VENT SYSTEM LOADS



SECTION 3-2.2.1 LOAD DESIGNATION			DIFFERENTIAL BELLOWS DISPLACEMENTS (in)			
LOAD TYPE	LOAD CASE NUMBER	AXIAL		LATERAL		
		COMPRESSION	EXTENSION	MERIDIONAL	LONGITUDINAL	
DEAD WEIGHT	1a	N/A	0.003	0.037	0.000	
SEISMIC	OBE 2a	0.005	0.005	0.003	0.009	
	SSE 2b	0.009	0.009	0.006	0.018	
INTERNAL PRESSURE	3b	0.025	N/A	0.035	0.000	
TEMPERATURE	3d	0.473	N/A	0.018	0.000	
VENT SYSTEM DISCHARGE	4a	0.059	N/A	0.015	0.000	
POOL SWELL	5a-5d	0.046	0.046	0.128	0.000	
CONDENSATION OSCILLATION	IBA 6a+6c	0.056	0.056	0.045	0.000	
	DBA 6b+6d	0.064	0.064	0.057	0.000	
CHUGGING	7a+7b	0.038	0.038	0.028	0.011	
PIPING REACTIONS	9a	0.044	0.044	0.139	0.153	

1. THE VALUES SHOWN ARE MAXIMUMS IRRESPECTIVE OF TIME FOR INDIVIDUAL LOAD TYPES AND MAY NOT BE ADDED TO OBTAIN LOAD COMBINATION RESULTS.

COM-02-041-3
Revision 0

3-2.186

Table 3-2.5-5
MAXIMUM VENT SYSTEM STRESSES
FOR CONTROLLING LOAD COMBINATIONS

ITEM	STRESS TYPE	LOAD COMBINATION STRESSES (ksi)										
		SBA II ⁽¹⁾		IBA I ⁽¹⁾		DBA I ⁽¹⁾		DBA II ⁽¹⁾		DBA III ⁽¹⁾		
		CALCULATED STRESS	CALCULATED ALLOWABLE ⁽²⁾	CALCULATED STRESS	CALCULATED ALLOWABLE ⁽²⁾	CALCULATED STRESS	CALCULATED ALLOWABLE ⁽²⁾	CALCULATED STRESS	CALCULATED ALLOWABLE ⁽²⁾	CALCULATED STRESS	CALCULATED ALLOWABLE ⁽²⁾	
COMPONENTS	DRYWELL SHELL	LOCAL PRIMARY MEMBRANE	17.07	0.59	12.68	0.44	18.56	0.49	17.39	0.46	20.35	0.40
		PRIMARY AND SECONDARY STRESS RANGE	61.09	0.90	47.44	0.70	N/A	N/A	58.26	0.86	N/A	N/A
	VENT LINE	PRIMARY MEMBRANE	18.15	0.94	16.18	0.84	17.03	0.88	16.94	0.88	25.57	0.75
		LOCAL PRIMARY MEMBRANE	9.86	0.34	8.69	0.30	5.39	0.14	9.09	0.24	10.21	0.20
		PRIMARY AND SECONDARY STRESS RANGE	30.82	0.45	26.91	0.40	N/A	N/A	27.75	0.41	N/A	N/A
	VENT LINE, VENT HEADER SPHERICAL JUNCTION ⁽³⁾	PRIMARY MEMBRANE	9.47	0.49	7.91	0.41	7.39	0.38	8.13	0.42	10.07	0.30
		LOCAL PRIMARY MEMBRANE	15.91	0.55	13.35	0.46	13.67	0.47	14.52	0.50	20.04	0.39
		PRIMARY AND SECONDARY STRESS RANGE	48.23	0.71	35.32	0.52	N/A	N/A	39.15	0.58	N/A	N/A
	VENT HEADER	PRIMARY MEMBRANE	17.46	0.91	14.66	0.76	18.68	0.97	17.85	0.93	25.98	0.77
		LOCAL PRIMARY MEMBRANE	20.93	0.72	9.27	0.32	18.96	0.50	18.59	0.49	19.87	0.39
		PRIMARY AND SECONDARY STRESS RANGE	51.67	0.76	29.27	0.43	N/A	N/A	47.38	0.70	N/A	N/A
	DOWNCOMER	PRIMARY MEMBRANE	8.52	0.44	3.80	0.20	11.88	0.62	5.67	0.29	16.25	0.48
		LOCAL PRIMARY MEMBRANE	20.05	0.69	9.96	0.34	16.63	0.44	16.92	0.45	18.96	0.37
		PRIMARY AND SECONDARY STRESS RANGE	34.70	0.51	10.85	0.16	N/A	N/A	34.81	0.51	N/A	N/A
	SUPPORT COLLAR PLATE	PRIMARY MEMBRANE	1.89	0.10	1.14	0.06	3.12	0.16	1.43	0.07	3.20	0.09
		LOCAL PRIMARY MEMBRANE	6.28	0.22	5.07	0.18	9.97	0.26	5.48	0.15	10.22	0.20
		PRIMARY AND SECONDARY STRESS RANGE	57.50	0.85	3.41	0.50	N/A	N/A	49.20	0.73	N/A	N/A

Table 3-2.5-5

MAXIMUM VENT SYSTEM STRESSES
FOR CONTROLLING LOAD COMBINATIONS
(Concluded)

ITEM	STRESS TYPE	LOAD COMBINATION STRESSES (ksi)										
		SBA I L ⁽¹⁾		IBA I ⁽¹⁾		DBA I ⁽¹⁾		DBA II ⁽¹⁾		DBA III ⁽¹⁾		
		CALCULATED STRESS	CALCULATED ⁽²⁾ ALLOWABLE	CALCULATED STRESS	CALCULATED ⁽²⁾ ALLOWABLE	CALCULATED STRESS	CALCULATED ⁽²⁾ ALLOWABLE	CALCULATED STRESS	CALCULATED ⁽²⁾ ALLOWABLE	CALCULATED STRESS	CALCULATED ⁽²⁾ ALLOWABLE	
COMPONENT SUPPORTS	SUPPORT COLUMNS	BENDING	9.70	0.50	6.73	0.35	3.07	0.16	11.73	0.60	6.93	0.27
		TENSILE	3.86	0.22	5.44	0.20	13.32	0.75	5.23	0.30	13.50	0.57
		COMBINED	0.72	0.72	0.55	0.55	0.91	0.91	0.90	0.90	0.84	0.84
		COMPRESSION	5.14	0.42	3.56	0.45	3.48	0.29	3.39	0.28	4.42	0.27
		INTERACTION	0.99	0.99	0.88	0.88	0.46	0.46	0.91	0.91	0.58	0.58
WELDS	COLUMN RING PLATE TO VENT HEADER	PRIMARY	6.79	0.45	4.45	0.30	10.64	0.71	6.00	0.40	10.99	0.42
		SECONDARY	11.29	0.25	7.14	0.16	N/A	N/A	9.50	0.21	N/A	N/A

- (1) REFERENCE TABLE 3-2.2-27 FOR LOAD COMBINATION DESIGNATION.
- (2) REFERENCE TABLE 3-2.3-1 FOR ALLOWABLE STRESSES.
- (3) LOCAL STRESSES ARE REPORTED AT THE VENT LINE-VENT HEADER JUNCTION. FOR LOCAL STRESSES AT THE VENT LINE-SRVDL AND VACUUM BREAKER PENETRATIONS, SEE VOLUMES 5 AND 6 RESPECTIVELY OF THIS REPORT.

COM-02-041-3
Revision 0

Table 3-2.5-6

MAXIMUM VENT LINE BELLOWS DIFFERENTIAL DISPLACEMENTS
FOR CONTROLLING LOAD COMBINATIONS

DISPLACEMENT COMPONENT		SBA II		IBA I		DBA II		DBA III	
		CALCULATED (in)	CALCULATED ALLOWABLE	CALCULATED (in)	CALCULATED ALLOWABLE	CALCULATED (in)	CALCULATED ALLOWABLE	CALCULATED (in)	CALCULATED ALLOWABLE
AXIAL	COMPRESSION	0.659	0.75	0.574	0.66	0.613	0.70	0.504	0.58
	TENSION	N/A	N/A	N/A	N/A	N/A	N/A	N/A	N/A
LATERAL	MERIDIONAL	0.427	0.68	0.422	0.68	0.350	0.56	0.431	0.69
	LONGITUDINAL	0.163	0.24	0.171	0.25	0.119	0.18	0.167	0.25

1. THE DBA III BELLOWS DISPLACEMENTS ENVELOP THOSE OF DBA I SINCE DBA III CONTAINS SRV DISCHARGE LOADS IN ADDITION TO THE OTHER LOADS IN DBA I, (TABLE 3-2.2-25).

3-2.188

Table 3-2.5-7

MAXIMUM FATIGUE USAGE FACTORS FOR VENT SYSTEM
COMPONENTS AND WELDS

EVENT (1) SEQUENCE	LOAD CASE CYCLES (1,2)				CONDENSATION OSCILLATION (sec)	(4) CHUGGING (sec)	EVENT USAGE FACTOR	
	SEISMIC	PRESSURE	TEMPERATURE	SRV (3) DISCHARGE			VENT (5) HEADER	WELD (6)
NOC W/SRV DISCHARGE	0	150	150	550	N/A	N/A	0.00	0.00
SBA 0. TO 600. SEC	0	0	0	50	N/A	300	0.31	0.10
SBA 600. TO 1200 SEC	1000 (2)	1	1	2	N/A	600	0.61	0.16
IBA 0. TO 900. SEC	0	0	0	25	900	N/A	0.59	0.01
IBA 900. TO 1100. SEC	1000 (2)	1	1	2	N/A	200	0.23	0.06
MAXIMUM CUMULATIVE USAGE FACTORS					NOC + SBA		0.92	0.26
					NOC + IBA		0.82	0.07

- (1) SEE TABLE 3-2.2-27 AND FIGURES 3-2.2-12 AND 3-2.2-13 FOR LOAD CYCLES AND EVENT SEQUENCING INFORMATION.
- (2) ENTIRE NUMBER OF LOAD CYCLES CONSERVATIVELY ASSUMED TO OCCUR DURING TIME OF MAXIMUM EVENT USAGE.
- (3) TOTAL NUMBER OF SRV ACTUATIONS SHOWN IS CONSERVATIVELY ASSUMED TO OCCUR IN SAME SUPPRESSION CHAMBER BAY.
- (4) EACH CHUG-CYCLE HAS A DURATION OF 1.4 SEC. SEE TABLE 3-2.2-17 FOR CHUGGING DOWNCOMER LOAD HISTOGRAM. THE MAXIMUM FATIGUE USAGE FACTOR FOR CHUGGING DOWNCOMER LOADS AT THE DOWNCOMER-VENT HEADER INTERSECTION IS 0.103.
- (5) THE MAXIMUM CUMULATIVE USAGE FOR A VENT SYSTEM COMPONENT OCCURS IN THE VENT HEADER AT THE DOWNCOMER-VENT HEADER INTERSECTION.
- (6) THE MAXIMUM CUMULATIVE USAGE FOR A VENT SYSTEM COMPONENT WELD OCCURS AT THE CONNECTION OF THE DOWNCOMER STIFFENER PLATE TO THE VENT HEADER.

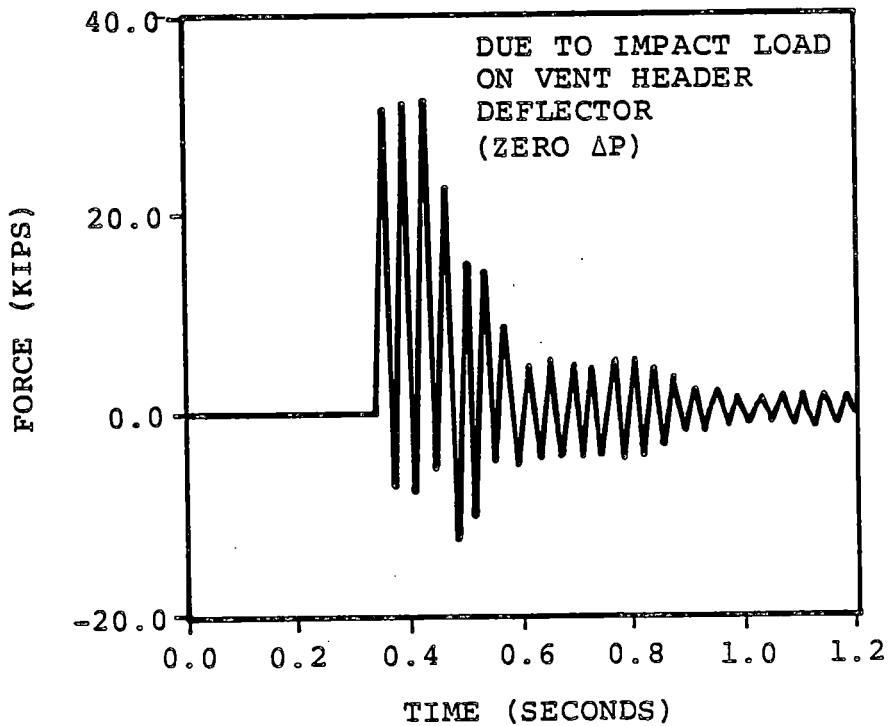
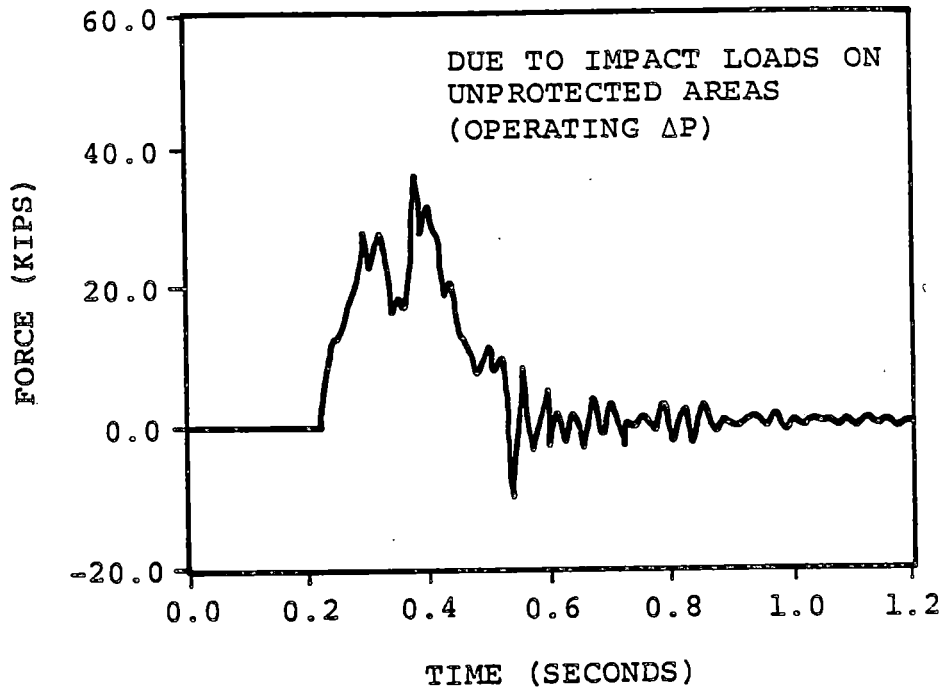


Figure 3-2.5-1

VENT SYSTEM SUPPORT COLUMN RESPONSE DUE TO POOL SWELL IMPACT LOADS - OUTSIDE COLUMN

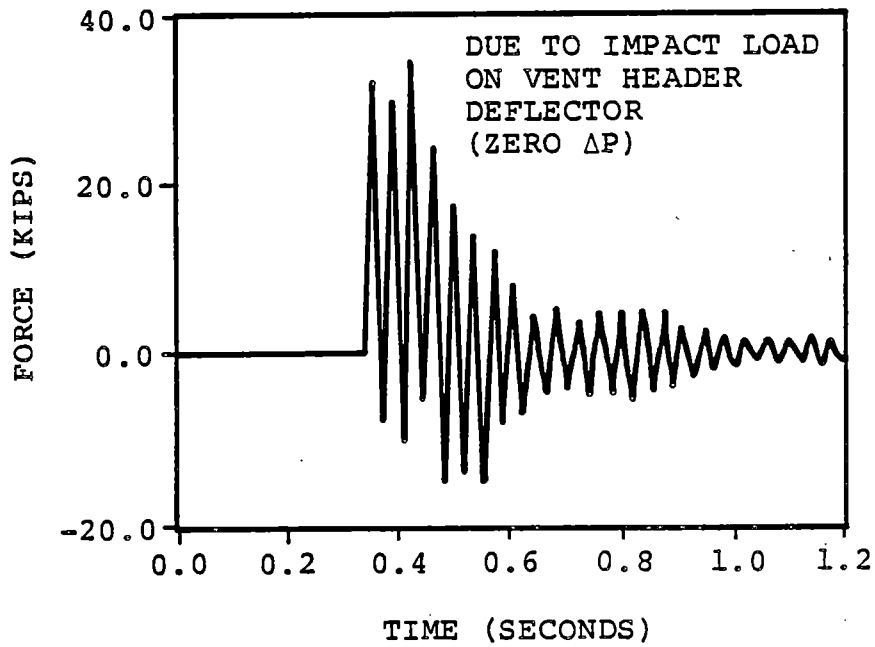
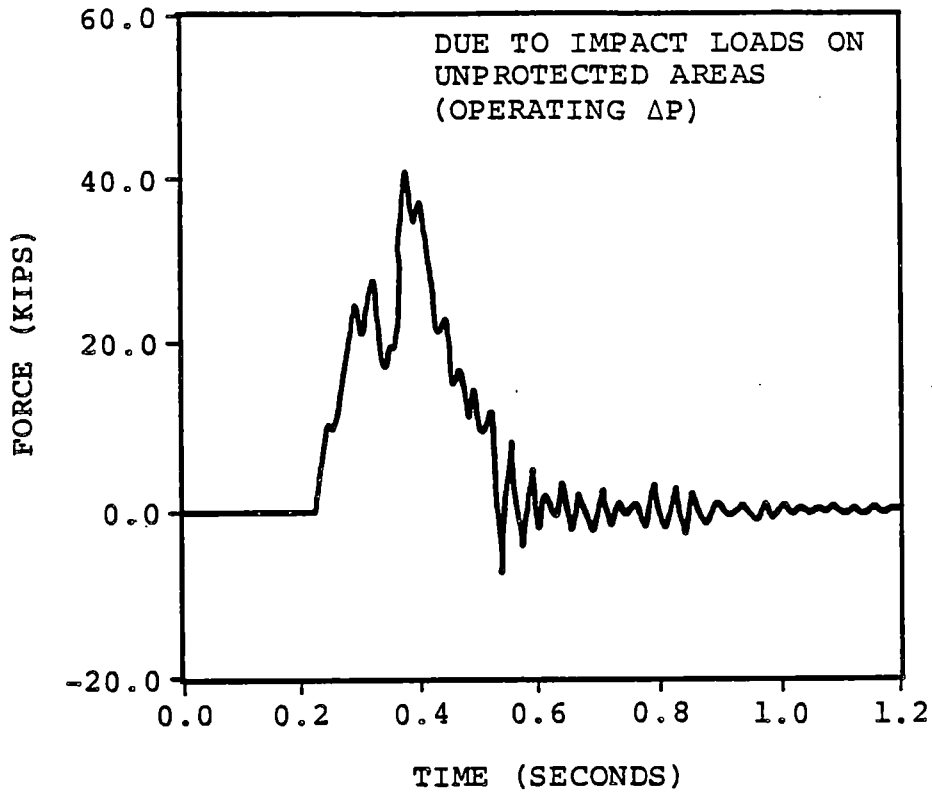


Figure 3-2.5-2

VENT SYSTEM SUPPORT COLUMN RESPONSE DUE TO POOL SWELL IMPACT LOADS - INSIDE COLUMN

3-2.5.1 Discussion of Analysis Results

The results (Table 3-2.5-1) indicate that the largest vent system primary membrane stresses occur for internal pressure loads, vent system discharge loads, pool swell impact loads, DBA CO downcomer loads, chugging downcomer lateral loads, and SRV discharge loads. The remaining loadings result in small primary stresses in the major vent system components.

Table 3-2.5-2 shows that the largest vent system support column reactions occur for internal pressure loads, vent system discharge loads, pool swell impact loads, chugging loads, and DBA CO loads. The distribution of loads between the inner and outer support columns varies from load case to load case. The magnitude and distribution of reaction loads on the drywell penetrations also vary from load case to load case (Table 3-2.5-3). Table 3-2.5-4 shows that the differential displacements of the vent line bellows are small for all loadings, except for thermal loadings.

The results (Table 3-2.5-5) indicate that the highest stresses in the vent system components, component supports, and associated welds occur for the SBA II and the DBA I load combinations. The vent line, spherical

junction, vent header, and downcomer stresses for the SBA II and DBA I load combinations are less than the allowable limits with stresses in other vent system components, component supports, and welds well within the allowable limits. The stresses in the vent system components, component supports, and welds for the IBA I, DBA II, and DBA III load combinations are also well within the allowable limits.

The results (Table 3-2.5-6) indicate that the vent line bellows differential displacements are all well within allowable limits. The maximum displacement occurs for the SBA II load combination.

The loads which cause the highest number of displacement cycles at the vent line bellows are seismic loads, SRV loads, and LOCA-related loads such as pool swell, CO, and chugging. The bellows displacements for these loads are small compared to the maximum allowable displacement, and their effect on fatigue is negligible. Thermal loads and internal pressure loads are the largest contributors to bellows displacements. The specified number of thermal load and internal pressure load cycles is 150. Since the bellows have a rated capacity of 1,000 cycles at maximum displacement, their adequacy for fatigue is assured.

The vent system fatigue usage factors (Table 3-2.5-7) are computed for the controlling events, which are Normal Operating plus SBA and Normal Operating plus IBA. The governing vent system component for fatigue is the vent header at the downcomer-vent header intersection. The magnitudes and cycles of downcomer lateral loads are the primary contributors to fatigue at this location.

The vent system welds are checked for fatigue, except for the SRVDL penetration, which is evaluated and discussed in Volume 5. The governing vent system weld for fatigue is at the downcomer-vent header intersection. Condensation oscillation, chugging, and the number of SRV actuations are the major contributors to fatigue at this location.

Fatigue effects at other locations in the vent system are less severe than at those described above, due primarily to lower stresses.

3-2.5.2 Closure

The vent system loads described and presented in Section 3-2.2.1 are conservative estimates of the loads postulated to occur during an actual LOCA or SRV discharge event. Applying the methodology discussed in Section 3-2.4 to examine the effects of the governing loads on the vent system results in bounding values of stresses and reactions in vent system components and component supports.

The load combinations and event sequencing defined in Section 3-2.2.2 envelop the actual events postulated to occur during a LOCA or SRV discharge event. Combining the vent system responses to the governing loads and evaluating fatigue effects using this methodology results in conservative values of the maximum vent system stresses, support reactions, and fatigue usage factors for each event or sequence of events postulated to occur throughout the life of the plant.

The acceptance limits defined in Section 3-2.3 are as restrictive (in many cases, more restrictive) as those used in the original containment design documented in the plant's safety analysis report. Comparing the resulting maximum stresses and support reactions to

these acceptance limits results in a conservative evaluation of the design margins present in the vent system and its supports. As demonstrated in the results discussed and presented in the preceding sections, all of the vent system stresses and support reactions are within these acceptance limits.

As a result, the vent system components described in Section 3-2.1, which are specifically designed for the loads and load combinations used in this evaluation, exhibit the margins of safety inherent in the original design of the primary containment as documented in the plant's safety analysis report. The NUREG-0661 requirements are therefore considered to be met.

LIST OF REFERENCES

1. "Mark I Containment Long-Term Program," Safety Evaluation Report, NRC, NUREG-0661, July 1980; Supplement 1, August 1982.
2. "Mark I Containment Program Load Definition Report," General Electric Company, NEDO-21888, Revision 2, November 1981.
3. "Mark I Containment Program Plant Unique Load Definition," Dresden Station Units 2 and 3, General Electric Company, NEDO-24566, Revision 2, April 1982.
4. "Containment Vessels Design Specification," Dresden Station Units 2 and 3, K-2152, Sargent & Lundy, Inc., March 19, 1966.
5. "Mark I Containment Program Structural Acceptance Criteria Plant Unique Analysis Applications Guide, Task Number 3.1.3," General Electric Company, NEDO-24583-1, October 1979.
6. ASME Boiler and Pressure Vessel Code, Section III, Division 1, 1977 Edition with Addenda up to and including Summer 1977.
7. "Safety Analysis Report (SAR)," Dresden Station Units 2 and 3, Commonwealth Edison Company, November 17, 1967.
8. "Containment Data," Dresden Unit 2, General Electric Company, 22A5743, Revision 1, April 1979.
9. "Containment Data," Dresden Unit 3, General Electric Company, 22A5744, Revision 1, April 1979.
10. "Dresden 2 and 3 Nuclear Generating Plants Suppression Pool Temperature Response," General Electric Company, NEDC-22170, July 1982.
11. Biggs, J. M., "Introduction to Structural Dynamics," McGraw-Hill Book Company, N.Y., 1964.